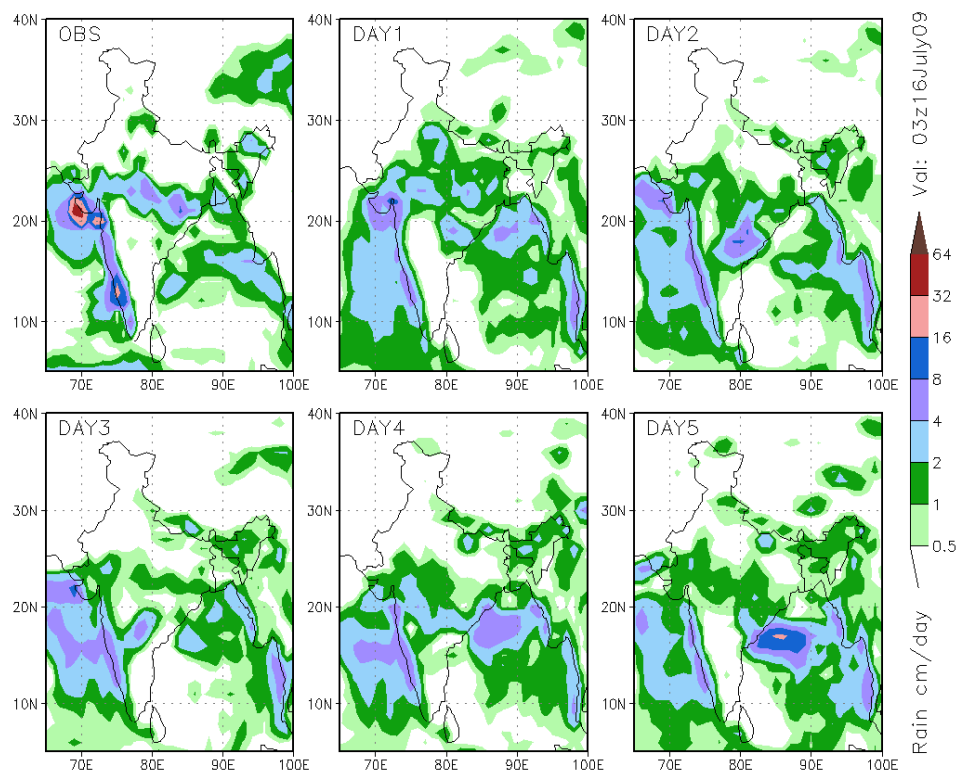


Monsoon-2009: Performance of T254L64 Global Assimilation–Forecast System



March 2010



सत्यमेव जयते


डॉ. शैलेश नायक
DR. SHAILESH NAYAK



FOREWORD

The Asian summer monsoon affects the lives and the economies of countries in the region. The variability of the Indian summer monsoon affects the Indian economy significantly. During last two decades, there has been a considerable improvement in the understanding of underlying physical and dynamical processes. There has also been a significant increase in the availability of data, especially from the satellites and development of efficient data assimilation schemes to ingest these data. The availability of enhanced computing power has made it possible to run operationally high resolution deterministic global models and an ensemble prediction system. The accuracy of numerical weather prediction (NWP) models has improved significantly. Verification/Diagnostics of the analysis/forecast products is a crucial component of research and development work in any operational NWP centre. A comprehensive set of verification scores/diagnostics not only provides a summary of the model's skill, but also indicates the suitability of the model for a variety of applications. It also provides crucial feedback for further model improvements.

NCMRWF is the lead MoES Centre in numerical modeling of weather and climate and is mandated to undertake tasks of developing models for all temporal and spatial scales. I am happy that NCMRWF has brought a detailed performance verification report titled " Monsoon-2009: Performance of the T254L64 Global Assimilation-Forecast System". This is the third consecutive year that the performance of this model has been evaluated in predicting the monsoon circulation and rainfall in medium range. Monsoon season of 2009 was characterised by a delay in advancement of monsoon over the central part of the country and a prolonged dry spell during August. Medium range forecasts could capture well the low-level flow patterns associated with these anomalous features. However, beyond day-3 the skill of rainfall forecast has to be improved further. This report will provide useful information to both scientists and operational forecasters engaged in monsoon prediction and research. I take this opportunity to congratulate the scientists of NCMRWF in bringing out this report and wish them all success in their goal of constantly contributing towards improving the modelling system especially for the Asian monsoon.


(SHAILESH NAYAK)



डॉ० अश्विनी कुमार बोहरा
प्रमुख एवम् सलाहकार

Dr. A.K.Bohra
Head & Advisor
email: akbohra@ncmrwf.gov.in

भारत सरकार
(पृथ्वी विज्ञान मंत्रालय)
राष्ट्रीय मध्यावधि मौसम पूर्वानुमान केन्द्र
ए-50, इंस्टिट्यूशनल एरिया,
फेज़-II सैक्टर-62, नोएडा-201307, उ०प्र०

GOVERNMENT OF INDIA
(Ministry of Earth Sciences)
National Centre for Medium Range Weather Forecasting
A-50, Institutional Area, Phase-II
Sector-62, NOIDA-201307 (UP)
09 March 2010

PREFACE

Numerical modelling is the core of modern meteorological information system. In India, at present, an end to end numerical weather prediction (NWP) system is in place at the National Centre for Medium Range Weather Forecasting (NCMRWF). NCMRWF uses a high resolution (T254L64) numerical model for generating medium range forecasts of monsoon. The associated data assimilation system is 3-D VAR based and has capabilities to assimilate various conventional as well as satellite observations including radiances from different polar orbiting and geostationary satellites. This is an adapted version of the NCEP GFS system.

Monsoon prediction has remained a formidable challenge as numerical modelling systems suffer from large systematic biases. There are a number of factors that generally contribute to poor prediction, viz. quality and quantity of available meteorological observations and the technique to assimilate the same for initializing the numerical model, model formulation, capability of model to handle various scales and their interactions.

NCMRWF is engaged in improving the accuracy of prediction, through better data utilization, enhanced model resolution, improved physics, and realistic interpretation of model products. Thorough performance evaluation and verification of NCMRWF analyses-forecast systems are conducted for every monsoon season. For a comprehensive view, all the main components of monsoon are evaluated individually. It is hoped that this report will provide useful feedback for further model development.

In 2009, Southwest monsoon activity during over Indian region was below normal, with rainfall only 77% of its long period average (LPA). This year though an early onset over Kerala declared by IMD on 23rd May, but there was hiatus in the advance of the monsoon during 8th - 20th June, resulting in rainfall only 53% of LPA in June 2009. This may be related to the weak onset of Arabian Sea branch of monsoon and subsequent weakening of cross-equatorial flow. Based on objective criteria, model predictions also show the delayed onset of over Kerala, and associated weak monsoon condition in June.

Cont....2/-

However, through out the season, observed main monsoon systems like north-south surface pressure gradient, heat low, monsoon trough, cross equatorial flow etc. were comparatively weak. In general, it is found that the model prediction tends to intensify heat low and monsoon trough compared to analyses. It is also noted that the movement of the monsoon disturbances in the T254L64 model is generally faster compared to the observations. The cross-equatorial flow near its core and the low level westerly jet's strength and positions near Somalia coast are captured realistically in the model this season. In most of the features related to low-level flow, it is noticed that the errors during 2009 season are lesser compared to those noticed during previous monsoon season.

During 2009 monsoon, model predicted winds show an easterly bias in the lower troposphere over eastern & central parts of India. Weakening of the Tropical Easterly Jet (TEJ) is seen in the model predictions. The model predictions are able to depict the active and weak spells of the monsoon flow reasonably well. Objective verification scores for wind computed against the analysis and observations show that the NCMRWF T254L64 model predictions compare well with that from the other major operational NWP centres. However the model rainfall predictions look realistic only up to day-3 prediction. Beyond that over the Indian region the model is able to capture the overall activity only. When particular sub-region of the country is examined, it is seen that for skills beyond day-3 forecasts, there is a need for further improvement.

In recent past India Meteorological Department under its modernisation plan have upgraded 10 radio-sonde stations by GPS-sonde, resulting in better quality of upper-air observations over India. These were used by NCMRWF assimilation-forecast system during monsoon-2009. Upcoming observations from Indian satellites viz. Oceansat-II and Insat-3D will facilitate enhanced data coverage over Indian region. NCMRWF is upgrading its high performance computing system to around 24 TF, which will enable further advanced modelling system. With enhanced observations and higher computing resources an overall improvement of model skill is envisaged in coming years.



(A. K. Bohra)

Please cite this report as given below:

NCMRWF, Ministry of Earth Sciences (MoES), Government of India, (March 2010): “**MONSOON-2009: Performance of the T254L64 Global Assimilation Forecast System**“, Report no. NMRF/MR/01/2010, 131 pages, Published by NCMRWF (MoES), A-50 Institute Area, Sector- 62, NOIDA, UP, INDIA 201307

Disclaimer:

The geographical boundaries shown in this report do not necessarily correspond to political boundaries.

Front Cover:

Front cover shows global T254L64 model predicted rainfall valid for 03UTC of 16 July 2009 (a typical active monsoon condition) along with observation.

This report was compiled and produced by:

A. K. Mitra, M. Das Gupta and G. R. Iyengar
NCMRWF/MoES

Acknowledgements:

Acknowledgement is also due to NCEP/NOAA for providing the GFS assimilation-forecast system codes and their support for its implementation in 2007. Observed rainfall data was provided by IMD.

For other details about NCMRWF see the website www.ncmrwf.gov.in

C o n t e n t s

<u>Topic</u>	<u>Page</u>
1. Overview of Global T254L64 Data Assimilation – Forecast System <i>E.N.Rajagopal, M. Das Gupta and V.S.Prasad</i>	1
2. Mean Circulation Characteristics of the Summer Monsoon <i>G. R. Iyengar</i>	8
3. (a) Systematic Errors in the Medium Range Prediction of the Summer Monsoon <i>G. R. Iyengar</i>	27
(b) Verification of Model Rainfall Forecasts <i>A. K. Mitra, G. R. Iyengar, R. G. Ashrit and S. Mohandas</i>	43
4. (a) Onset and Advancement of Monsoon <i>M. Das Gupta</i>	56
(b) Monsoon Indices: Onset, Strength and Withdrawal <i>D. Rajan and G. R. Iyengar</i>	64
5. Heat Low, Monsoon Trough, Lows and Depressions <i>R. G. Ashrit and J. P. George</i>	75
6. Mascarene High, Cross-Equatorial Flow, Low-Level Jet and North-South Pressure Gradient <i>A. K. Mitra, M. Dasgupta and G. R. Iyengar</i>	85
7. Tropical Easterly Jet, Tibetan High and Mid-Latitude Interaction <i>S. Mohandas and L. Harenduprakash</i>	103
8. Location Specific and Customized Weather Forecast for Cities and Districts: Evaluation of Forecast Skills <i>Ashok Kumar, E.N.Rajagopal, J.V.Singh and Ranjeet Singh</i>	111

Overview of Global T254L64 Data Assimilation - Forecast System

E. N. Rajagopal, M. Das Gupta and V.S. Prasad

1. Introduction

The global high-resolution assimilation-forecast system T254L64 (T254 spectral waves in horizontal and 64 layers in vertical) was implemented at NCMRWF in January 2007 (Rajagopal et al., 2007). In this report an attempt is made to verify and compare the evolutions of various weather systems and semi-permanent monsoon features during June-September 2009, in the T254L64 analysis-forecast system. The salient features of T254L64 global data assimilation-forecast system are presented briefly in this chapter.

Global Forecast System (GFS) is the operational numerical weather analysis-forecast system of National Centers for Environmental Prediction (NCEP), USA. This system was acquired by NCMRWF under a USAID training programme. The GFS was implemented on CRAY-X1E and Param Padma (IBM P5 cluster) in 2007. GFS has capabilities to assimilate various conventional as well as satellite observations including radiances from different polar orbiting and geostationary satellites.

2. Data Pre-Processing and Quality Control

The meteorological observations from all over the globe and from various observing platforms are received at Regional Telecommunication Hub (RTH), New Delhi through Global Telecommunication System (GTS) and the same is made available to NCMRWF through a dedicated link at half hourly interval. In decoding step, all the GTS bulletins are decoded from their native format and encoded into NCEP BUFR format using the various decoders. Satellite radiances (level 1b) from AMSU-A, AMSU-B/MHS & HIRS on board NOAA-15, 16, 18, Metop-A and SBUV ozone profiles from NOAA-16 & 17 are downloaded from NOAA/NESDIS ftp server. The same are processed and encoded in NCEP BUFR.

Global data assimilation system (GDAS) of T254L64 access the observational database at a set time each day (i.e., the data cut-off time, presently set as 6 hour), four times a day. Observations of a similar type [e.g., satellite-derived winds ("satwnd"), surface land reports ("adpsfc")] are dumped into individual BUFR files in which, duplicate reports are removed, and upper-air report parts (i.e. AA,BB,CC,DD) are merged.

Last step of conventional data processing is the generation of "prebufr" files. This step involves the execution of series of programs designed to assemble observations dumped from a number of decoder databases, encode information about the observational error for each data type as well the background (first guess) interpolated to each data location, perform both rudimentary multi-platform quality control and more complex platform-specific quality control. Quality control of satellite radiance data is done within the global analysis scheme.

3. Global Analysis Scheme

The Gridpoint Statistical Interpolation (GSI) [Wu et al. 2002] replaced Spectral Statistical Interpolation (SSI) in the operational global suite with effect from 1 January 2009. Some positive impacts of GSI were seen in the parallel analysis system experiment conducted in August 2008 using NCMRWF's T254L64 model (Rajagopal et al., 2008) and hence it was decided to make GSI operational from January 2009.

GSI replaces spectral definition for background errors with grid point version based on recursive filters. Diagonal background error covariance in spectral space allows little control over the spatial variation of the error statistics as the structure function is limited to being geographically homogeneous and isotropic about its center (Parrish and Derber 1992; Courtier et al. 1998). GSI allows greater flexibility in terms of inhomogeneity and anisotropy for background error statistics. The major improvement of GSI over SSI analysis scheme is its latitude-dependent structure functions and has more appropriate background errors in the tropics. The background error covariances are isotropic and homogenous in the zonal direction. It has the advantage of being capable of use with forecast systems in both global and regional scale. It also has capability to assimilate newer satellite, radar, profiler and surface data. Assimilation capability of cosmic GPS – Radio Occultation, Doppler radial velocities and reflectivity, precipitation, cloud and ozone observations are the scientific advancement in GSI over SSI. A detailed description of GSI code and its usage can be found in GSI User's Guide (DTC, 2009)

The analysis variables in GSI are stream function, surface pressure, unbalanced velocity potential, unbalanced virtual temperature, unbalanced surface pressure, relative humidity, surface skin temperature, ozone mixing ratio and cloud condensate mixing ratio. Horizontal resolution of the analysis system is quadratic T254 Gaussian grid (approximately 0.5 x 0.5

degree). The analysis is performed directly in the model's vertical coordinate system. This sigma ($\sigma = p/p_s$) coordinate system extends over 64 levels from the surface (~997.3 hPa) to top of the atmosphere at about 0.27hPa. This domain is divided into 64 layers with enhanced resolution near the bottom and the top, with 15 levels is below 800 hPa, and 24 levels are above 100 hPa. Meteorological observations from various types of observing platform, assimilated in T254L64 global analysis scheme at NCMRWF are shown Table I.

Table I: Observations currently used in T254L64

<i>Observation type</i>	<i>Variables</i>
Radiosonde	u, v, T, q, p _s
Pibal winds	u, v
Wind profilers	u, v
Surface land observations	p _s
Surface ship and buoy observations	u, v, T, q, p _s
Conventional Aircraft observations (AIREP)	u, v, T
AMDAR Aircraft observations	u, v, T
ACARS Aircraft observations	u, v, T
GMS/MTSAT AMV (BUFR)	u, v, T
INSAT AMV (SATOB)	u, v, T
METEOSAT AMV (BUFR)	u, v, T
GOES (BUFR)	u, v, T
SSM/I	Surface wind speed
Scatterometer (QSCAT)	10m u, v
AMSU-A radiance	Bright. Temp.
AMSU-B radiance	Bright. Temp.
HIRS radiance	Bright. Tem
SBUV ozone	Total Ozone

The NOAA level 1b radiance data sets obtained from NESDIS/NOAA contain raw instrument counts, calibration coefficients and navigation parameters. The data is in a packed format and all the band data exists in a 10 bit format. The data product, in addition to video data, contains ancillary information like Earth Location Points (ELPs), solar zenith angle and calibration.. The raw counts in the level 1b files are transformed using the calibration coefficients in the data file to antenna temperatures and then to brightness temperatures (for AMSU-A data) using the algorithm of Mo (1999). The geometrical and channel brightness temperature data extracted from orbital data are then binned in 6 hour periods (+/-3hrs) of the analysis time for use in the assimilation system. The use of the level 1b data requires the application of quality control, bias correction, and the appropriate radiative transfer model (Derber & Wu, 1998; McNally et al., 1999). The radiative transfer model (CRTM) uses the OPTRAN transmittance model to calculate instrument radiances and brightness temperatures and their Jacobians.

4. Forecast Model

The forecast model is a primitive equation spectral global model with state of art dynamics and physics (Kanamitsu 1989, Kanamitsu et al. 1991, Kalnay et al. 1990). Model horizontal and vertical resolution & representation are same as described in analysis scheme. The main time integration is leapfrog for nonlinear advection terms. Semi-implicit method is used for gravity waves and for zonal advection of vorticity and moisture. An Asselin (1972) time filter is used to reduce computational modes. The model time step for T254 is 7.5 minutes for computation of dynamics and physics. The full calculation of longwave radiation is done once every 3 hours and shortwave radiation every hour (but with corrections made at every time step for diurnal variations in the shortwave fluxes and in the surface upward longwave flux). Mean orographic heights on the Gaussian grid are used. Negative atmospheric moisture values are not filled for moisture conservation, except for a temporary moisture filling that is applied in the radiation calculation.

Various physical parameterization schemes used in the model are summarized briefly in Table II.

Table II: Physical Parameterization schemes in T254L64 Model

Physics	Scheme
Surface Fluxes	Monin-Obukhov similarity
Turbulent Diffusion	Non-local Closure scheme (Hong and Pan (1996))
SW Radiation	Based on Hou et al. 2002 –invoked hourly
LW Radiation	Rapid Radiative Transfer Model (RRTM) (Mlawer et al. 1997). – invoked 3 hourly
Deep Convection	SAS convection (Pan and Wu (1994))
Shallow Convection	Shallow convection Following Tiedtke (1983)
Large Scale Condensation	Large Scale Precipitation based on Zhao and Carr (1997)
Cloud Generation	Based on Xu and Randall (1996)
Rainfall Evaporation	Kessler's scheme
Land Surface Processes	NOAH LSM with 4 soil levels for temperature & moisture Soil moisture values are updated every model time step in response to forecasted land-surface forcing (precipitation, surface solar radiation, and near-surface parameters: temperature, humidity, and wind speed).
Air-Sea Interaction	Roughness length determined from the surface wind stress (Charnock (1955), Observed SST, Thermal roughness over the ocean is based on a formulation derived from TOGA COARE (Zeng et al., 1998).
Gravity Wave Drag	Based on Alpert et al. (1988)

5. Computational Performance

One cycle of analysis (GSI) takes about 70 minutes of computing time in on 27 MSPs (Multi-Streaming Processors) Cray X1E. The forecast model takes about 120 minutes of computation time in 27 MSPs of Cray X1E for a 168-hr model forecast. Due to this large computational time required for T256L64, analysis-forecast system runs 4 times a day for four assimilation cycle (i.e. 0000, 0600,1200,1800 UTC) with a strict data-cut off of 6 hours.

References

- Alpert, J.C., S-Y Hong and Y-J Kim, 1996: Sensitivity of cyclogenesis to lower troposphere enhancement of gravity wave drag using the Environmental Modeling Center medium range model. *Proc. 11th Conference. on NWP, Norfolk*, 322-323.
- Asselin, R., 1972: Frequency filter for time integrations. *Mon. Wea. Rev.*, 100, 487-490.
- Charnock, H., 1955: Wind stress on a water surface. *Quart. J. Roy. Meteor. Soc.*, 81, 639-640.
- Courtier, P., and Coauthors, 1998: "The ECMWF implementation of the three-dimensional variational assimilation (3D-Var). I: Formulation, Quarterly Journal of Royal Meteorological Society, 124, pp. 1783-1807.
- Derber, J. C. and W.-S. Wu, 1998: The use of TOVS cloud-cleared radiances in the NCEP SSI analysis system. *Mon. Wea. Rev.*, 126, 2287 - 2299
- Derber, J. C., D.F. Parrish and S. J. Lord, 1991: The new global operational analysis system at the National Meteorological Center. *Weather and Forecasting*, 6, 538-547.
- DTC, 2009: Gridpoint Statistical Interpolation (GSI) Version 1.0 User's Guide, NCAR/NCEP, NOAA/GSD, ESRL, NOAA, 77 p.
(http://www.dtcenter.org/com-GSI/users/docs/users_guide/GSIUserGuide_V1.0.pdf/)
- Hong, S.-Y. and H.-L. Pan, 1996: Nonlocal boundary layer vertical diffusion in a medium-range forecast model. *Mon. Wea. Rev.*, 124, 2322-2339.
- Hou, Y-T, K. A. Campana and S-K Yang, 1996: Shortwave radiation calculations in the NCEP's global model. *International Radiation Symposium, IRS-96, August 19-24, Fairbanks, AL.*
- Kalnay, M. Kanamitsu, and W.E. Baker, 1990: Global numerical weather prediction at the National Meteorological Center. *Bull. Amer. Meteor. Soc.*, 71, 1410-1428.
- Kanamitsu, M., 1989: Description of the NMC global data assimilation and forecast system. *Weather and Forecasting*, 4, 335-342.
- Kanamitsu, M., J.C. Alpert, K.A. Campana, P.M. Caplan, D.G. Deaven, M. Iredell, B. Katz, H.-L. Pan, J. Sela, and G.H. White, 1991: Recent changes implemented into the global forecast system at NMC. *Weather and Forecasting*, 6, 425-435.
- McNally, A. P., J. C. Derber, W.-S. Wu and B.B. Katz, 2000: The use of TOVS level-1 radiances in the NCEP SSI analysis system. *Quart.J.Roy. Meteorol. Soc.* , 129, 689-724
- Mlawer, E.J., S.J. Taubman, P.D. Brown, M.J. Iacono, and S.A. Clough, 1997: Radiative transfer for inhomogeneous atmospheres: RRTM, a validated correlated-k model for the longwave. *J. Geophys. Res.*, 102, 16663-16682.

- NCMRWF, Ministry of Earth Sciences (MoES), Government of India (January 2008): Monsoon-2007: Performance of the NCMRWF Global Assimilation Forecast System, Report No. NMRF/MR/01/2008, 143 pages, Published by NCMRWF (MoES), A-50, Sector-62, NOIDA, UP, INDIA 201307.
- Parrish, D.E. and J.C. Derber, 1992. The National Meteorological Center's spectral statistical-interpolation analysis system. *Mon. Wea. Rev.*, 120, 1747-1763.
- Pan, H.-L. and W.-S. Wu, 1995: Implementing a Mass Flux Convection Parameterization Package for the NMC Medium-Range Forecast Model. *NMC Office Note, No. 409*, 40 pp.
- Rajagopal, E.N., M. Das Gupta, Saji Mohandas, V.S. Prasad, John P. George, G.R. Iyengar and D. Preveen Kumar, 2007: Implementation of T254L64 Global Forecast System at NCMRWF, *NMRF/TR/1/2007*, 42 p.
- Rajagopal, E.N., Surya K. Dutta, V.S. Prasad, Gopal R. Iyengar and M. Das Gupta, 2008: Impact of Gridpoint Statistical Interpolation Scheme over Indian Region, Extended Abstracts - Int'l Conf. on Progress in Weather and Climate Modelling over Indian Region, 9-12 December 2008, NCMRWF, NOIDA, 202-205.*
- Tiedtke, M., 1983: The sensitivity of the time-mean large-scale flow to cumulus convection in the ECMWF model. *ECMWF Workshop on Convection in Large-Scale Models, 28 November-1 December 1983, Reading, England*, pp. 297-316.
- Wan-Shu Wu, R. James Purser, and David F. Parrish, 2002: Three-Dimensional Variational Analysis with Spatially Inhomogeneous Covariances. *Monthly Weather Review*, 130, 2905–2916.
- Xu, K. M., and D. A. Randall, 1996: A semiempirical cloudiness parameterization for use in climate models. *J. Atmos. Sci.*, 53, 3084-3102.
- Zeng, X., M. Zhao, and R.E. Dickinson, 1998: Intercomparison of bulk aerodynamical algorithms for the computation of sea surface fluxes using TOGA COARE and TAO data. *J. Climate*, 11, 2628-2644.
- Zhao, Q. Y., and F. H. Carr, 1997: A prognostic cloud scheme for operational NWP models. *Mon. Wea. Rev.*, 125, 1931-1953.

Mean Circulation Characteristics of the Summer Monsoon

G. R. Iyengar

1. Introduction

In this chapter, mean circulation characteristics of the summer monsoon- and their anomalies are examined. The anomalies are calculated from the archived mean analysis fields of NCMRWF (1994-2003).

2. Wind Fields

The geographical distribution of the mean wind field for the months of June, July, August and September at 850, 700, 500 and 200hPa and their monthly anomalies are shown in Fig. 1(a-b) to Fig. 16(a-b) respectively. The anomalous features identified from the mean circulation of each month of monsoon- 2009 are listed below.

2.1 June

At 850, 700 and 500 hPa levels, an anomalous anti-cyclonic circulation was seen over the central and western parts of India. This anomalous circulation feature was associated with the prolonged hiatus in the advancement of monsoon over India during the second and third weeks of June. A strong upper level cyclonic circulation anomaly was well established over west-central Asia around early June. This type of anomalous extratropical circulation pattern could have induced stagnation in the progress of monsoon. An anomalous cyclonic circulation was also seen over the south-central Arabian Sea at 850 and 700 hPa levels. At 200 hPa level, anomalous westerlies were seen over the southern peninsular India, indicating that the Tropical Easterly Jet was weaker than normal.

2.2 July

In the lower tropospheric levels (850 and 700hPa) an anomalous east-west cyclonic circulation was seen over the central parts of India. Anomalous westerlies were also seen over the Arabian Sea. These features were associated with the positive rainfall anomalies over the west coast and central parts of India. At 500 hPa level, an anomalous cyclonic circulation was

seen over the northwest Bay of Bengal. At 200 hPa level, anomalous westerlies were seen over the southern peninsular India, indicating that the Tropical Easterly Jet was weaker than normal.

2.3 August

In the lower tropospheric levels (850 and 700hPa) anomalous anti-cyclonic circulations were seen over the entire northern and central parts of India. Anomalous easterlies were also seen over the peninsular India in the lower tropospheric levels. This feature was also observed at 500 hPa level. The observed rainfall activity over the country was very subdued during this month.

2.4 September

In the lower tropospheric levels (850 and 700hPa) anomalous cyclonic circulation was seen over the Bay of Bengal and adjoining eastern parts of the country. At 500hPa an anomalous anti cyclonic circulation was seen over the north-western parts of India. At 200 hPa level, anomalous westerlies were seen over the peninsular India

Legends for figures:

Figure 1: Geographical distribution of mean wind field (a) and anomaly (b) at 850hPa; for June 2009. Anomalies are departures from the 1994-2003 base period. [Units: m/s, Contour interval: 5m/s for analyses and 3m/s for anomalies]

Figure 2: Same as in Figure 1, but for 700hPa.

Figure 3: Same as in Figure 1, but for 500hPa.

Figure 4: Same as in Figure 1, but for 200hPa. [Units: m/s, Contour interval: 10m/s for analyses and 5m/s for anomalies]

Figure 5: Same as in Figure 1, but for July 2009.

Figure 6: Same as in Figure 2, but for July 2009.

Figure 7: Same as in Figure 3, but for July 2009.

Figure 8: Same as in Figure 4, but for July 2009.

Figure 9: Same as in Figure 1, but for August 2009.

Figure 10: Same as in Figure 2, but for August 2009.

Figure 11: Same as in Figure 3, but for August 2009.

Figure 12: Same as in Figure 4, but for August 2009.

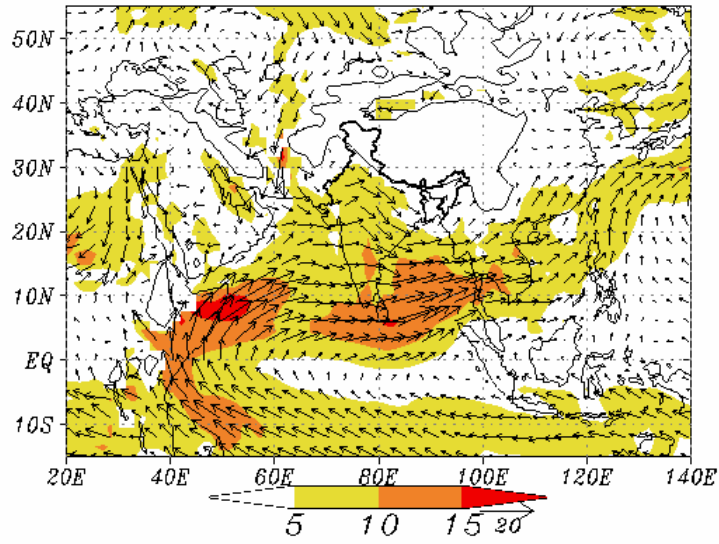
Figure 13: Same as in Figure 1, but for September 2009.

Figure 14: Same as in Figure 2, but for September 2009.

Figure 15: Same as in Figure 3, but for September 2009.

Figure 16: Same as in Figure 4, but for September 2009.

MEAN ANALYSIS 850hPa WINDS JUN 2009



ANOMALY 850hPa WINDS JUN 2009

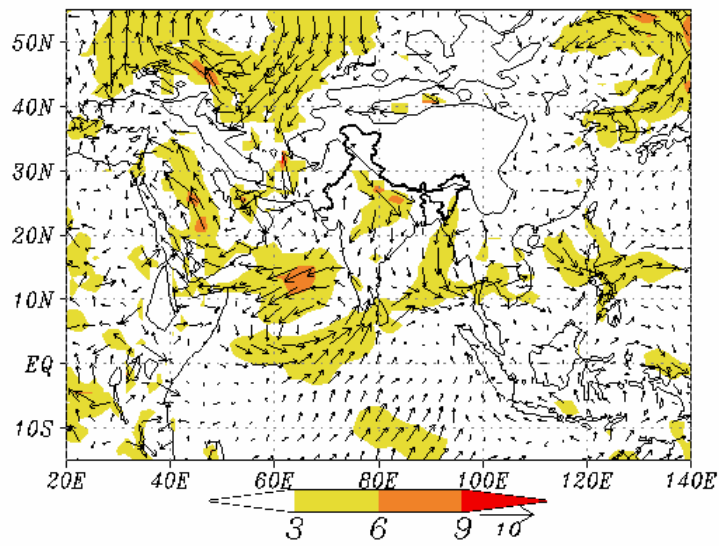
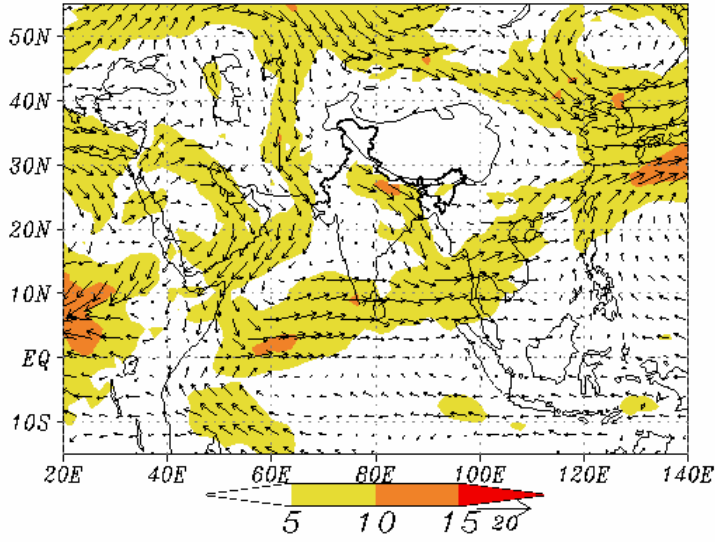


Fig.1

MEAN ANALYSIS 700hPa WINDS JUN 2009



ANOMALY 700hPa WINDS JUN 2009

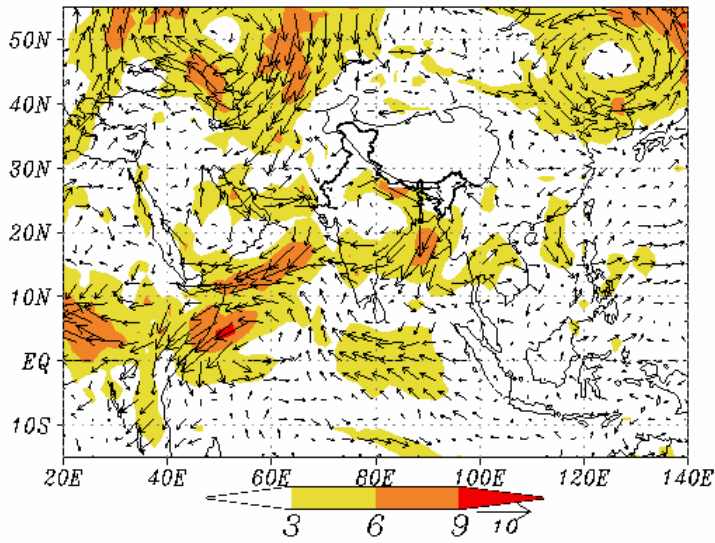
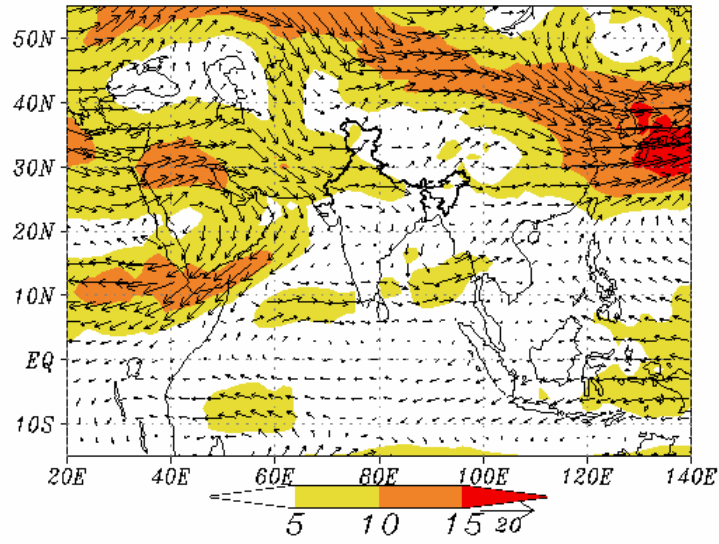


Fig.2

MEAN ANALYSIS 500hPa WINDS JUN 2009



ANOMALY 500hPa WINDS JUN 2009

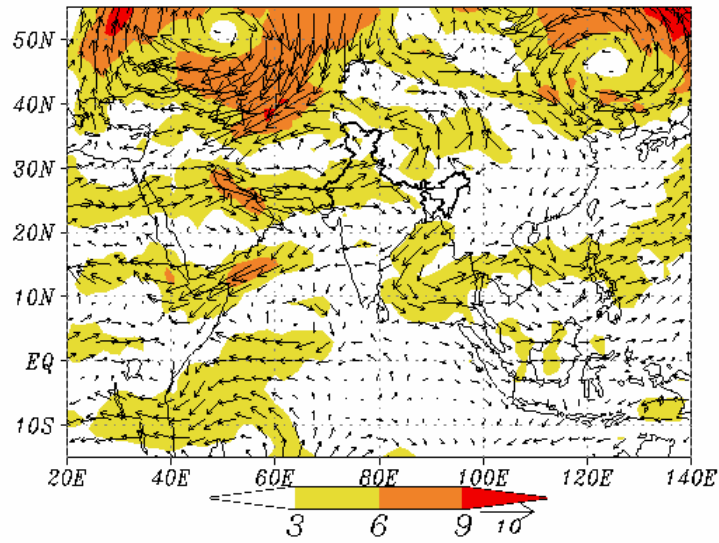
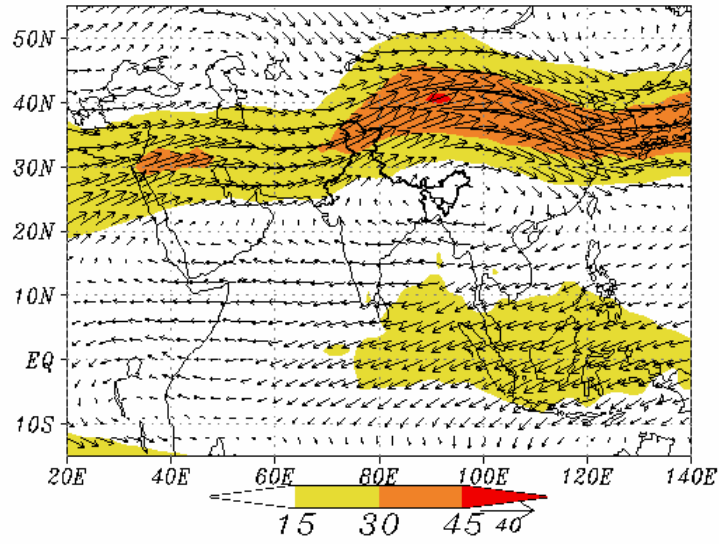


Fig.3

MEAN ANALYSIS 200hPa WINDS JUN 2009



ANOMALY 200hPa WINDS JUN 2009

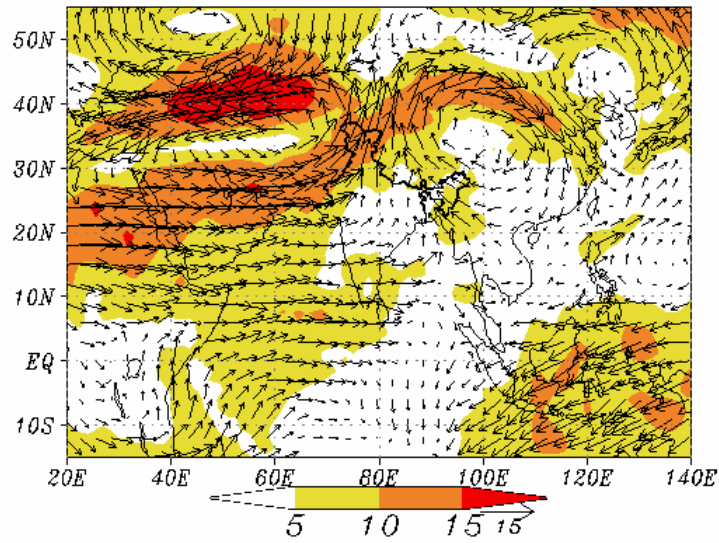
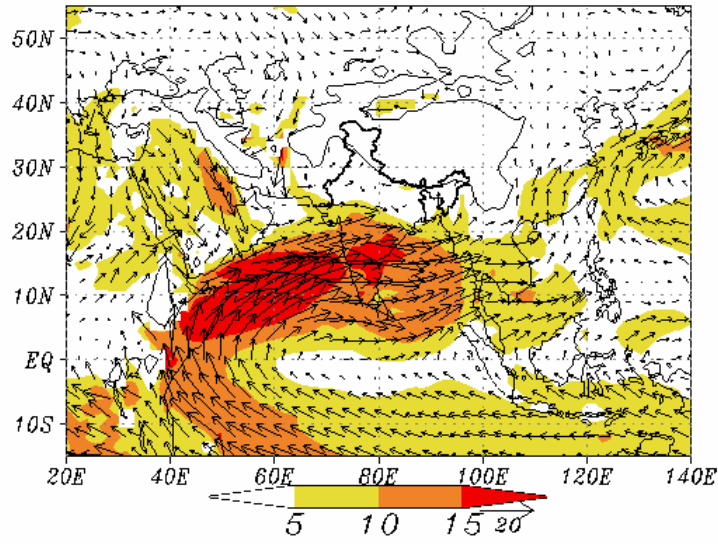


Fig. 4

MEAN ANALYSIS 850hPa WINDS JUL 2009



ANOMALY 850hPa WINDS JUL 2009

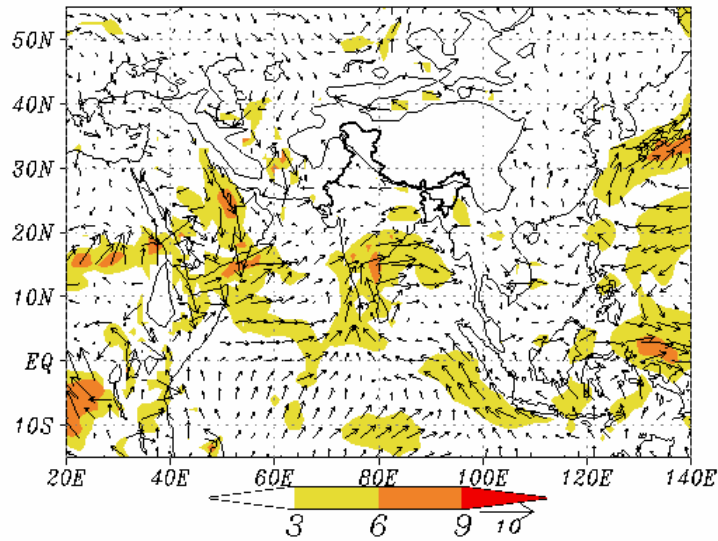
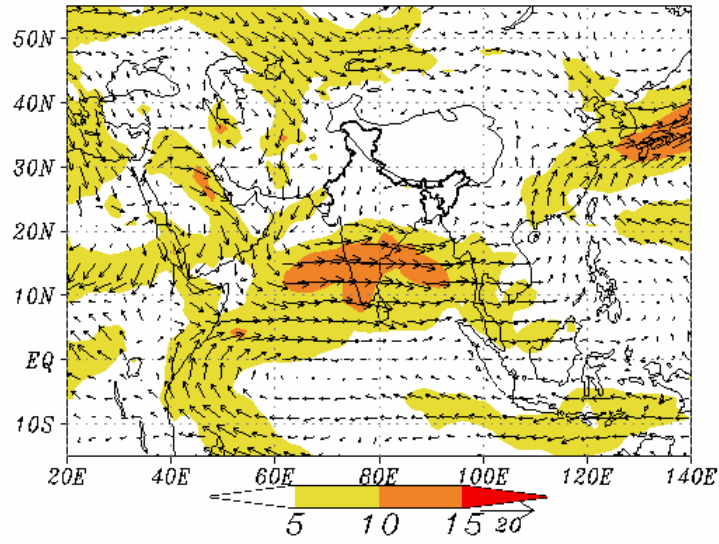


Fig. 5

MEAN ANALYSIS 700hPa WINDS JUL 2009



ANOMALY 700hPa WINDS JUL 2009

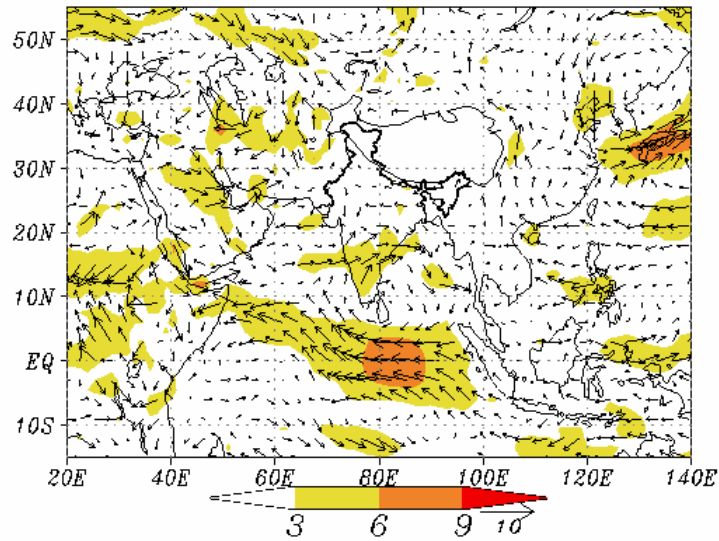
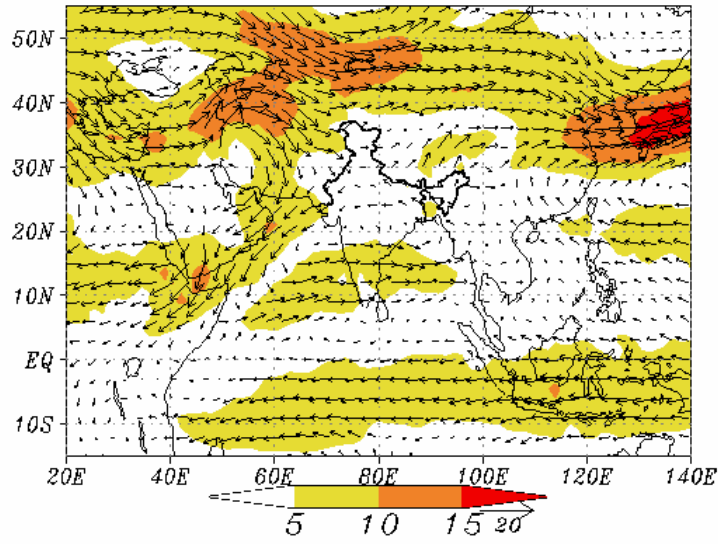


Fig. 6

MEAN ANALYSIS 500hPa WINDS JUL 2009



ANOMALY 500hPa WINDS JUL 2009

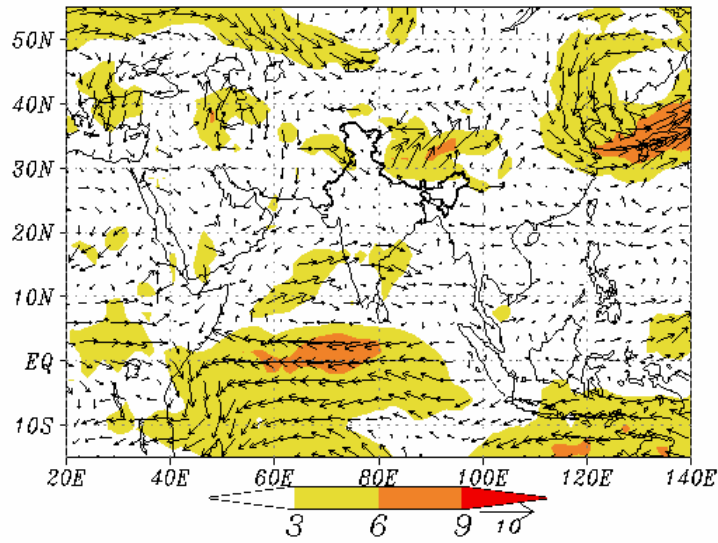
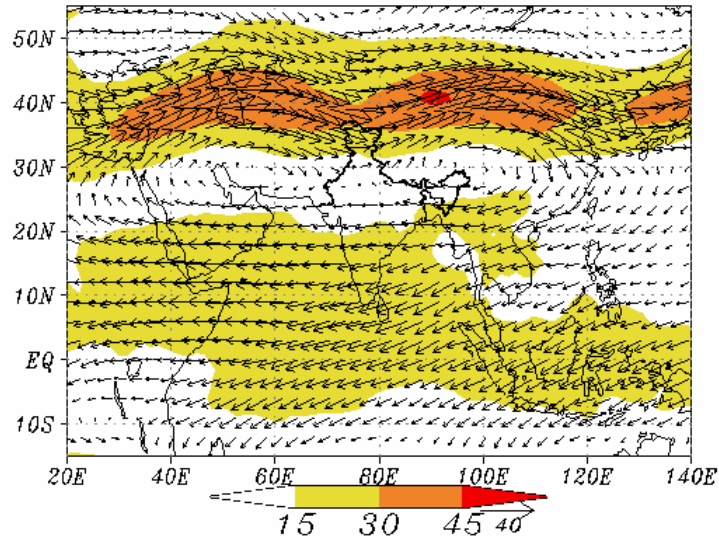


Fig. 7

MEAN ANALYSIS 200hPa WINDS JUL 2009



ANOMALY 200hPa WINDS JUL 2009

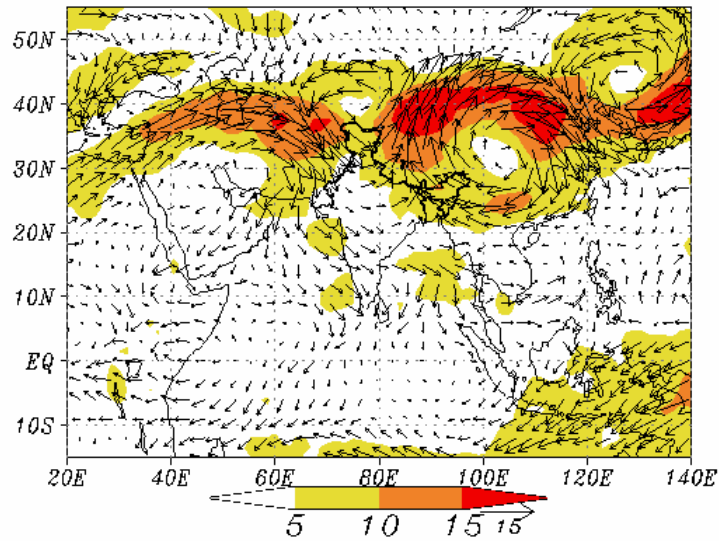
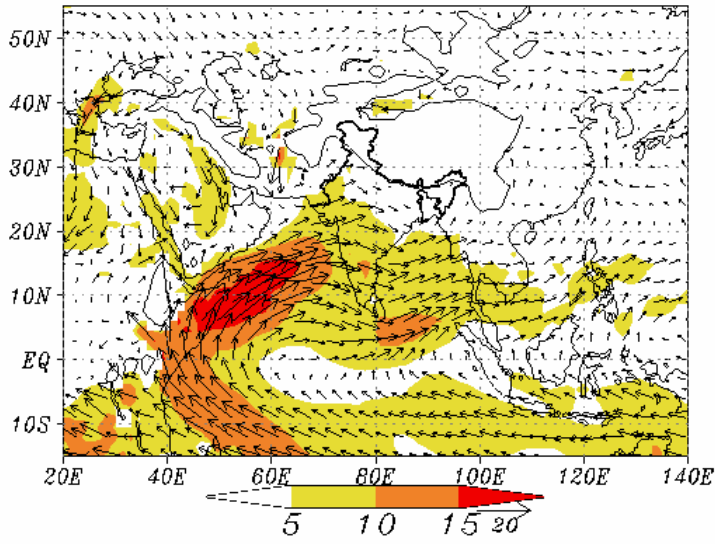


Fig. 8

MEAN ANALYSIS 850hPa WINDS AUG 2009



ANOMALY 850hPa WINDS AUG 2009

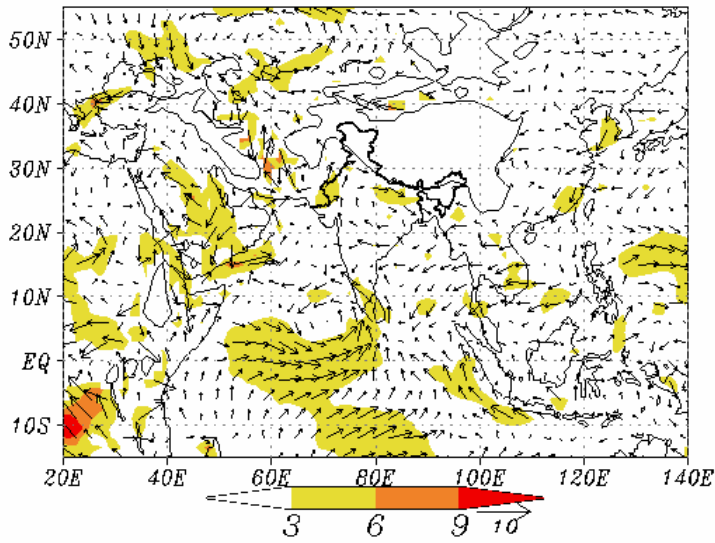
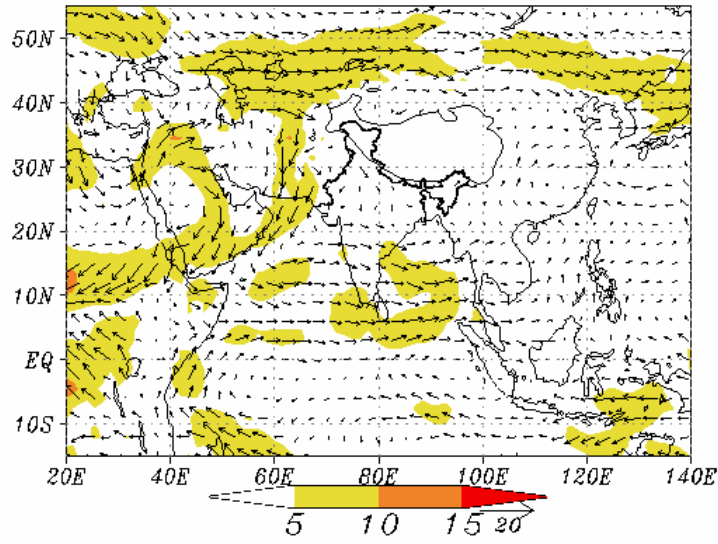


Fig. 9

MEAN ANALYSIS 700hPa WINDS AUG 2009



ANOMALY 700hPa WINDS AUG 2009

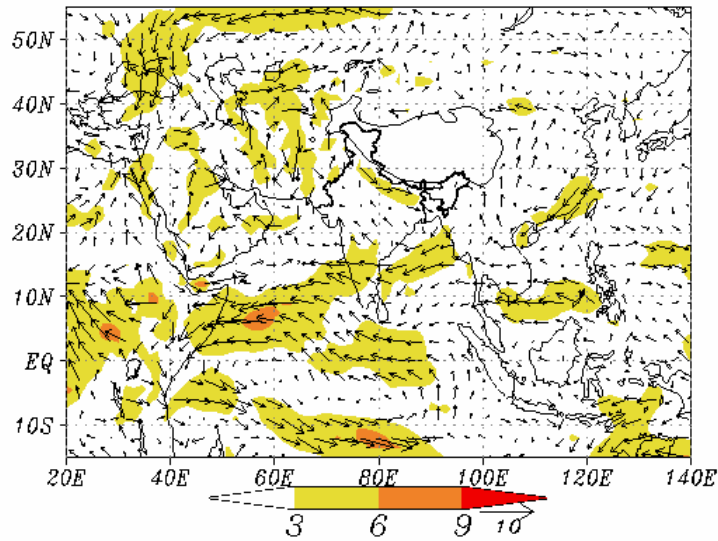
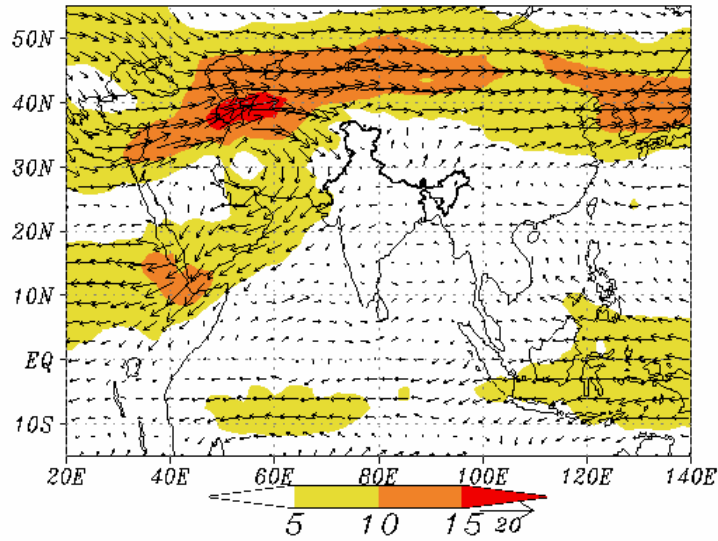


Fig. 10

MEAN ANALYSIS 500hPa WINDS AUG 2009



ANOMALY 500hPa WINDS AUG 2009

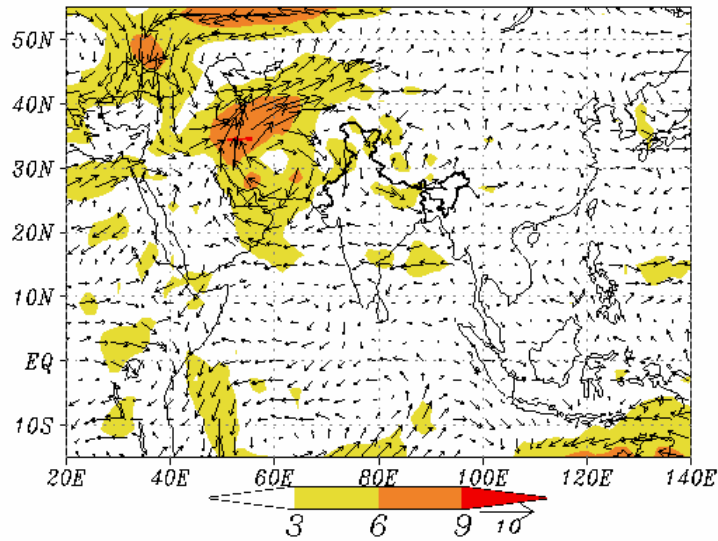
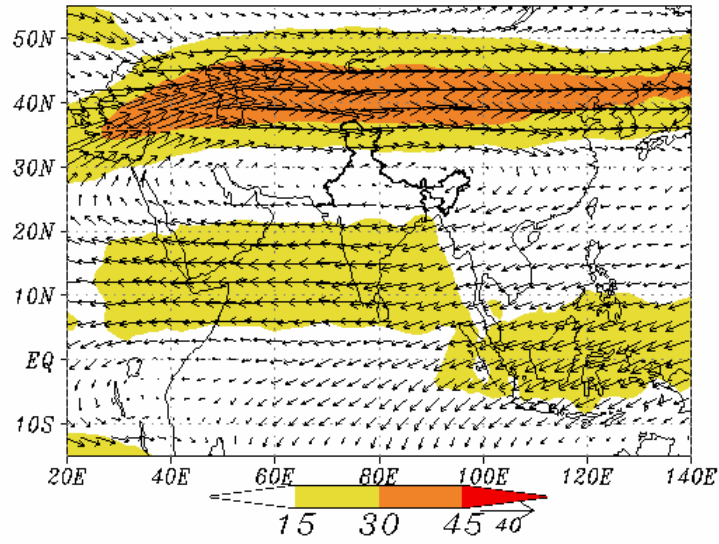


Fig. 11

MEAN ANALYSIS 200hPa WINDS AUG 2009



ANOMALY 200hPa WINDS AUG 2009

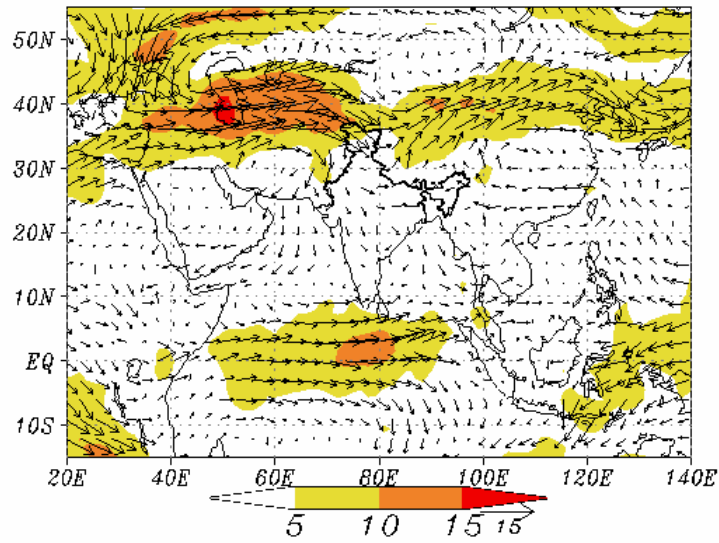
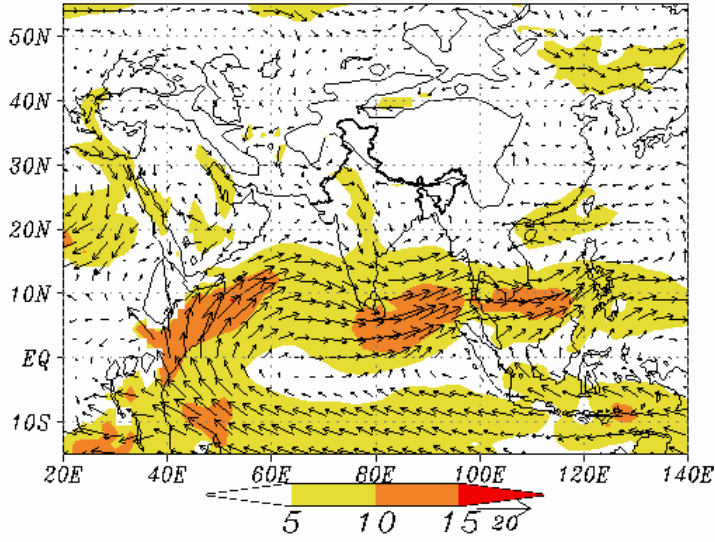


Fig. 12

MEAN ANALYSIS 850hPa WINDS SEP 2009



ANOMALY 850hPa WINDS SEP 2009

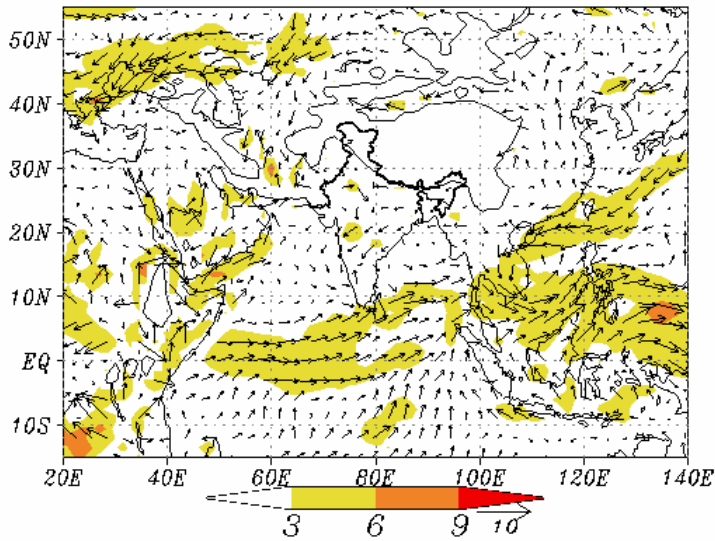
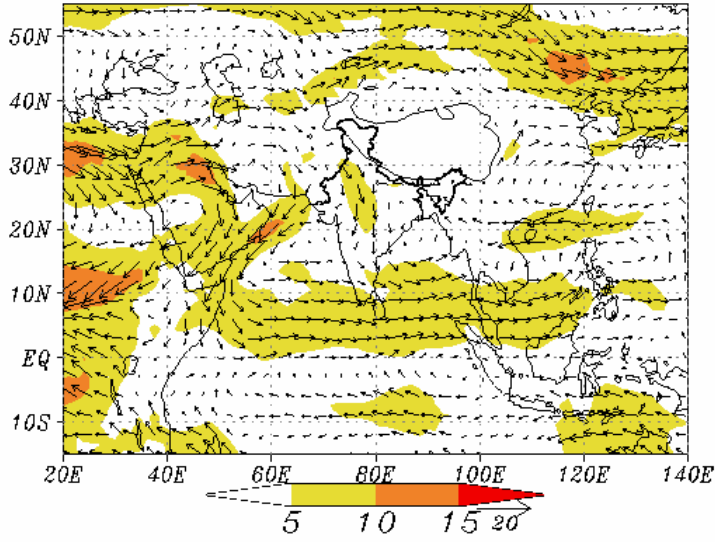


Fig. 13

MEAN ANALYSIS 700hPa WINDS SEP 2009



ANOMALY 700hPa WINDS SEP 2009

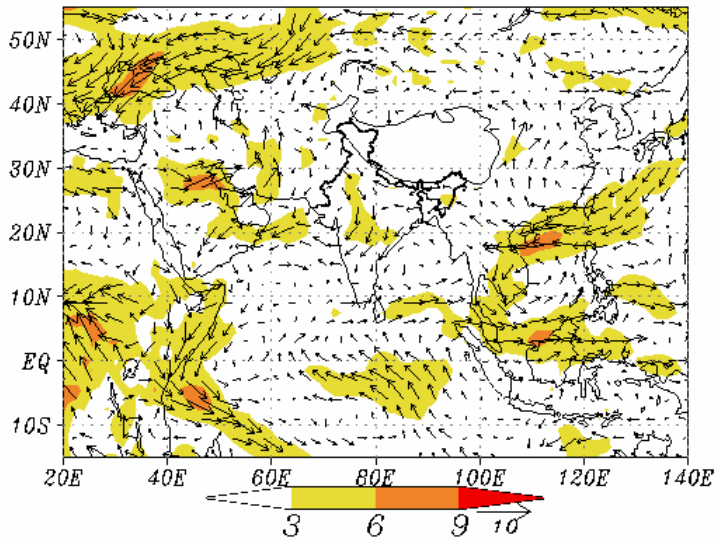
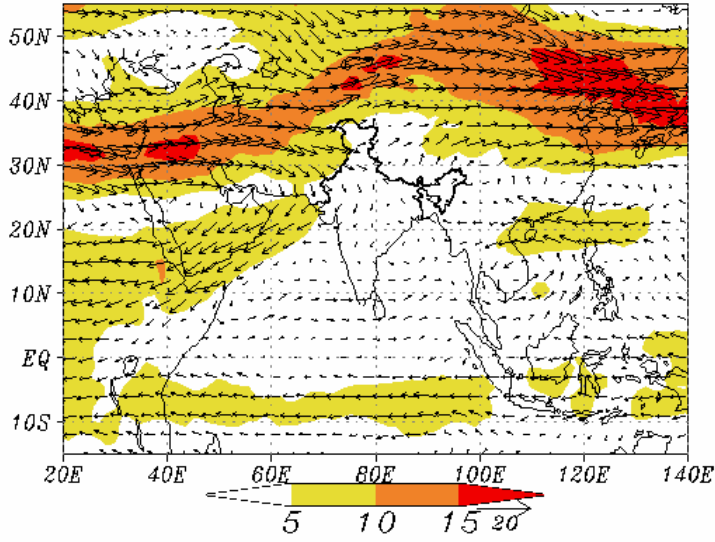


Fig. 14

MEAN ANALYSIS 500hPa WINDS SEP 2009



ANOMALY 500hPa WINDS SEP 2009

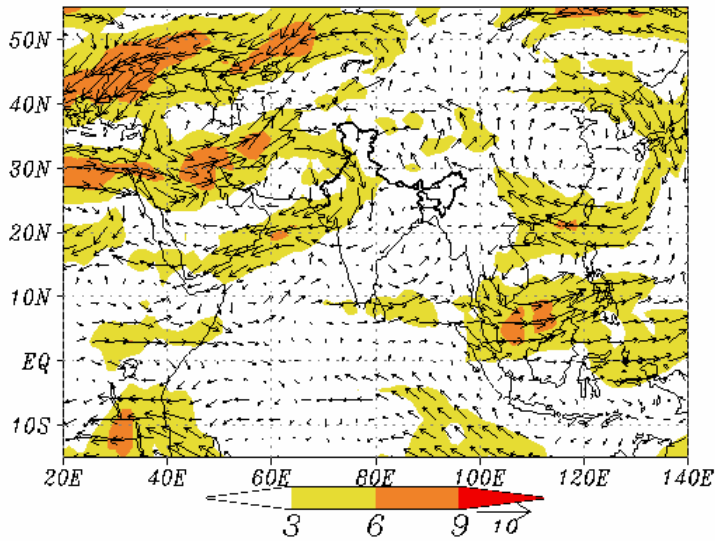
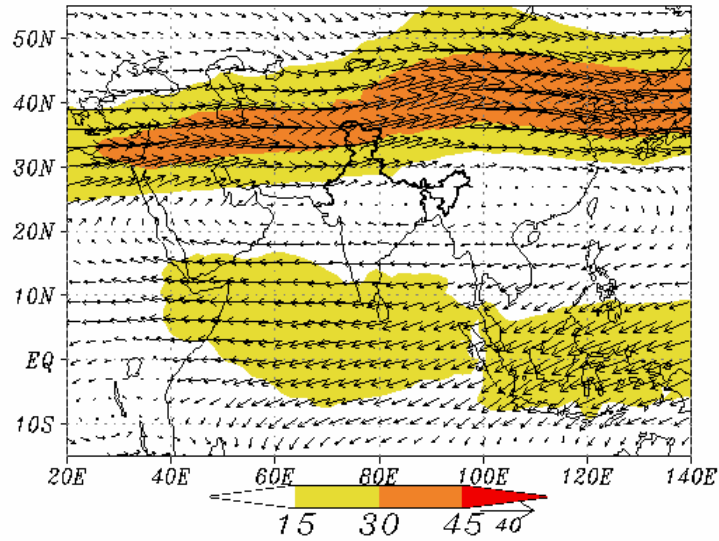


Fig. 15

MEAN ANALYSIS 200hPa WINDS SEP 2009



ANOMALY 200hPa WINDS SEP 2009

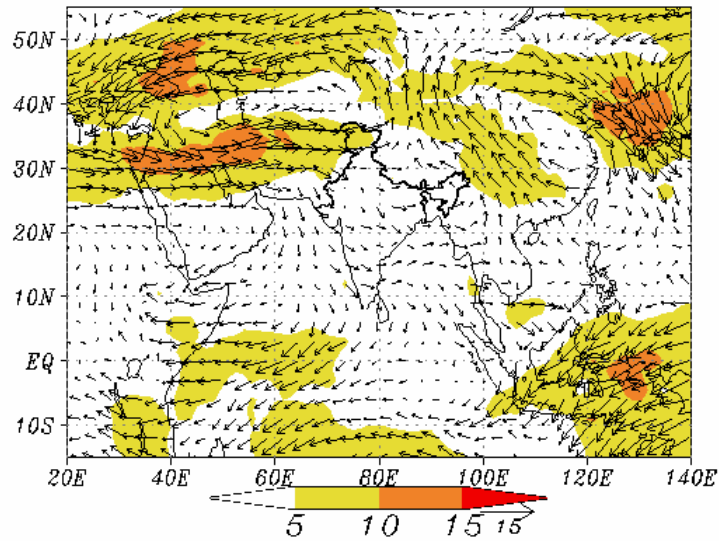


Fig. 16

Systematic Errors in the Medium Range Prediction of the Summer Monsoon

G. R. Iyengar

1 Introduction

The nature and distribution of systematic errors seen in the NCMRWF global T254 model forecasts are discussed in this chapter using the seasonal (June-September) means of analyses and medium range (Day-1 through Day-5) forecasts.

2 Circulation Features:

Geographical distribution of the mean analysed wind field and the systematic forecast errors for the T254 model at 850hPa, 700hPa, 500hPa and 200hPa are shown in figures 1(a-d) - 4(a-d) respectively. The notable features seen in the systematic errors of the 850hPa flow pattern are the anomalous easterlies over eastern & central parts of India. This feature is also seen at 700 and 500hPa levels. An anomalous cyclonic circulation is also seen over the north-west parts of India and adjoining Pakistan at 850hPa level. The incursion of dry air could be reason for the scanty rainfall observed in the model forecasts over the northwest parts of India. An anomalous cyclonic circulation is also seen over the extreme southern peninsula and adjoining Arabian Sea. At 700 and 500hPa levels, a broad east-west anomalous cyclonic circulation is seen over the peninsula and adjoining oceanic areas. At 200hPa, the most significant feature in the systematic errors is the weakening of the Tropical Easterly Jet.

The strong cross-equatorial low level jet stream with its core around 850 hPa is found to have large intraseasonal variability. Figure 5 shows the Hovmoller diagram of zonal wind (U) of 850 hPa averaged over the longitude band 60–70E and smoothed by a 5-day moving average for the period 1 June–30 September 2009. The top panel shows the analysis and the middle and the lower panel depict the day-3 and day-5 forecasts respectively. The active monsoon spells are characterized by strong cores of zonal wind. The monsoon set in over Kerala on 23 May. There was a prolonged hiatus in the advancement of monsoon during 8-24 June. As seen from the analysis panel the zonal

wind flow was quite weak in the month of June. The low level westerly flow picked up strength with a core of zonal wind of about 20 ms^{-1} in the first week of July and remained so till the end of the month. This was followed by a spell of weak core of zonal wind for a period of two weeks. Another spell of strong core of zonal wind of about 15 ms^{-1} was seen in the first week of September. The day-3 and day-5 forecasts agree reasonably well with the analyses and are able to depict the active and weak spells of the monsoon flow. However the wind strength is weaker during the active spell in the day 5 forecasts.

Figure 6 shows the Hovmoller diagram of zonal wind (U) of 850 hPa averaged over the longitude band 75–80E and smoothed by a 5-day moving average for the period 1 June–30 September 2009. The top panel shows the analyses and the middle and the lower panel depict the day-3 and day-5 forecasts respectively. The analyses show the northward movement of the core of zonal wind during the fourth week of June to the third week of July. Another weak spell is seen from the fourth week of August to the second week of September. The day-3 forecasts compare well with the analyses. However the day 5 forecasts are not able depict the northward movement of the core of zonal wind.

3 Temperature:

Geographical distribution of the mean systematic forecast temperature errors for the T254 model at 850hPa and 200hPa level are shown in figures 7(a-d) and 8(a-d) respectively. The T254 model forecasts also show a warm bias in the lower troposphere over the northwest parts of India, and a cold bias over the peninsular India and adjoining Bay of Bengal. In the upper troposphere, the T254 model also shows a cold bias over the northern parts of India and a warm bias over the central & peninsular India. Fig. 9(a-d) shows the geographical distribution of the mean systematic forecast humidity errors for the T254 model at 850hPa level. The T254 model forecasts show a dry bias over the entire country.

4 Verification of wind and temperature forecasts:

Objective verification scores against the analysis and observations are computed every day valid for 00UTC at standard pressure levels for different areas as recommended by the WMO. Monthly averages are then computed from the daily values of all forecasts verifying within the relevant month.

Figure 10 shows the rmse of winds for the NCMRWF operational model day 03 forecasts against the radiosonde observations over the Indian region since January 1999. The errors of the T254 model during May and June 2009 were more as compared to that in 2008. However the errors decreased in July, August and September 2009 and were less as compared to that in 2008.

Figures 11 (a-d) and 12 (a-d) show the rmse of winds for the T254, NCEP, UKMO and ECMWF model forecasts against the radiosonde observations over the Asian region (25° - 65° N & 60° -145° E) for June, July, August and September 2009 at 850 & 200hPa levels respectively. These figures show that ECMWF model forecasts have the least rmse among the four models.

Legends for figures:

Figure 1. Mean T254 analysed wind field (a) and systematic forecast errors for Day-1 (b), Day-3 (c) and Day-5 (d) at 850 hPa. [Units: m/s, Contour interval: 5m/s for analyses and 2m/s for forecast errors]

Figure 2. Mean T254 analysed wind field (a) and systematic forecast errors for Day-1 (b), Day-3 (c) and Day-5 (d) at 700 hPa. . [Units: m/s, Contour interval: 10m/s for analyses and 5m/s for forecast errors]

Figure 3. Mean T254 analysed wind field (a) and systematic forecast errors for Day-1 (b), Day-3 (c) and Day-5 (d) at 500 hPa. [Units: m/s, Contour interval: 5m/s for analyses and 2m/s for forecast errors]

Figure 4. Mean T254 analysed wind field (a) and systematic forecast errors for Day-1 (b), Day-3 (c) and Day-5 (d) at 200 hPa. . [Units: m/s, Contour interval: 10m/s for analyses and 5m/s for forecast errors]

Figure 5. Hovmoller diagram of zonal wind (U) of 850 hPa averaged over the longitude band 60–70E and smoothed by a 5-day moving average for the period 1 June–30 September 2009.

Figure 6. Hovmoller diagram of zonal wind (U) of 850 hPa averaged over the longitude band 75–80E and smoothed by a 5-day moving average for the period 1 June–30 September 2009.

Figure 7. Mean T254 analysed temperature field (a) and systematic forecast errors for Day-1 (b), Day-3(c) and Day-5 (d) of temperature at 850 hPa.: [Units: K, Contour interval: 2 K for analyses and 1 K for forecast errors]

Figure 8. Mean T254 analysed temperature field (a) and systematic forecast errors for Day-1 (b), Day-3(c) and Day-5 (d) of temperature at 200 hPa.: [Units: K, Contour interval: 2 K for analyses and 1 K for forecast errors]

Figure 9. Mean T254 analysed specific humidity field (a) and systematic forecast errors for Day-1 (b), Day-3(c) and Day-5 (d) of specific humidity at 850 hPa.: [Units: gm/kg, Contour interval: 2 for analyses and 1 for forecast errors]

Figure 10. RMSE of wind (m/s) against the radiosonde observations for the NCMRWF operational model forecasts at 850hPa level over the India region The blue line corresponds to T80L18 model and the red line corresponds to the T254L64 model.

Figure 11. RMSE of wind (m/s) against the radiosonde observations for the T254 , UKMO, NCEP and ECMWF model forecasts at 850hPa level over the Asian region for June(a), July(b), August(c) and September(d)

Figure 12. RMSE of wind (m/s) against the radiosonde observations for the T254 , UKMO, NCEP and ECMWF model forecasts at 200hPa level over the Asian region for June(a), July(b), August(c) and September(d)

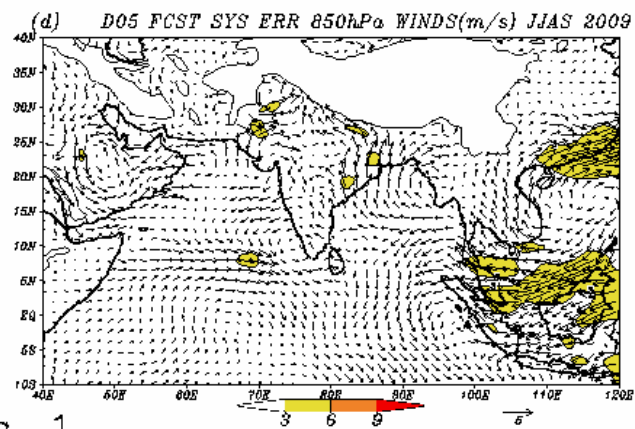
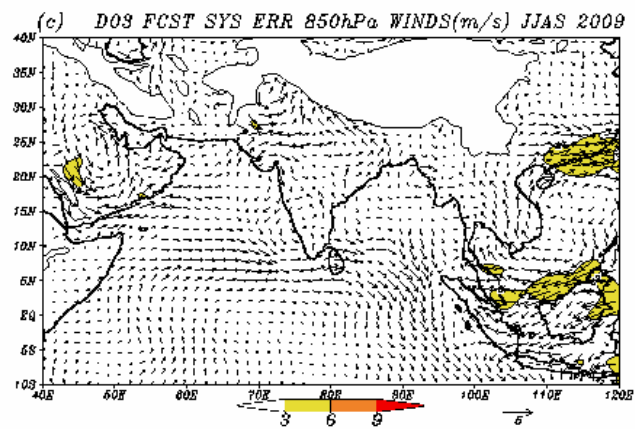
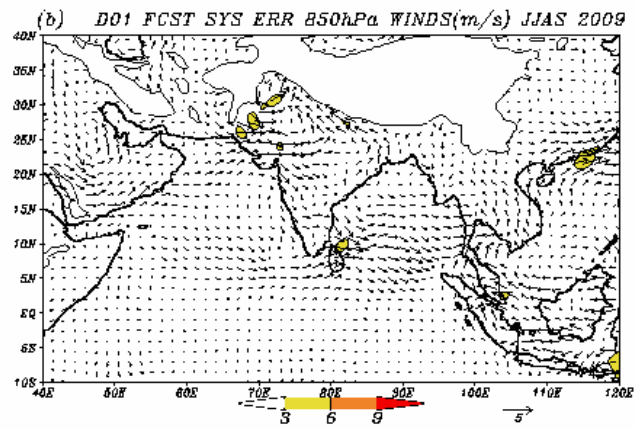
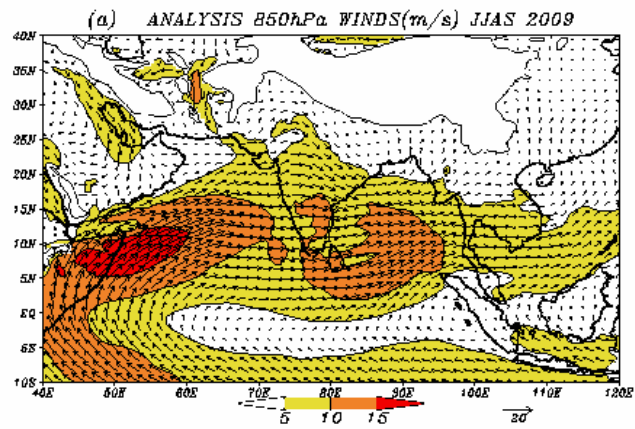


Fig. 1

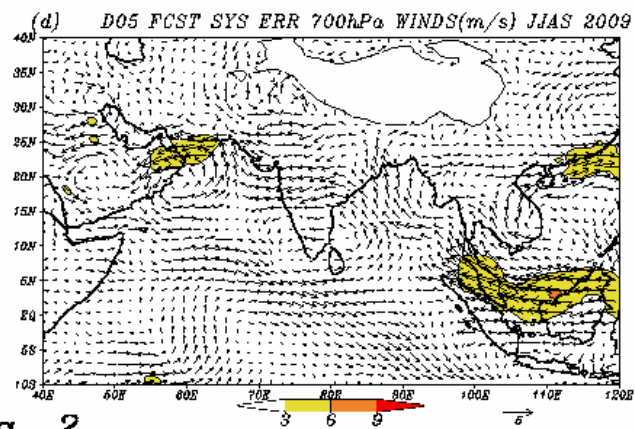
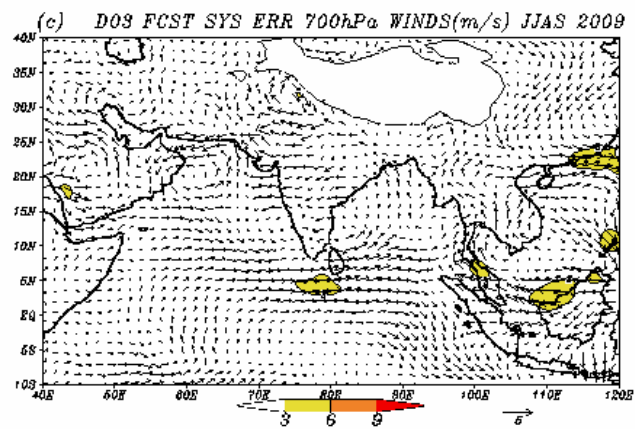
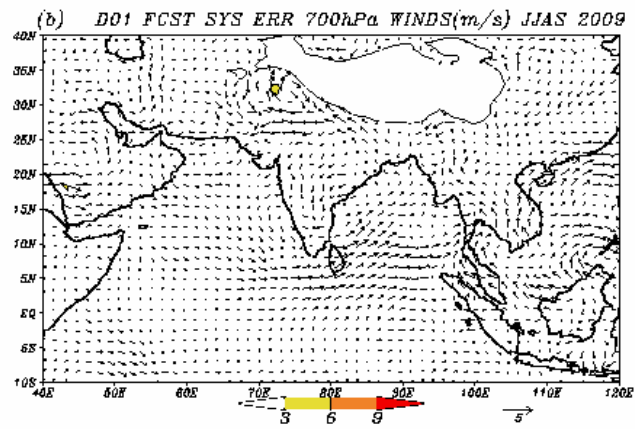
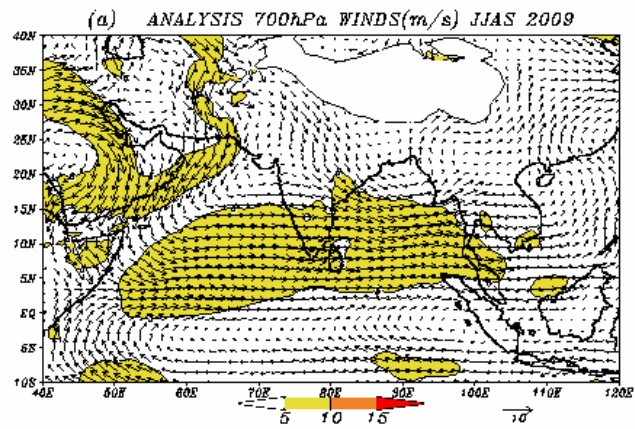


Fig. 2

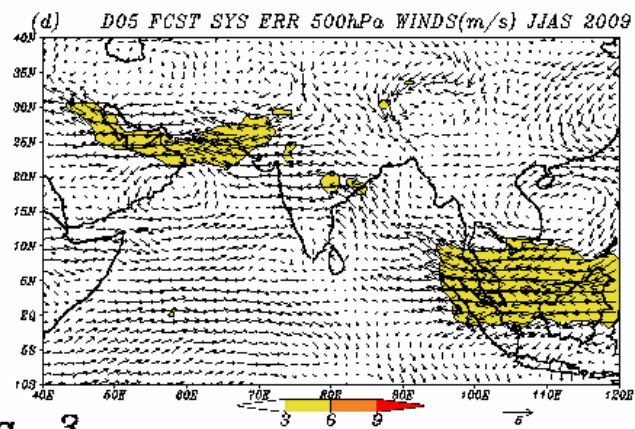
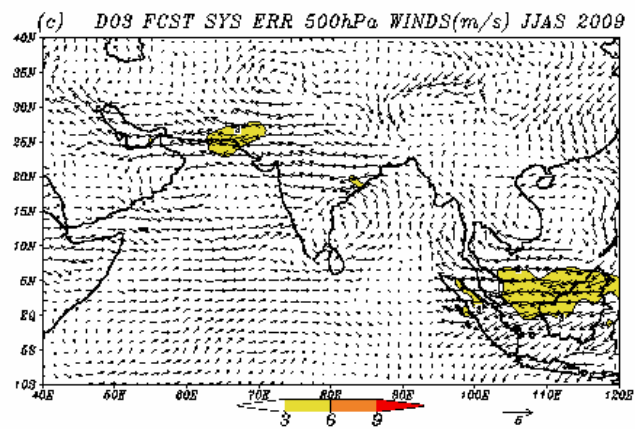
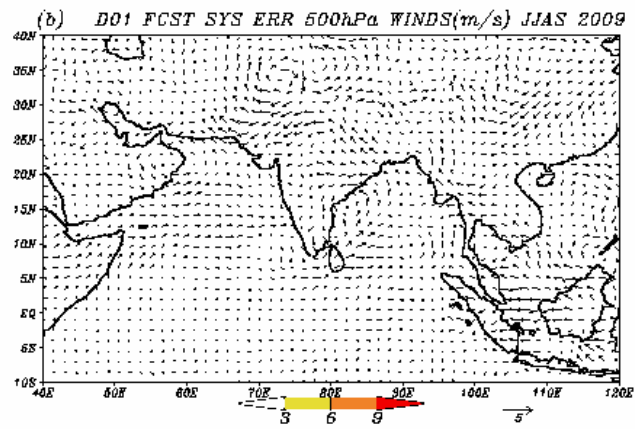
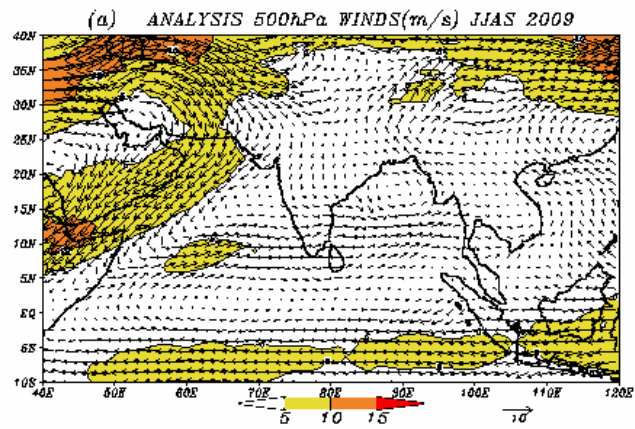


Fig. 3

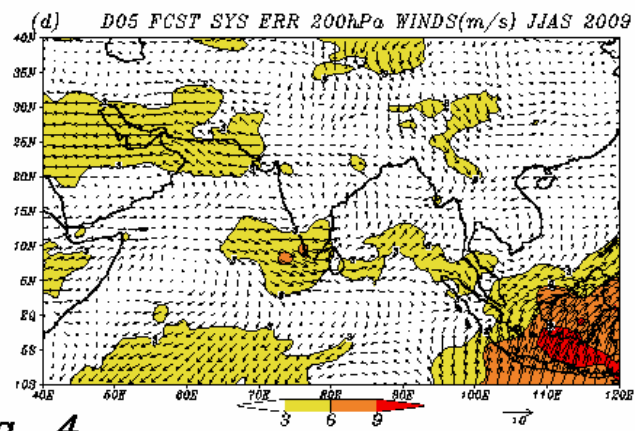
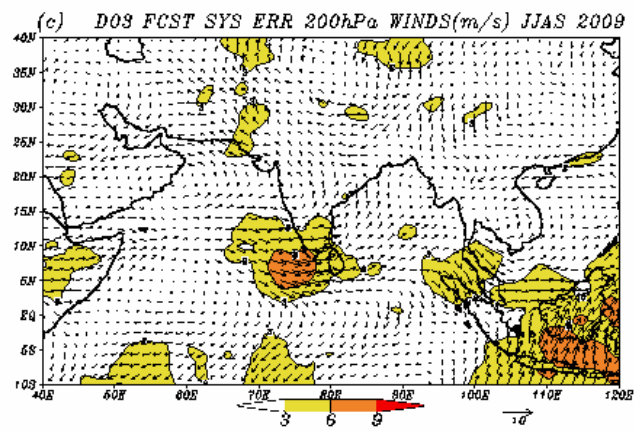
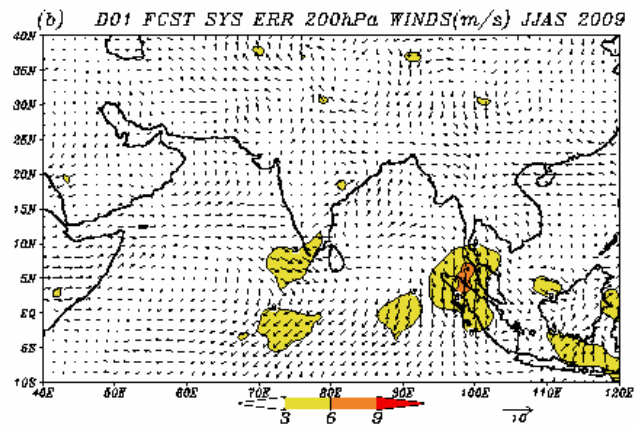
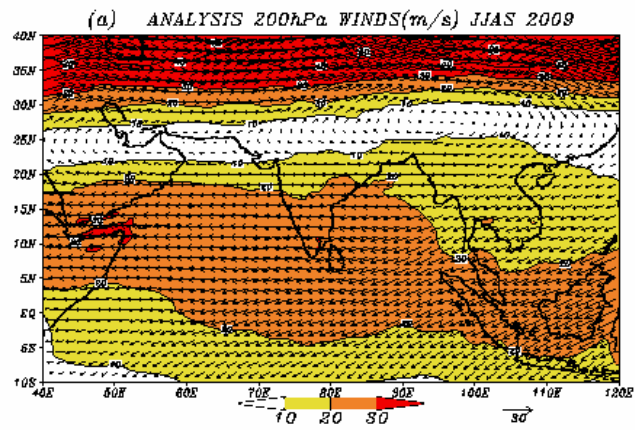


Fig. 4

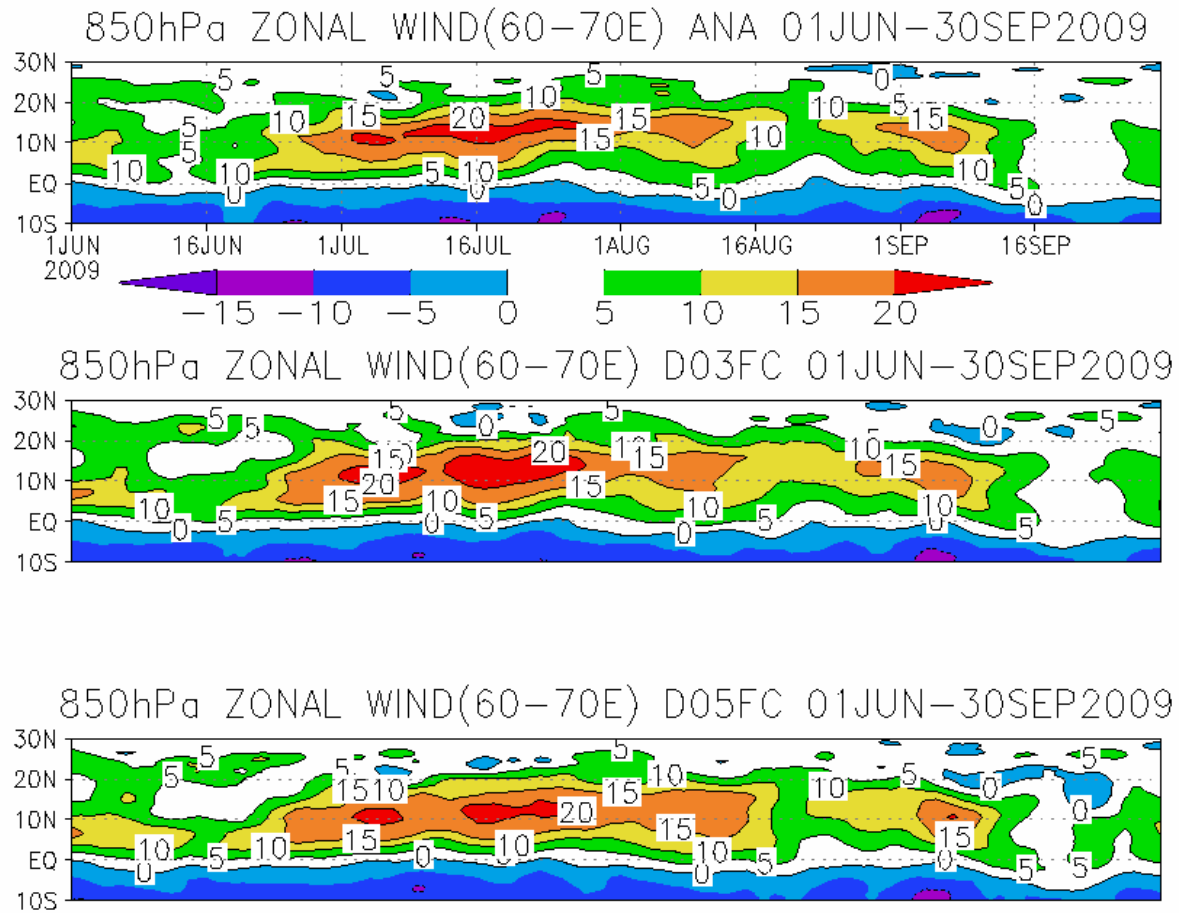


Fig. 5

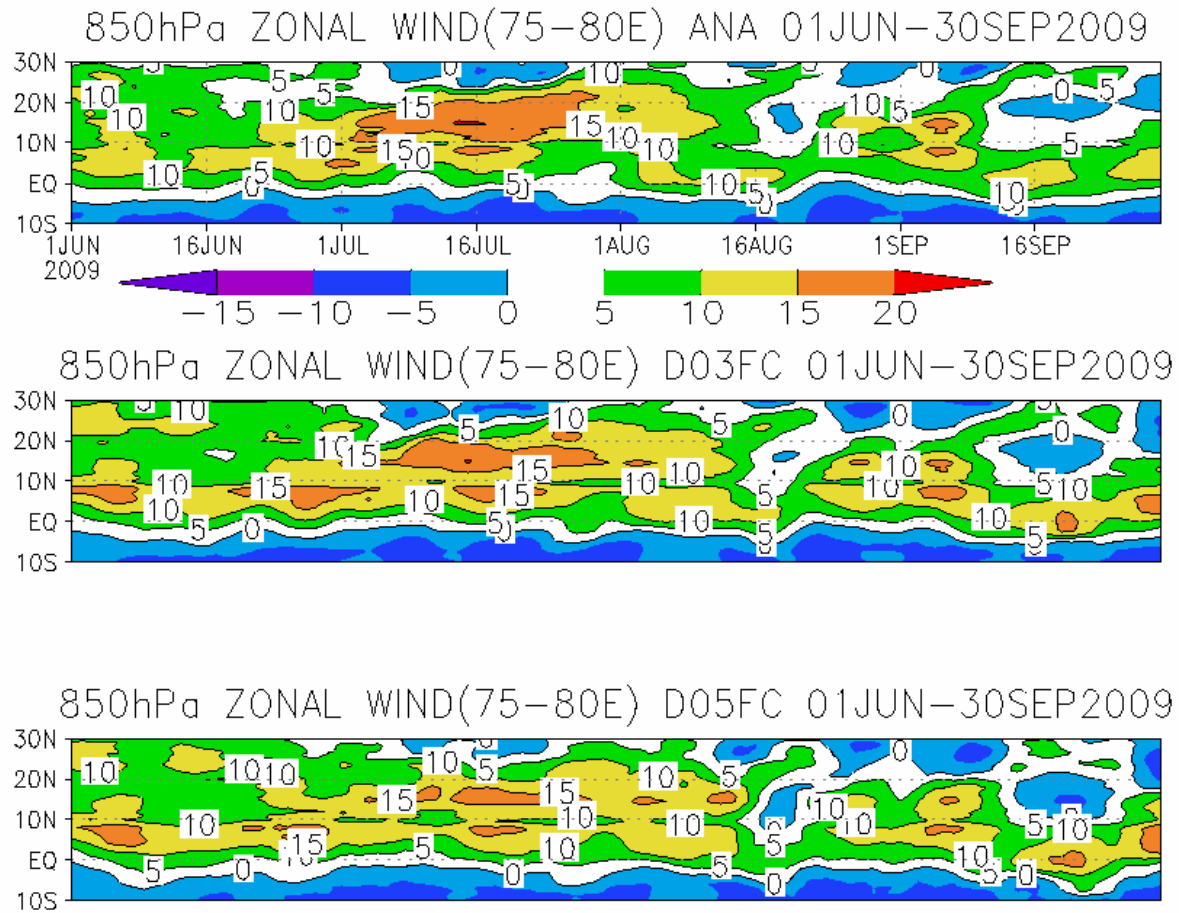
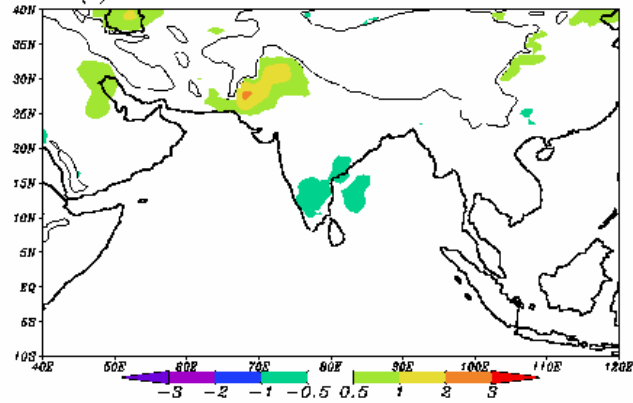
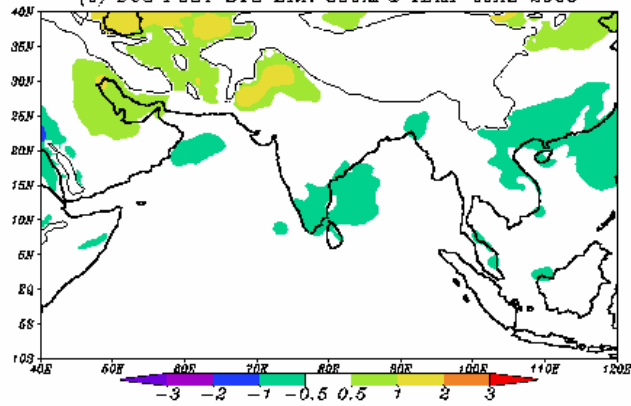


Fig. 6

(b) D01 FCST SYS ERR 850hPa TEMP JJAS 2009



(c) D03 FCST SYS ERR 850hPa TEMP JJAS 2009



(d) D05 FCST SYS ERR 850hPa TEMP JJAS 2009

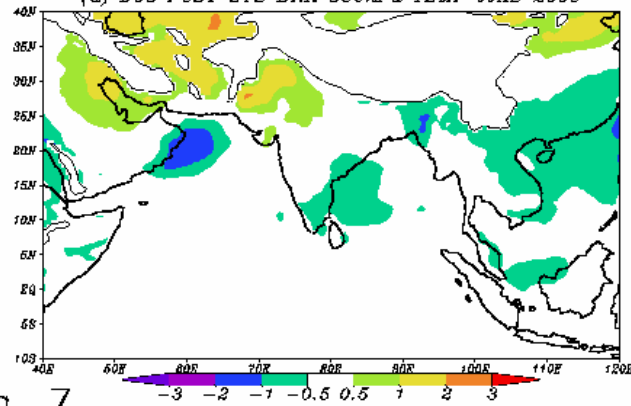
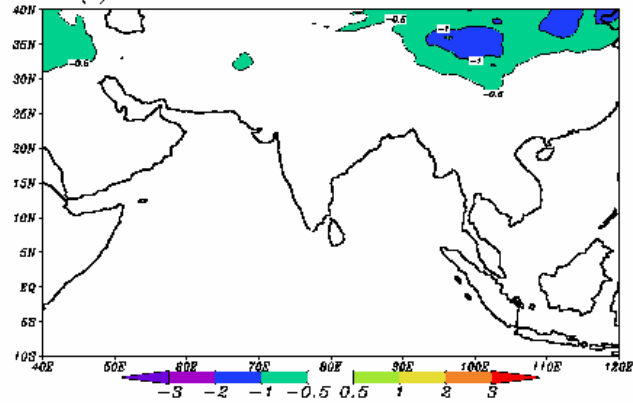
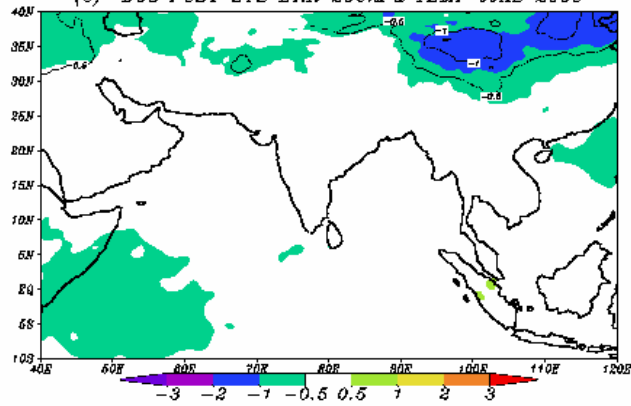


Fig. 7

(b) D01 FCST SYS ERR 200hPa TEMP JJAS 2009



(c) D03 FCST SYS ERR 200hPa TEMP JJAS 2009



(d) D05 FCST SYS ERR 200hPa TEMP JJAS 2009

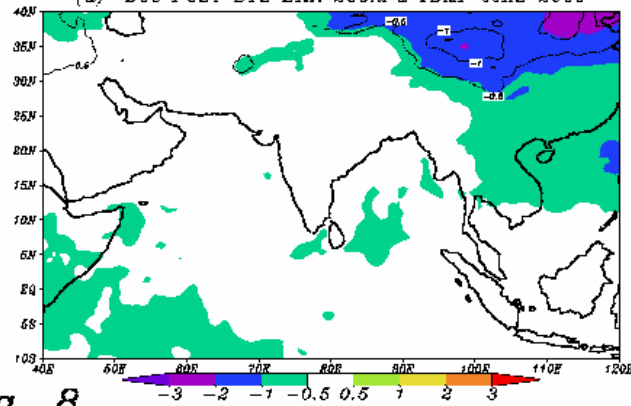
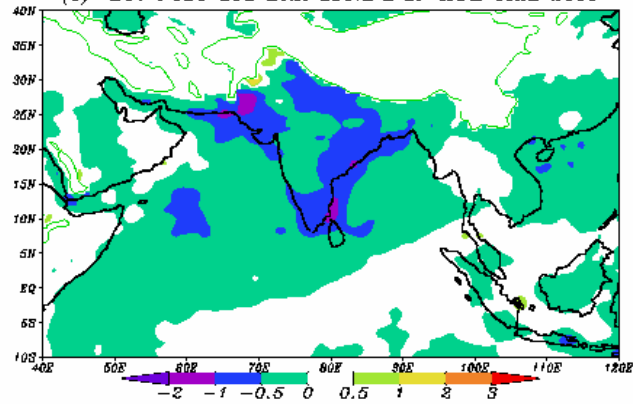
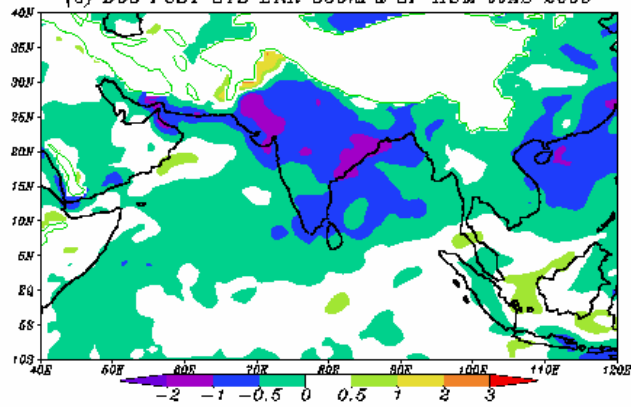


Fig. 8

(b) D01 FCST SYS ERR 850hPa SP HUM JJAS 2009



(c) D03 FCST SYS ERR 850hPa SP HUM JJAS 2009



(d) D05 FCST SYS ERR 850hPa SP HUM JJAS 2009

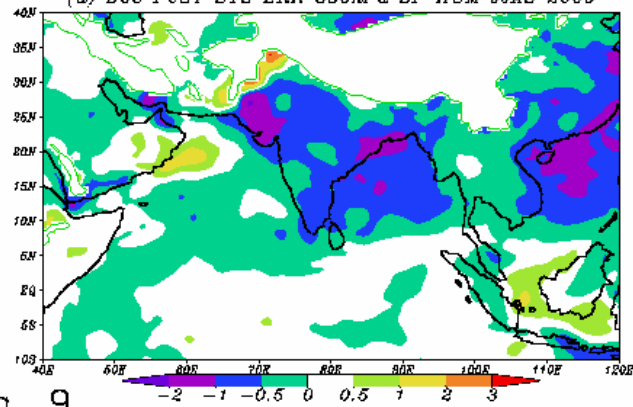


Fig. 9

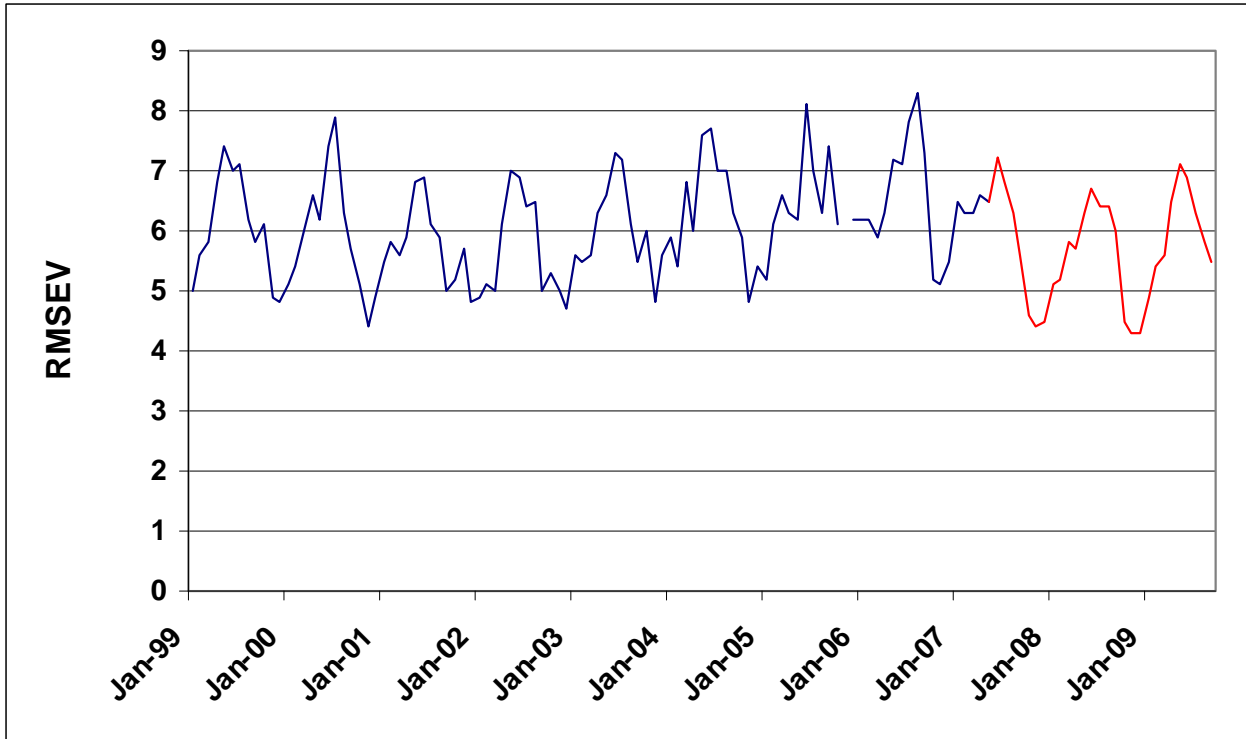


Figure 10

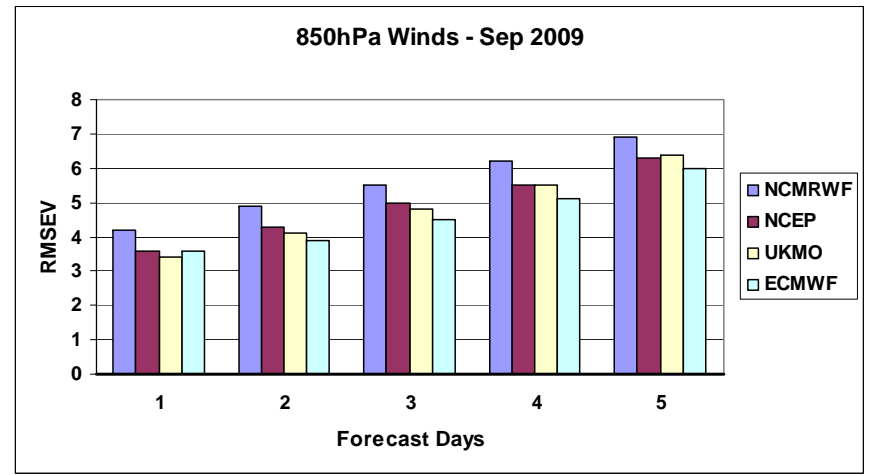
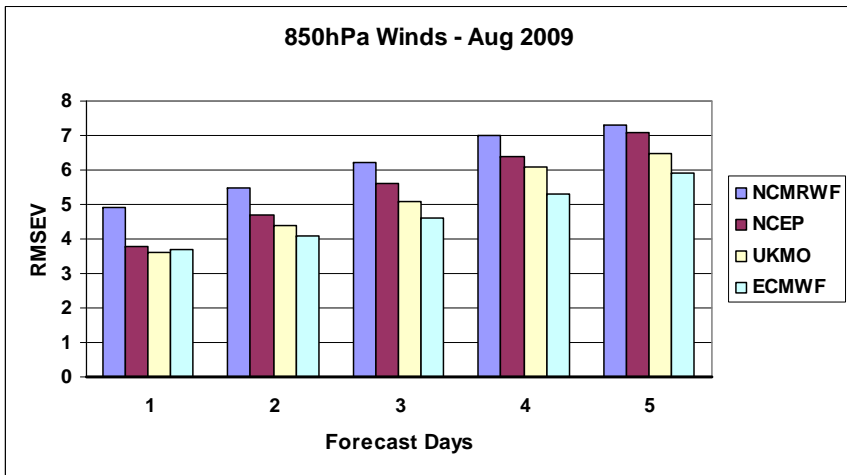
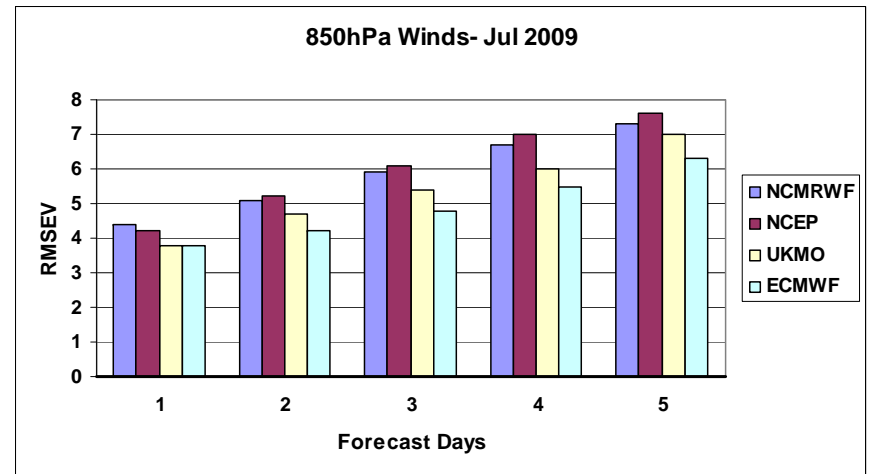
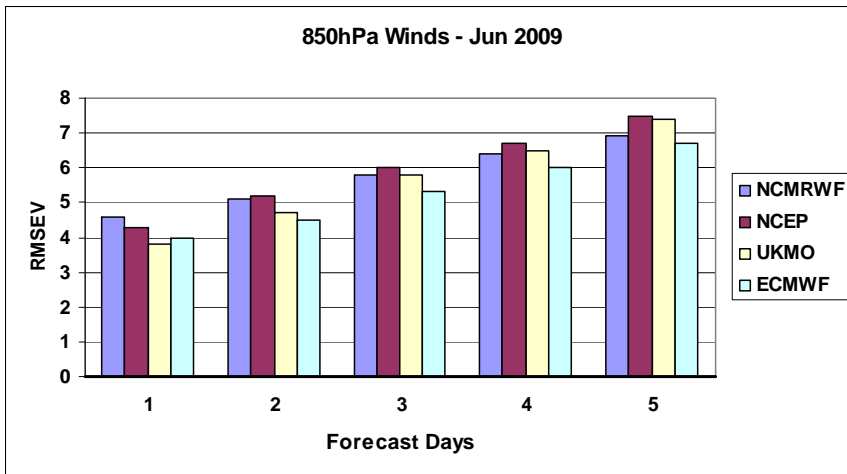


Figure 11

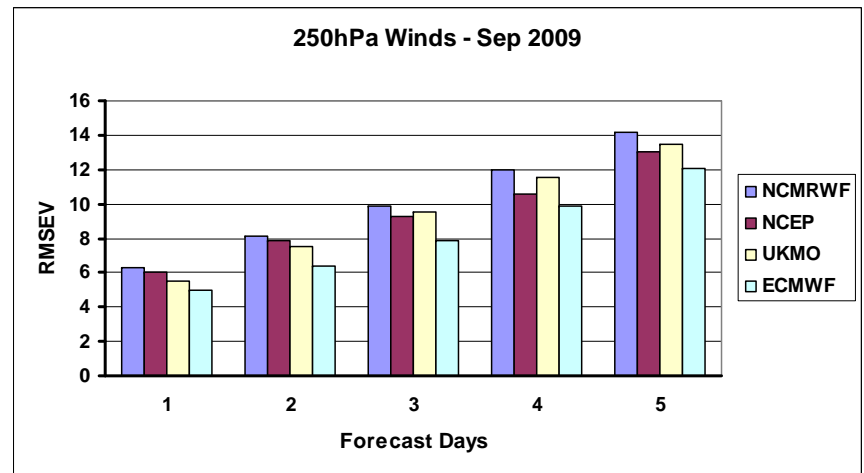
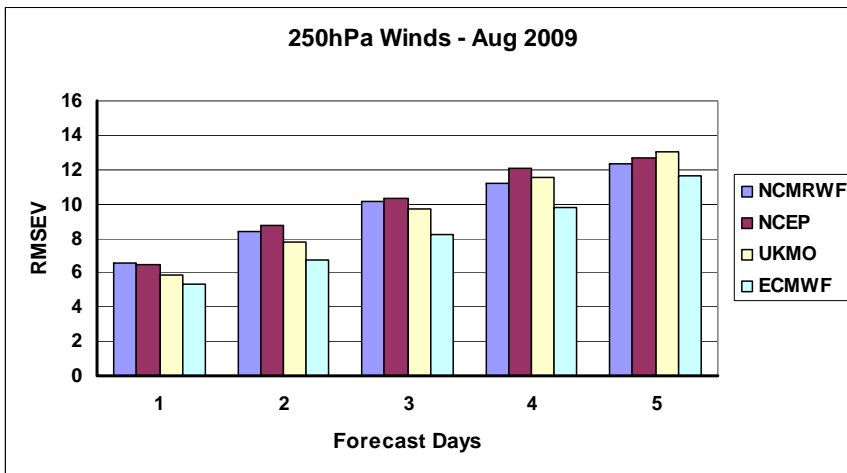
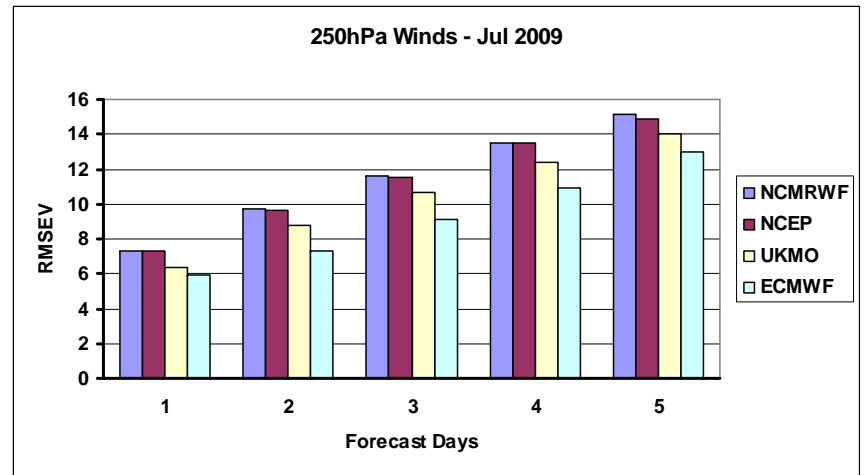
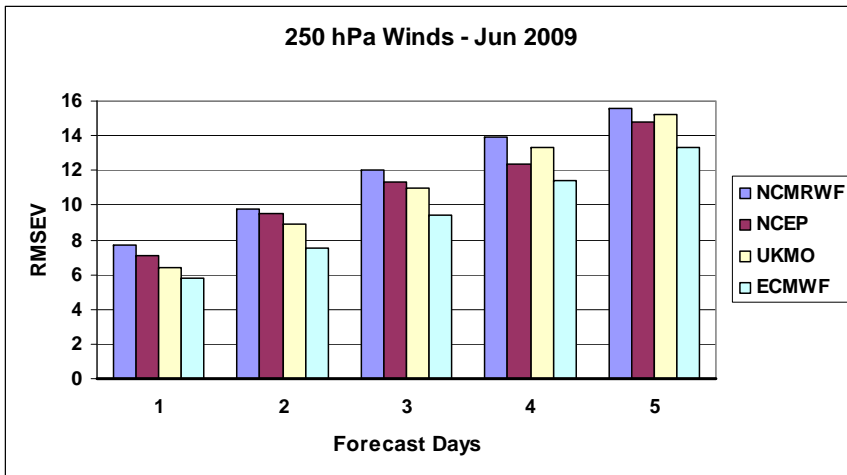


Figure 12

Verification of Model Rainfall Forecasts

A. K. Mitra, G. R. Iyengar, R. G. Ashrit and Saji Mohandas

In this section the performance of rainfall prediction from the global T254L64 high resolution modeling system are discussed. Monsoon 2009 was an anomalous one, where the rainfall during the season was well below normal. It was a drought year. There were many days during the season, when there was no rainfall activity. Therefore, examining the model rainfall forecast in this typical season will be of interest, and the model performance might be different compared to a normal year like 2008. Here, for model verification purpose, mostly the reference observed rain is the daily gridded merged satellite (meteosat-7) and rain-gauge data for the Indian region. These daily observed rainfall are past 24 hours accumulated rainfall valid at 03 UTC. The model forecast values used here are also valid at 03 UTC. For the all India rainfall (AIR) comparisons the AIR values provided by IMD are used. Panels in figure 1 shows the seasonal total rainfall amounts from observations and model forecasts. Broadly it shows that the model is able to represent the large-scale monsoon rain spatial pattern reasonably well. However, on closer examination we see different amounts in observations and the model predictions. For example, in the monsoon trough region, the model forecasts are showing higher rainfall for day-1. And for day-3 and day-5 amounts and regions of maximum rainfall in monsoon trough zone are closer to observations. The differences of forecasts (day-1, day-3 and day-5) minus the observations for the season are shown in figure 2, where the anomalies are seen more clearly. These mean seasonal anomalies are also called the mean error in forecasts from the model. Over central India day-1 has the maximum error, and by day-5 these errors reduce. Off Kerala coast, in the Arabian Sea, the positive biases (wet) increases from day-1 through day-5. And near the head Bay of Bengal region, the dry bias is seen to increase with time. Eastern side of the Bay of Bengal (Arakan coastal region) also shows significant biases.

Different threshold based skill scores for rainfall for the season is shown in figure 3 to figure 6. These calculations are based on collecting points above a certain intended rainfall threshold amount. We have considered six thresholds of 1 to 6 cm per day. Different skill scores like equitable threat score, hit rate and bias scores are computed from observed and model rainfall data. Equitable threat score (ETS) is a measure of relative accuracy of the forecasts including chance (expected number of randomly correct forecasts above a threshold) as a

parameter. ETS should vary between 0 to 1. Hit rate (HR) also known as success rate is the ratio of number of correctly forecasted points above a threshold to the number of forecasted points above that threshold. HR values are between 0 to 1. Bias score (BS) is the ratio of number of forecasted points above a threshold to the number of observation points above that threshold. If the BS is closer to 1, then it shows that the model rainfall forecast has less bias. Higher values (> 1) means positive (wet) bias, and lower values (< 1) indicated negative (dry) biases.

Figure 3 shows the threshold based skill scores for the central India region (73-90 E; 22-28 N). This region is representative of the region where the monsoon trough is generally seen. Most of the models have difficulty in representing this monsoon trough related features realistically. In ETS all scores are below 0.2, and only 1 cm threshold shows the highest score. Forecasts for thresholds of 3 cm and above have a poor score of 0.05 or less. The HR for all threshold and all days are below 0.4, showing the non-satisfactory performance. For threshold of 2 cm and above the scores become 0.2 or lesser. In BS for lower threshold (1 and 2 cm), forecasts show a slight positive bias (wetter). But for thresholds of 3 cm and above, the biases is very less for the central India region (particularly for day-1).

Figure 4 shows the threshold based skill scores for the peninsular India region (74-85 E; 7-21 N). The ETS falls rapidly with increasing thresholds. For threshold of 2 cm and above the ETS scores are seen to be 0.2 and lesser. For higher rainfall amounts ($> 4\text{cm}$) the scores become very low. The scores for HR also fall rapidly with increasing thresholds. The BS shows that the model has really higher positive (wet) biases for threshold of 4 cm and above for the peninsular India region.

Figure 5 shows the threshold based skill scores for the west coast region of India (70-78 E; 10-20 N). ETS are mostly lower than 0.15, for all thresholds and days. Beyond the thresholds of 3 cm and above, the ETS are around 0.1 and less. The HR also falls rapidly with increasing thresholds. For 3 cm and above thresholds the HR becomes 0.3 or lesser. For west coast also the BS shows a positive (wet) bias for heavier rainfalls ($> 4\text{ cm}$).

Figure 6 shows the performance for the All India region (67 - 100 E; 7 - 37 N). For each threshold the ETS decreases from day-1 to day-5 gradually. Only for 1 cm threshold and day-1 to day-3 we see the skill scores are above 0.2, and for rest of the thresholds and all, days the scores are all mostly below 0.2 indicating unsatisfactory skills. For threshold 4 cm and above the scores

become very low (0.1 and less), and by day-5 they all reach a low score of 0.05. The HR also falls rapidly with thresholds for different days. Only forecasts for 1 cm threshold looks good, and for heavier rainfall (> 2 cm) the scores are below 0.4 indicating poor performances by model. The BS indicates that for thresholds of 1 cm, 5 cm and 6 cm the model has some positive biases.

Apart from verifying the model's capability to forecast rainfall at different ranges, it is also important to know the model's capability to distinguish between rain and no-rain type of regions on a day. This yes/no forecast (irrespective of the rainfall amount) is also an important model diagnostics and also useful from forecasting point. To demonstrate the spatial distribution of yes/no rainfall forecast skill, two skill scores have been computed at each grid point from data of 122 days during monsoon 2009, (a)ETS and (b) Odd Ratio (ODR). These forecast skill are computed for prediction of rainy day (rainfall > 0.5 cm). Here ETS tells us how well the forecast "yes" events corresponded to the observed "yes" events (accounting for hits due to chance). This score ranges from $-1/3$ to 1. An ETS value of 0 indicates no skill and 1 meaning perfect score. But the minimum value depends on the verification sample climatology. For rare events, the minimum ETS value is near 0, while the absolute minimum is obtained if the event has a climatological frequency of 0.5, and there are no hits. If the score goes below 0 then the chance forecast is preferred to the actual forecast, and the forecast is said to be unskilled. The gray shading in the plots indicates no skill. As can be seen from figure 7, day-1 forecast feature small areas with no skill over Rajasthan, J&K, parts of NE India and isolated pockets over the peninsula. However, the areas of no skill spread with forecast lead time and in Day-5 forecasts feature relatively larger regions with no skill. The gray shaded region in the Day-5 forecast showing no skill along the west coast is of great interest. West coast of the peninsula features high number of rainy days and the Day-5 forecasts have no skill in predicting the rainy days. Over Gujarat and Madhya Pradesh, the forecast skill is very high and persists in Day-3 and Day-5 forecasts. Similarly over Rajasthan and J&K and parts of NE India the forecast skill is same in Day-1, Day-3 and Day-5. Over Peninsula and central India the forecast skill is reasonable (ets > 0.2) in Day-1 and Day-3 and decreases in Day-5.

The Odd ratio (OR) gives the ratio of the odds of a "yes" forecast being correct, to the odds of a "yes" forecast being wrong. The OR ranges from 0 to infinity, with a score of 1 indicating no skill and the perfect score is infinity. It measures the ratio of the odds of making a hit to the odds of making a false alarm. This score considers prior probabilities. It gives better

scores for rarer events. It is less sensitive to hedging. This score is not to be used if any of the cells in the contingency table are equal to 0. The figure 8 shows the OR computed for the model forecasts. The area with shading in white indicate region with poor skill or no skill. As can be seen from figure 8 this area of no skill is increasing from Day-1, Day-3 and Day-5 forecasts. The dark blue shading over Gujarat in the Day-1 forecasts ($ODR > 30$) show that the odds of a 'yes' forecast being correct are 30 times greater than the odds of a 'yes' forecast being incorrect. The light blue shaded regions suggesting values of ODR over 5, 10 and 20 can be seen over most parts of India in the Day-1 forecast. It is confined to only western, northwestern India and small region over eastern peninsula in the Day-5 forecast.

The all India rainfall (AIR) variability from model (compared to observations) in time scales like daily, weekly, monthly and also in a season are useful model diagnostics, which depicts important aspects of the model skill to capture the monsoon over the Indian region in a broad sense. Several forecasters at IMD also seek (monitor) this AIR figures from the model to infer about the monsoon strength in medium range time-scale. In figures 9 and 10, the variability of AIR from observations and model are shown. It is seen that, there is a good correspondence between the observed and model in day-1 prediction and as the forecast lead time increases to day-3 and day-5, the resemblance reduces (Fig. 9). Panel (a) in figure 10 shows the comparison of model AIR for the whole season. The values are seen to be quite reasonable and close to the observations for day-3 and day-5 forecasts. However, day-1 forecasts show some over estimation (wetter). This is also seen (consistent) in all the monthly comparisons in panel (b) of figure 10. Just for reference, in these two panels (a) and (b), CLIM shows the observed long period averaged values (climatology) of AIR. Panel (c) in figure 10 shows the comparison of the weekly (7 days accumulated predicted rainfall) AIR from model and observations during monsoon 2009. These weekly forecasts are made from a single initial condition once a week. The trends in AIR rainfall (changes from one week to the next during the progression of season) from global model matches well with the observed trend. However, there are some biases in values during few weeks which are obvious and consistent with the skills examined in daily scores for all India region.

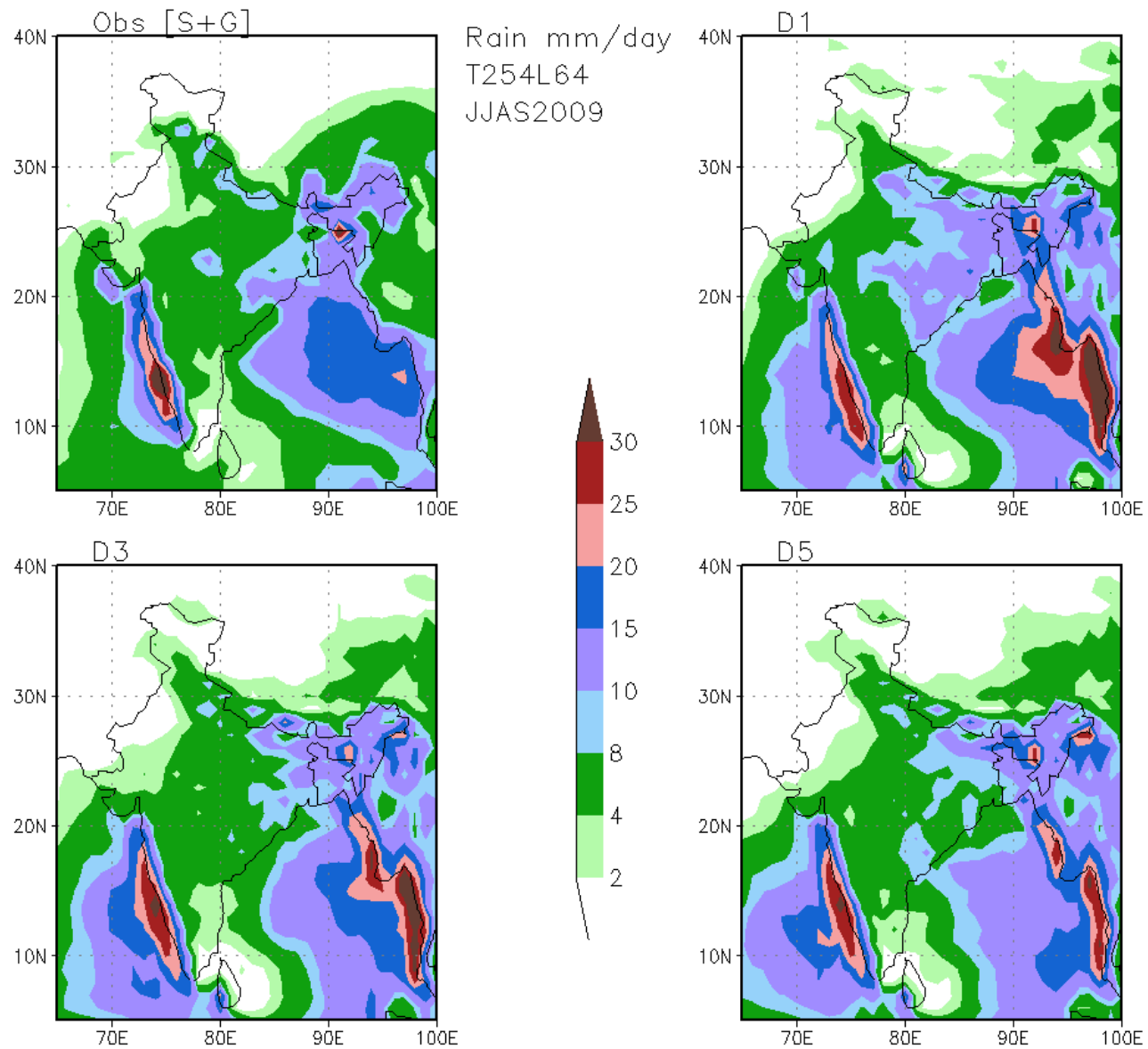


Fig. 1: Observed and day-1, day-3 and day-5 rainfall forecasts from the model for the 2009 monsoon season

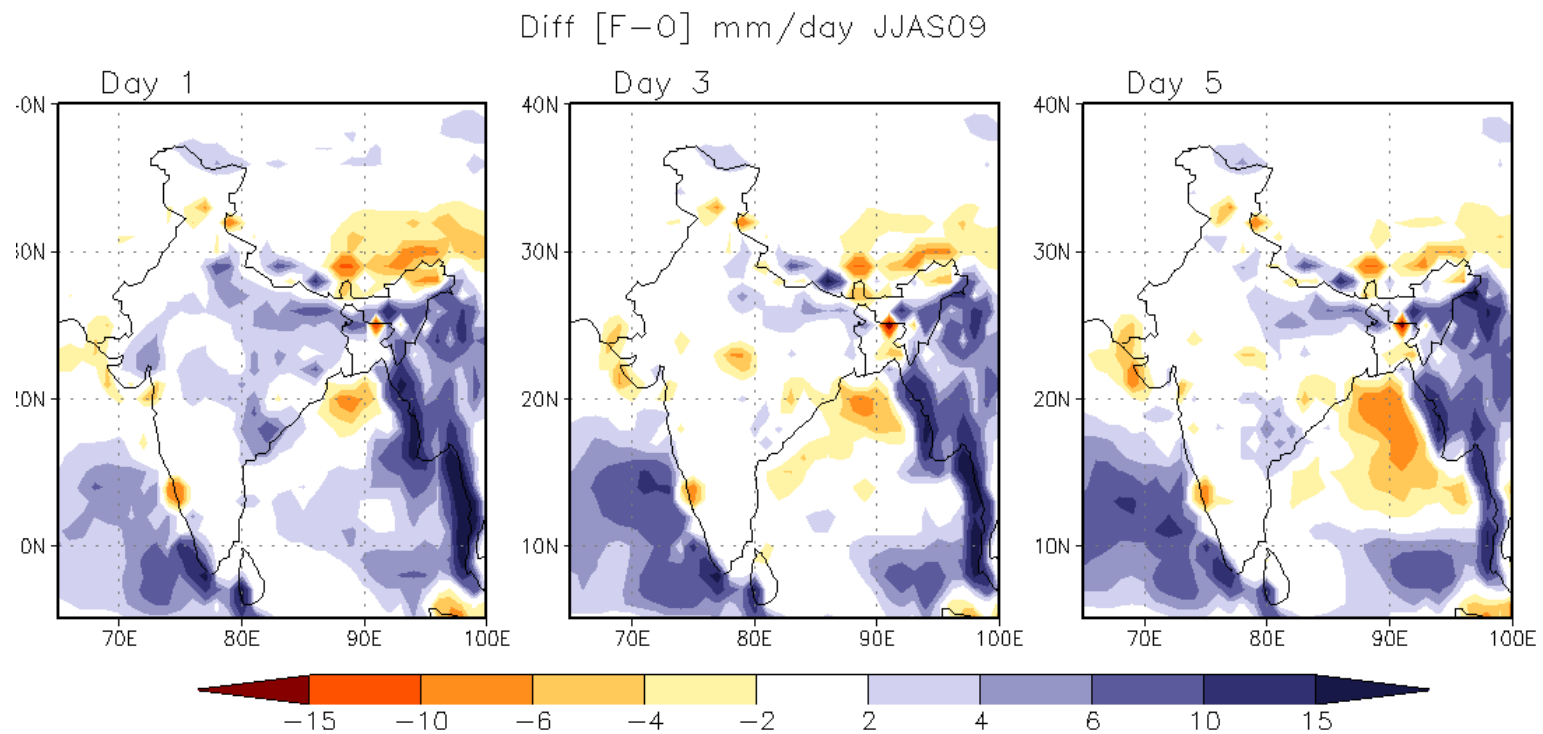


Fig. 2: Difference (Forecast - Observation) rainfall for day-1, day-3 and day-5 for the 2009 monsoon season

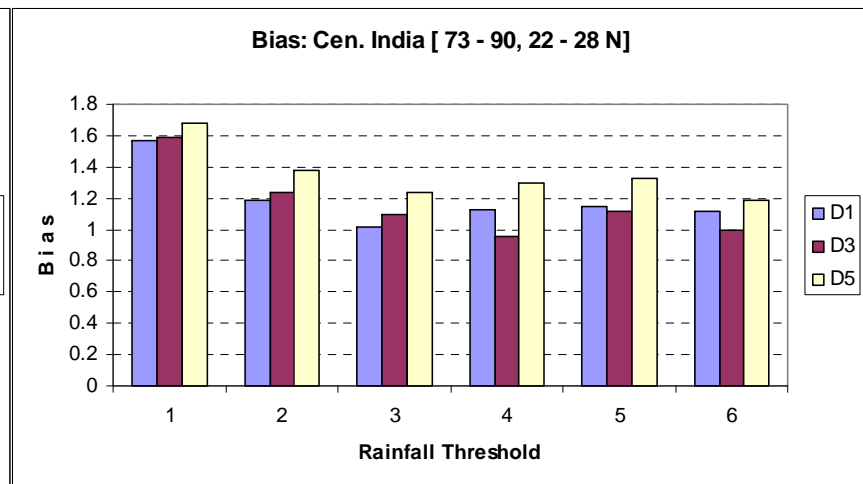
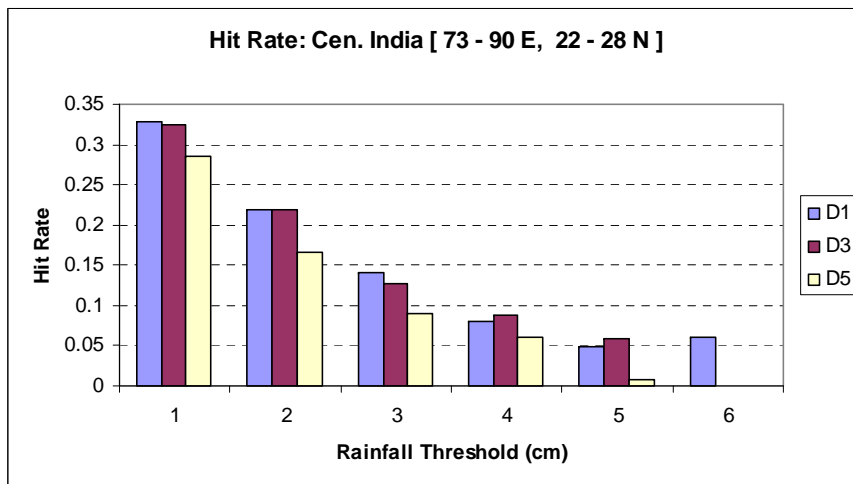
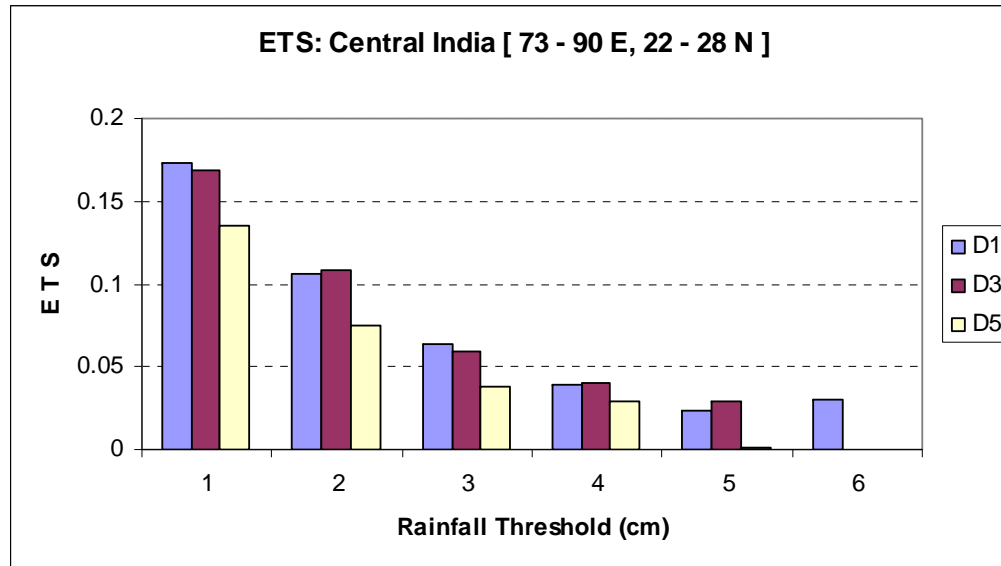


Fig. 3: Rainfall threshold based skill scores for Central India Region for the 2009 monsoon season

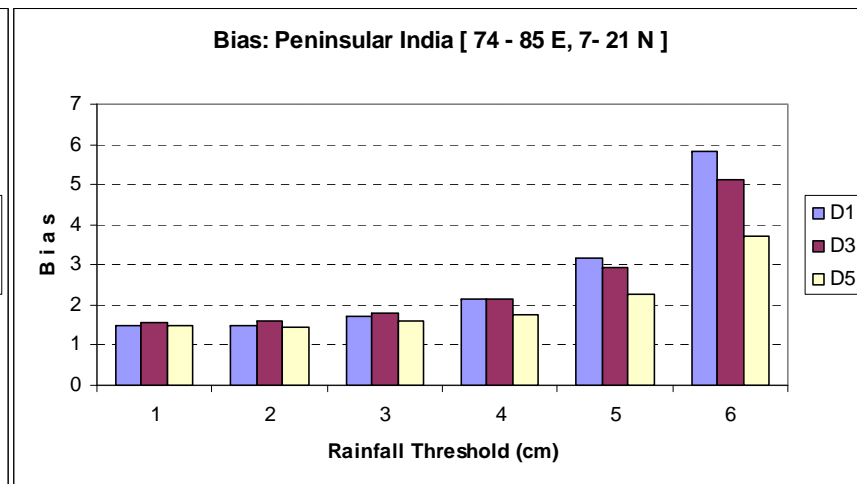
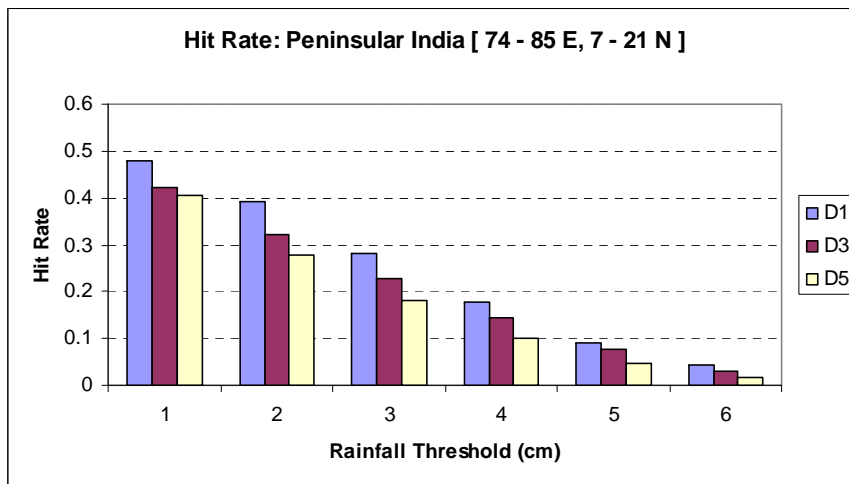
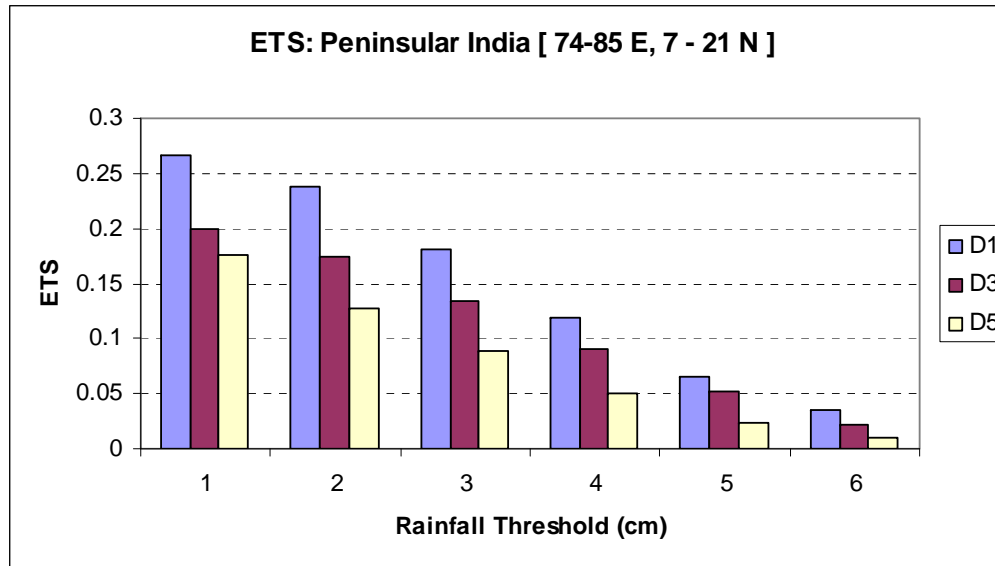


Fig. 4: Rainfall threshold based skill scores for Peninsular India Region for the 2009 monsoon season

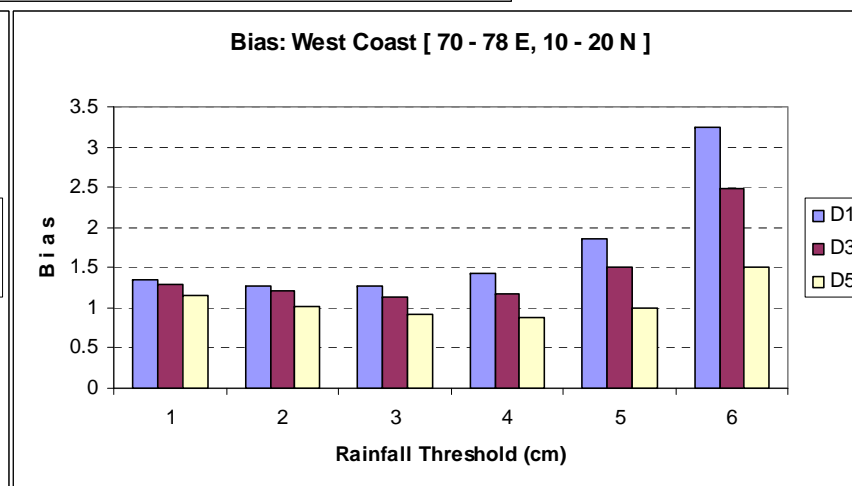
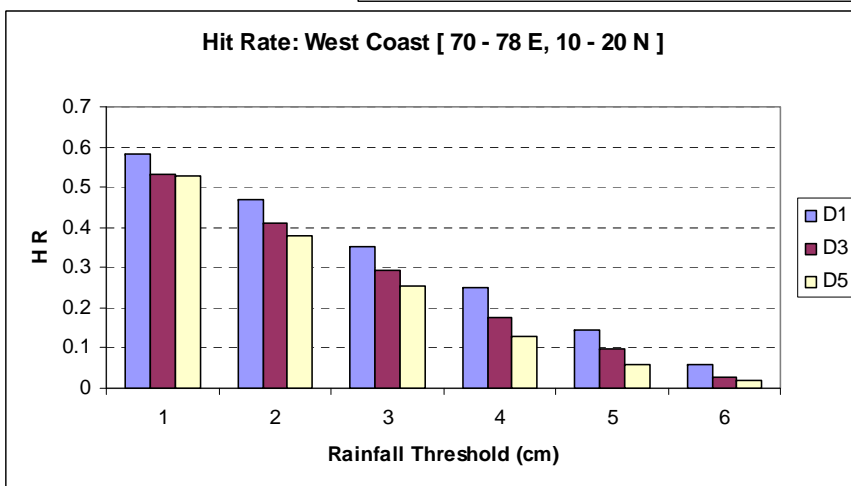
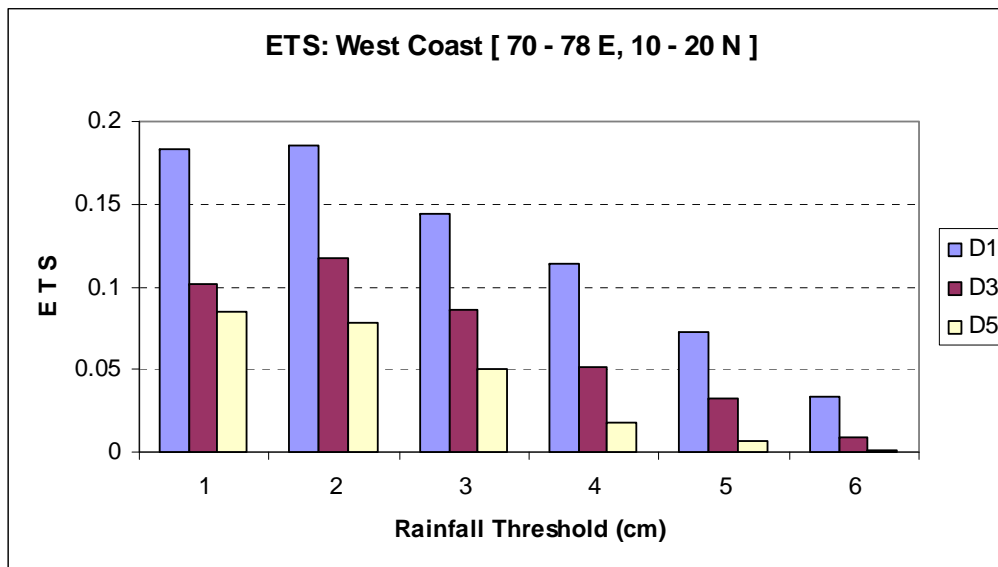


Fig. 5: Rainfall threshold based skill scores for West Coast Region for the 2009 monsoon season

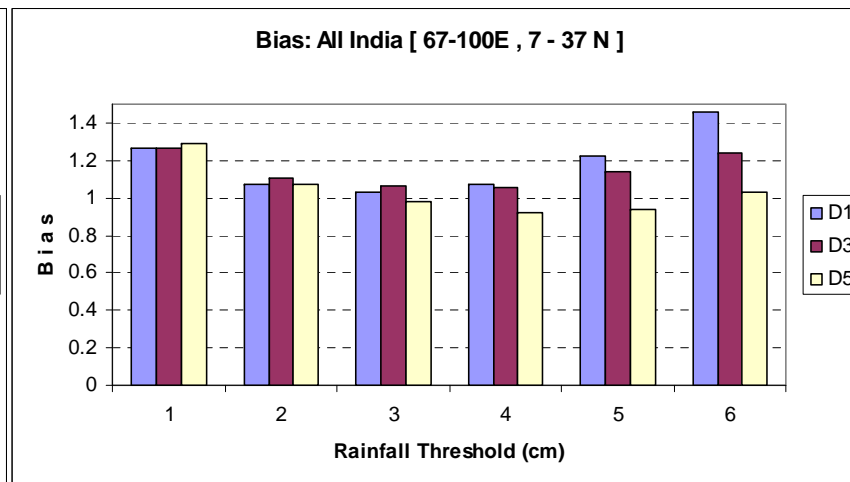
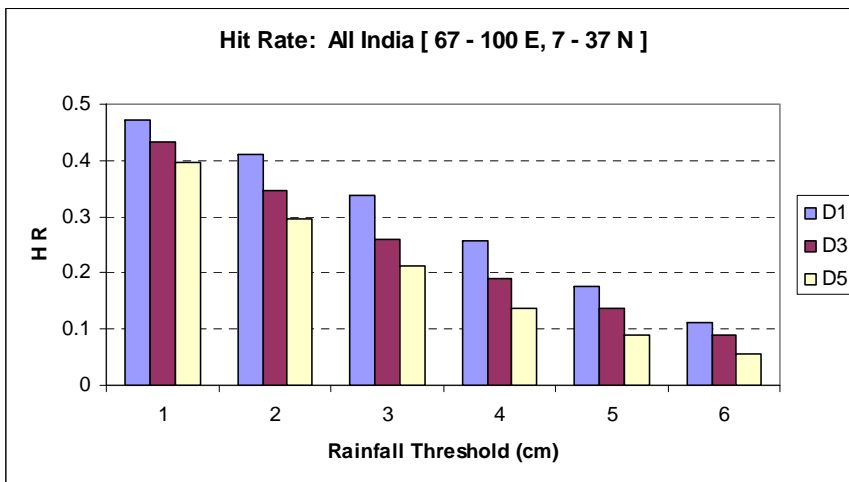
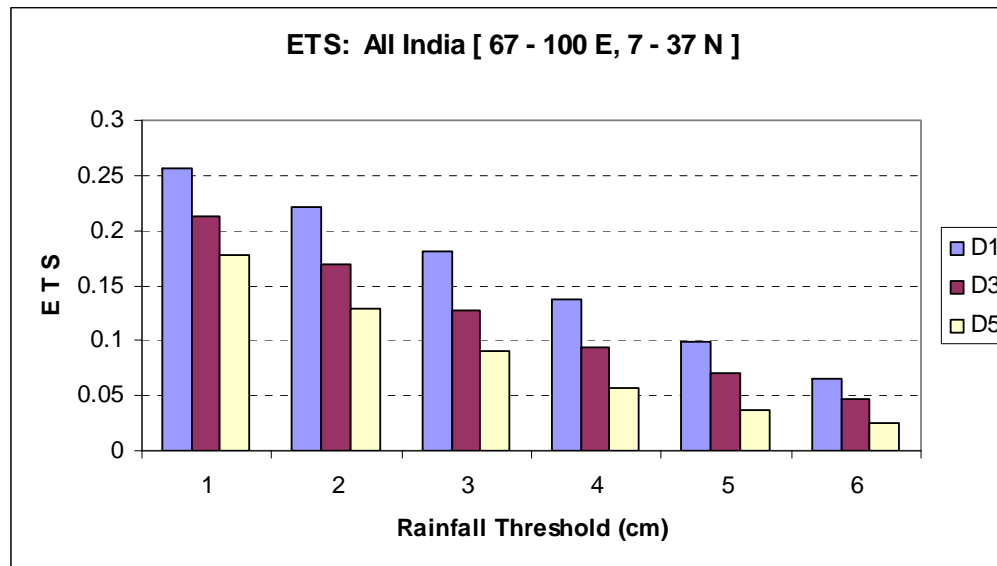


Fig. 6: Rainfall threshold based skill scores for All India Region for the 2009 monsoon season

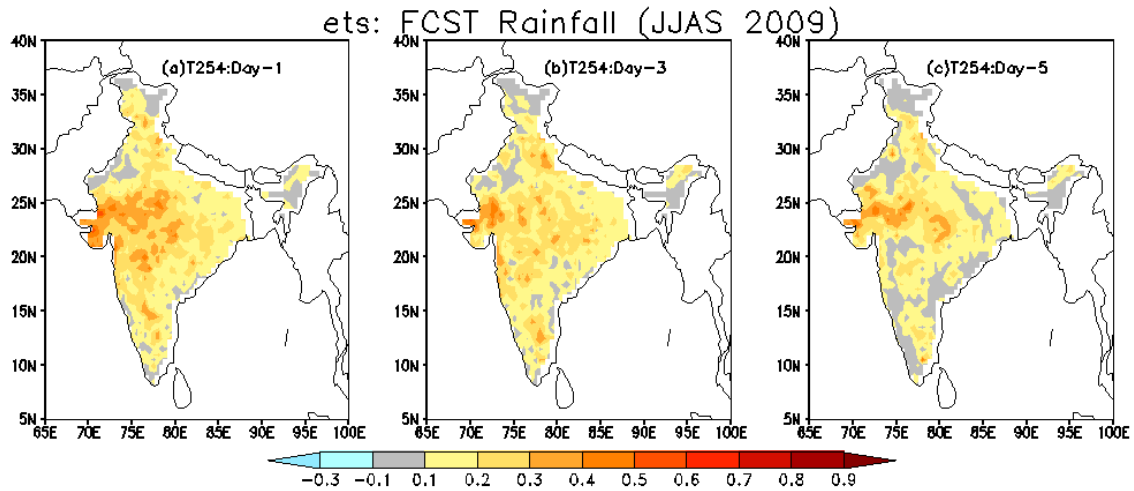


Fig. 7. Spatial distribution of equitable threat score over India during JJAS 2009. An ETS value of 0 indicates no skill and 1 meaning perfect score.

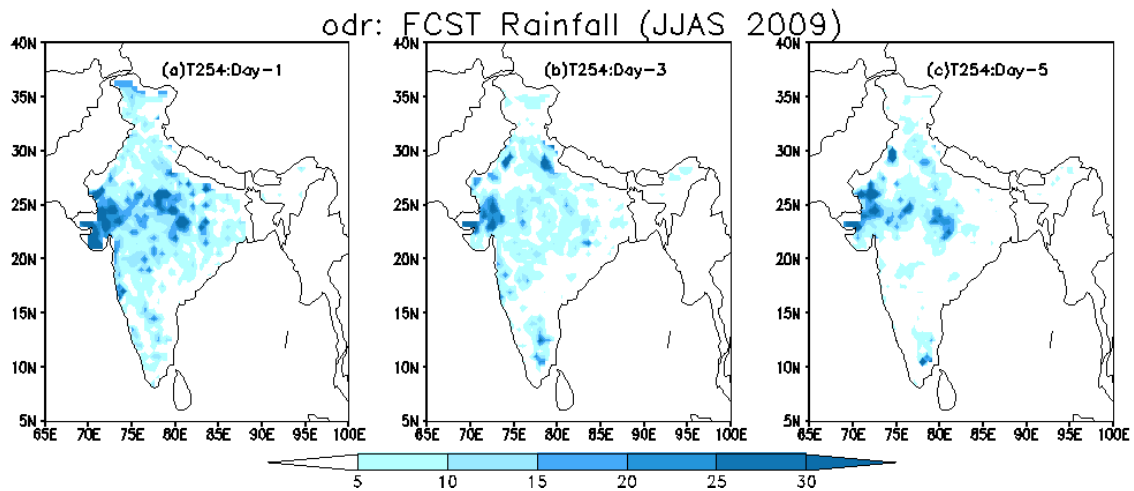
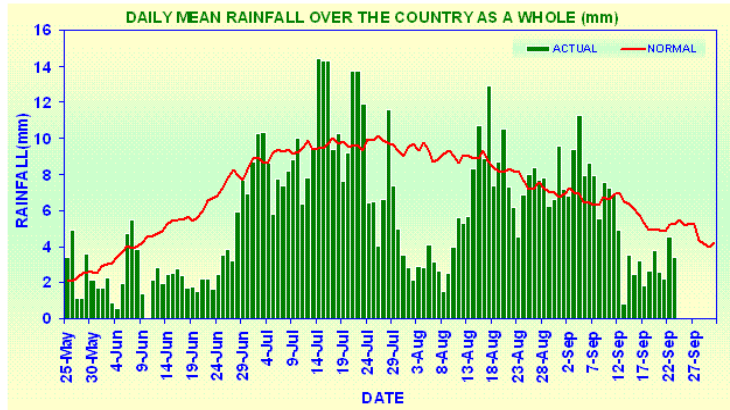


Fig. 8. Spatial distribution of odd ratio over India during JJAS 2009. OR ranges from 0 to infinity, with a score of 1 indicating no skill and the perfect score is infinity.

Monsoon 2009
Observed IMD



All_India Daily Rainfall (mm)
Observed vs. T254L64 forecast

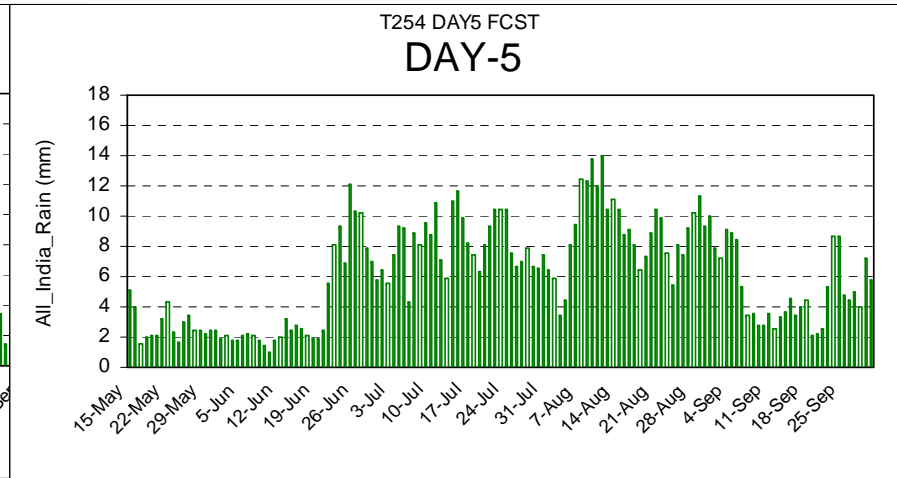
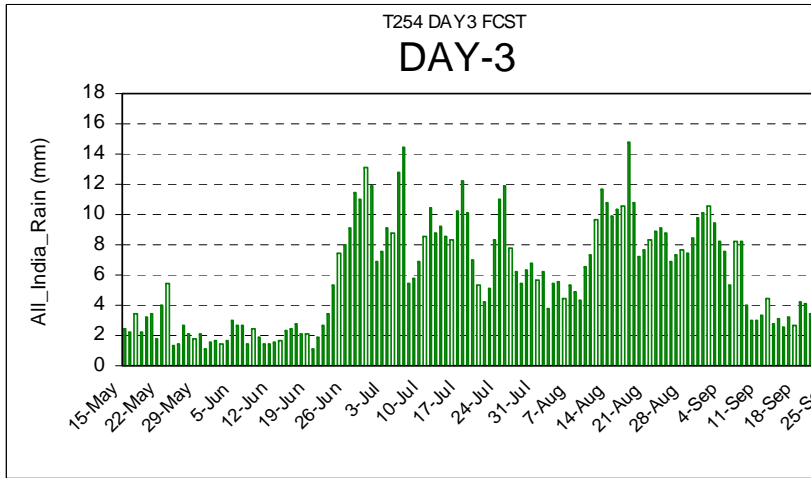
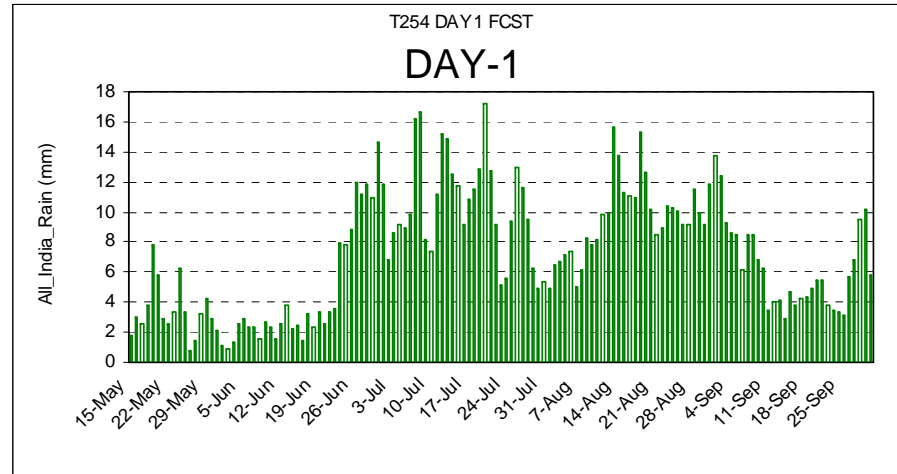


Fig.9: All India daily rainfall (mm) predicted by T254L64 for day-1, day-3 and day-5, against observed rainfall during Monsoon 2009

Monsoon-2009

All India Rainfall (mm)

Observed vs. T254L64

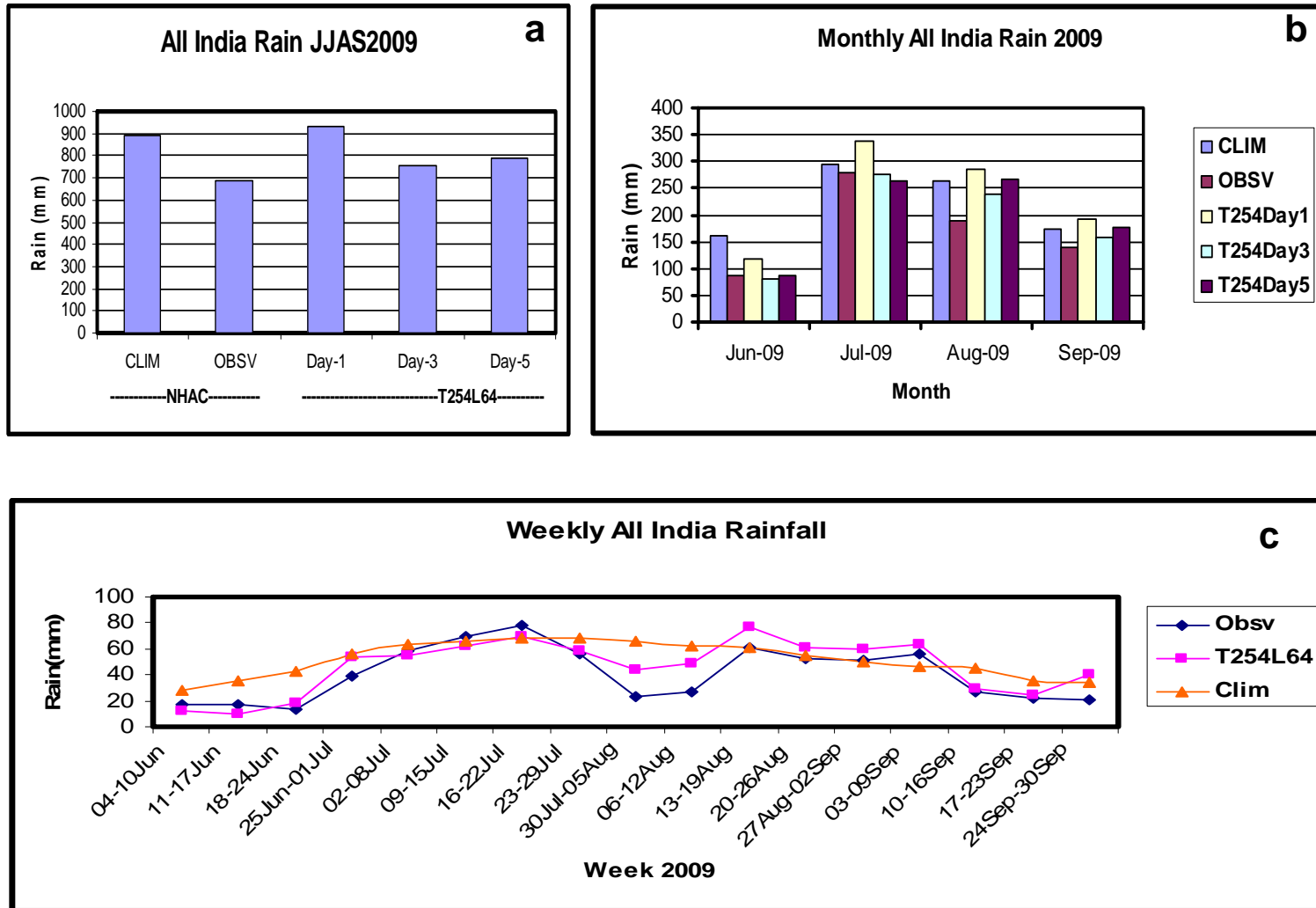


Fig. 10: All India rainfall (mm) from T254L64 against observed; (a) Seasonal, from day-1, day-3 and day-5 forecasts (b) Monthly, from day-1, day-3 and day-5 forecasts (c) Weekly forecasts from single initial condition, once a week [CLIM shows the observed long period averaged values (climatology)]

Onset and Advancement of Monsoon

M. Das Gupta

1. Introduction

Southwest monsoon activity during JJAS 2009 over Indian region was below normal, rainfall received was only 77% of its long period average (LPA). During monsoon 2009, though an early onset over Kerala was seen by 23rd May (normal date is 1st June), but there was hiatus in the advance of the monsoon during 8th - 20th June, resulting rainfall only 53% of LPA in June 2009. Rainfall activity subsequently increased in the later part of June and monsoon covered the entire country by 3rd July, about 12 days earlier than the normal date (15th July). However through out the season, main monsoon systems like north-south surface pressure gradient, monsoon trough, cross equatorial flow etc. was comparatively weak, resulting over all below normal rainfall activity.

The onset of Monsoon not only affects the rainfall over land but the tropospheric wind, humidity and temperature fields also undergo major transitions. An objective method for predicting monsoon onset, advancement and withdrawal date using dynamic and thermodynamic precursors from NCMRWF T80L18 analysis-forecast system was developed (Ramesh et al. 1996, Swati et al. 1999.) and used since 1995 at NCMRWF. The same has been extended for NCMRWF T254L64 analysis-forecast system during monsoon 2008 (Das Gupta and Mitra, 2009). The onset and advancement of monsoon, based on the above mentioned objective method from NCMRWF T254L64 analysis-forecast system during monsoon 2009 will be discussed here.

2. Onset over Bay of Bengal:

The advancement summer monsoon over southwest Bay of Bengal (BOB) normally takes place prior to that over Arabian Sea (ARB) around 2nd-3rd week of May. The evolution of monsoon onset was monitored routinely from the first week of May by monitoring the daily variations of the analysed and predicted value of 850 hPa kinetic energy(KE), net tropospheric (1000hPa-300hPa) moisture (NTM) and mean tropospheric

(1000hPa-100hPa) temperature (MTT) computed over BOB(0°N -19.5°N,78°E-96°E). Figure 1 depicts the daily variations of KE, NTT and MTT over BOB form 1st May to 1st October 2009 for 0000UTC analysis (black line) and subsequent day-1(24hr.) to day-7(168 hr.) predictions.

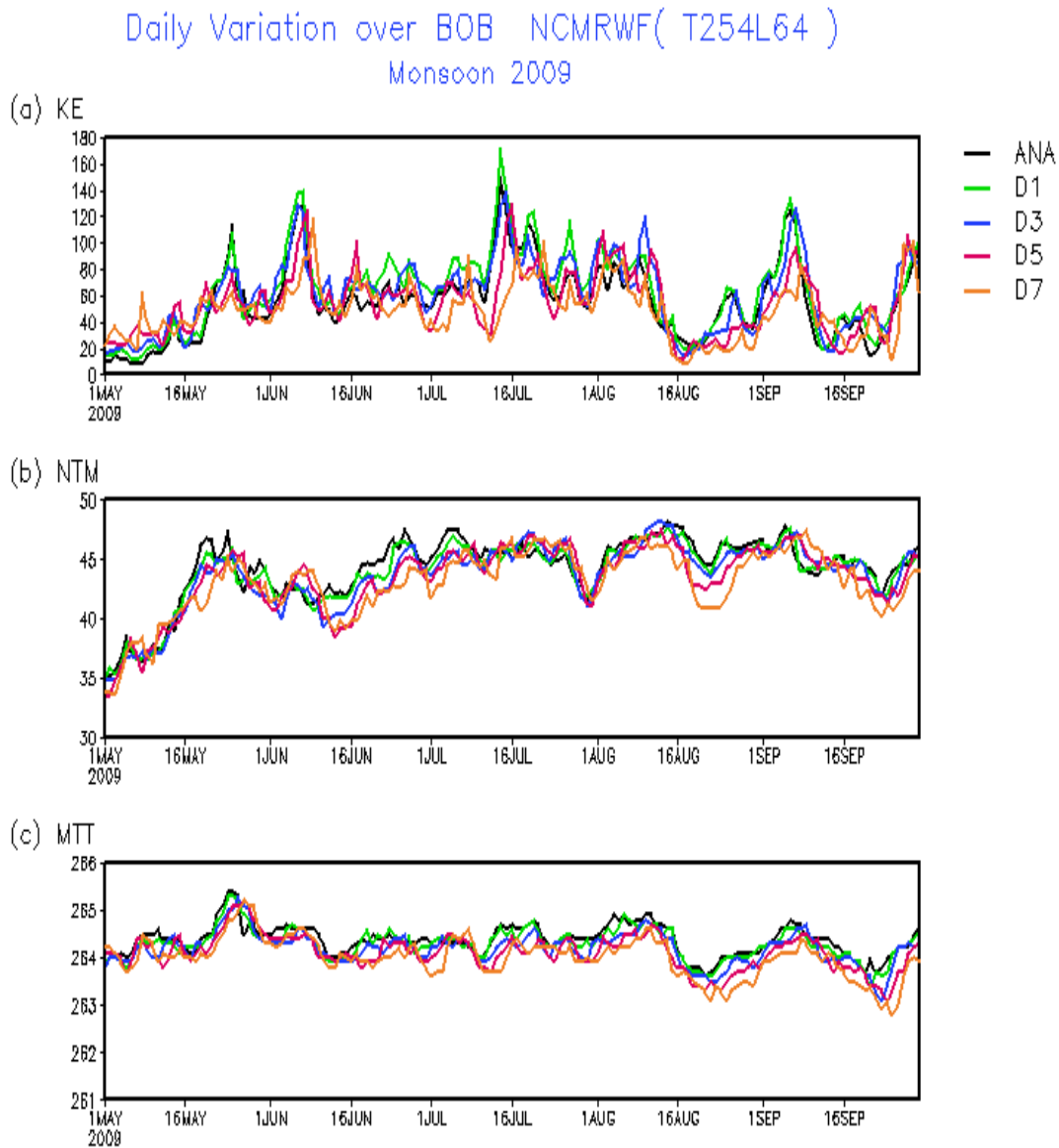


Fig.1 Daily variation of (a) Kinetic energy, (b) Net Tropospheric Moisture and (c) Mean Tropospheric Temperature over Bay of Bengal during JJAS 2009

As seen from the plot there were several episodes of active monsoon condition over BOB, corresponding with the peaks in KE analysis plot (Fig 1a). In general all these

active and weak phases of monsoon over BOB are captured well in predictions also. Steady increase of KE above $60\text{m}^2\text{s}^{-2}$ at 850 hPa over BOB was noticed first on analysis and predictions (from day-1 to day-7) valid for 21st May. There was a rise in NTM above 40 mm on 21st May, followed by a sudden fall on 25th May. Fall in the MTT was also noticed almost around the same time. The changes in prevailing wind regimes over certain selected points monitored over BOB also indicated the conducive changes around 25th May. So, following the objective criteria, NCMRWF T254L64 analysis-forecast system suggested the date of onset over BOB as 25th May, 2009. However, based on conventional procedure, India Meteorological Department (IMD) declared the onset over southwest Bay on 20 May, 2009.

3. Onset over Kerala (Arabian Sea Branch):

The Arabian Sea branch of monsoon generally first hits the Western Ghats of the coastal state of Kerala around 1st June with standard deviation of 8 days. This year IMD declared the monsoon onset over Kerala on 23rd May, 8 days prior to the normal date. But this onset was rather weak. Though the monsoon along the west coast was advanced up to 17°N by 7th June, but after that, due to weakening of cross-equatorial flow, there was no further advancement of monsoon along the west coast till 21st June.

Figure 2 depicts the daily variations of analysed and predicted KE at 850 hPa, NTM and MTT computed over ARB (0-19.5° N; 55.5°E-75°E) from 1st May 2009 onwards. This weak onset phase was very well captured by T254L64 system. KE at 850hPa over ARB reached above the threshold value $60\text{m}^2\text{s}^{-2}$ in 48-hr prediction valid for 25th May, based on 23rd May initial analysis, but the rise of KE in the subsequent predictions was marginal (only up to $77\text{m}^2\text{s}^{-2}$ in 168hr FCST valid for 30th May). By this time NTM was also not reached threshold value 40mm. After that, for next two consecutive weeks KE started reducing and its value was well below $60\text{m}^2\text{s}^{-2}$. So, based on the objective criteria, T254L64 system did not predict the monsoon onset over Kerala in the month of May.

Rise of KE above $60\text{m}^2\text{s}^{-2}$ again was seen in 144hr prediction valid for 21st June onwards based on 15th June initial condition. But NTM was below 40 mm. Based on 20th

June initial condition, all subsequent predictions beyond 48 hr. satisfied the objective criteria for onset (except the fact that the NTM was just 40mm for a day only). Hence objectively the date of onset over Kerala, as analysed/predicted by T254L64 system, is determined as 22nd June.

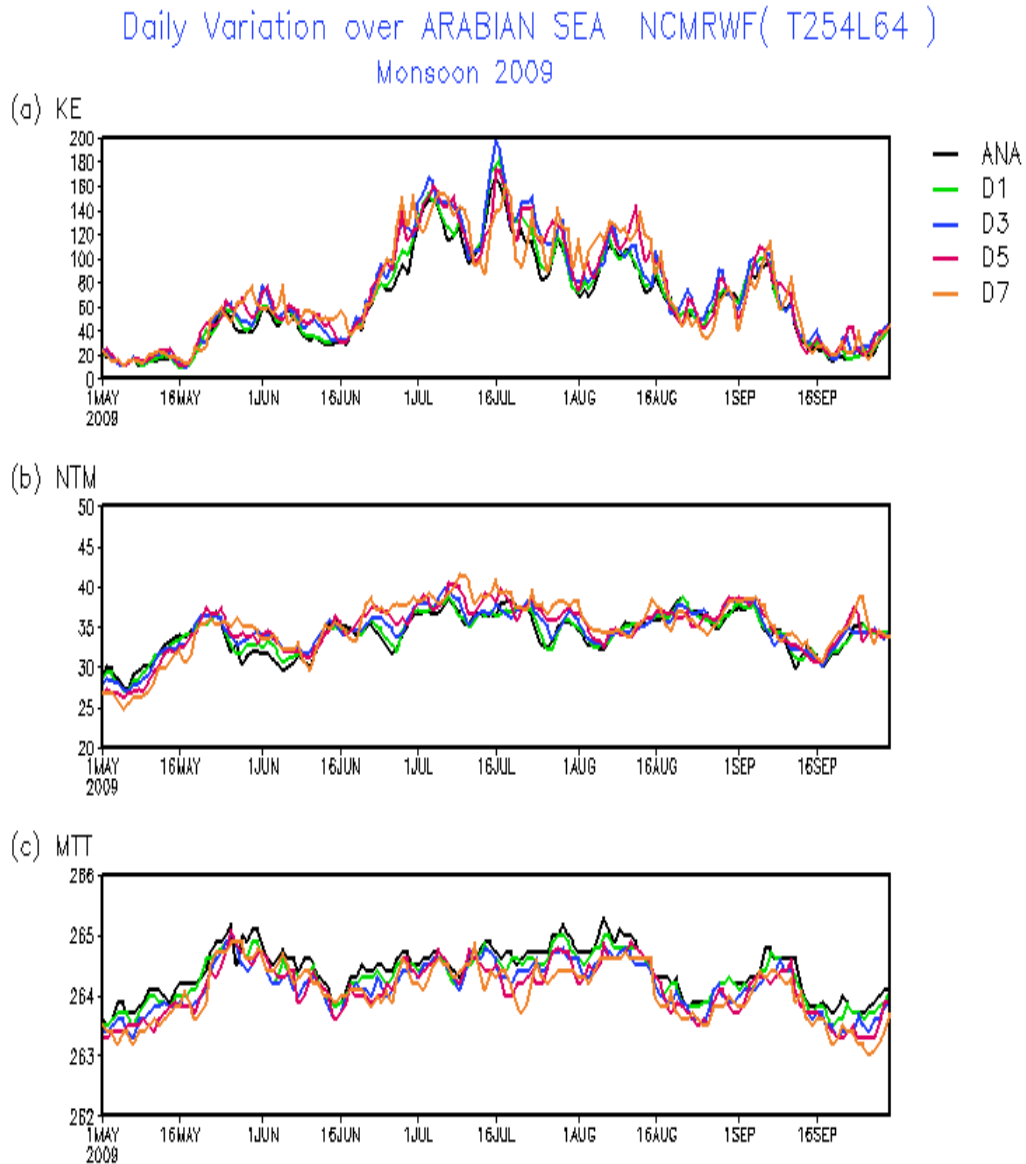


Fig.2 Daily variation of (a) Kinetic energy, (b) Net Tropospheric Moisture and (c) Mean Tropospheric Temperature over Arabian Sea for JJAS 2009

4. Advancement of Monsoon:

Advancement of Monsoon over India during monsoon-2009 was rather different from its normal pattern. Bay of Bengal branch of monsoon showed rapid advancement due to formation of cyclonic storm Aila in end of May. This resulted in early onset of monsoon over North-eastern states of India and West Bengal, well before its normal date. On the other side the advancement over west coast was very sluggish and no advancement beyond 17°N along the west coast took place from 7th -20th June.

According to objective criteria the advancement of monsoon over main land of India is determined by examining changes in NTM together with the flow characteristics at 850hPa in analyses and subsequent predictions. The criteria adopted for determining the progress of monsoon over a particular location are as follows:

- (i) Steady increase of NTM under the influence of expected wind regime at 850 hPa
- (ii) Sharp fall in the net moisture content and subsequent rise there after under the influence of same wind regime
- (iii) Date for advancing the northern limit of monsoon over a location is fixed on the day of fall in the net moisture content, which is believed to be utilized for producing the rainfall associated with the advancement of monsoon over that region

For determining the advancement of monsoon over different locations over Indian main land, NTM MTT and wind direction and speed at 850hPa in analysis and predictions are examined over 43 locations over India.

Figure 3 depicts the same for Kolkata during 1st May to 27th June 2009. As seen from the plot, rapid increase of NTM value at Kolkata was seen in subsequent day predictions with initial condition of 25th May. It also showed the sharp fall of NTM on 27th May indicating occurrence of rain. Based on these objective criteria, the date of advancement of monsoon over Kolkata was determined as 27th May. However IMD's northern limit of monsoon line covered Kolkata on 25th May.

Table 1 depicts the dates of advancement of monsoon at few important locations over India using NCMRWF objective criteria along with that declared by IMD (as northern limit of monsoon).

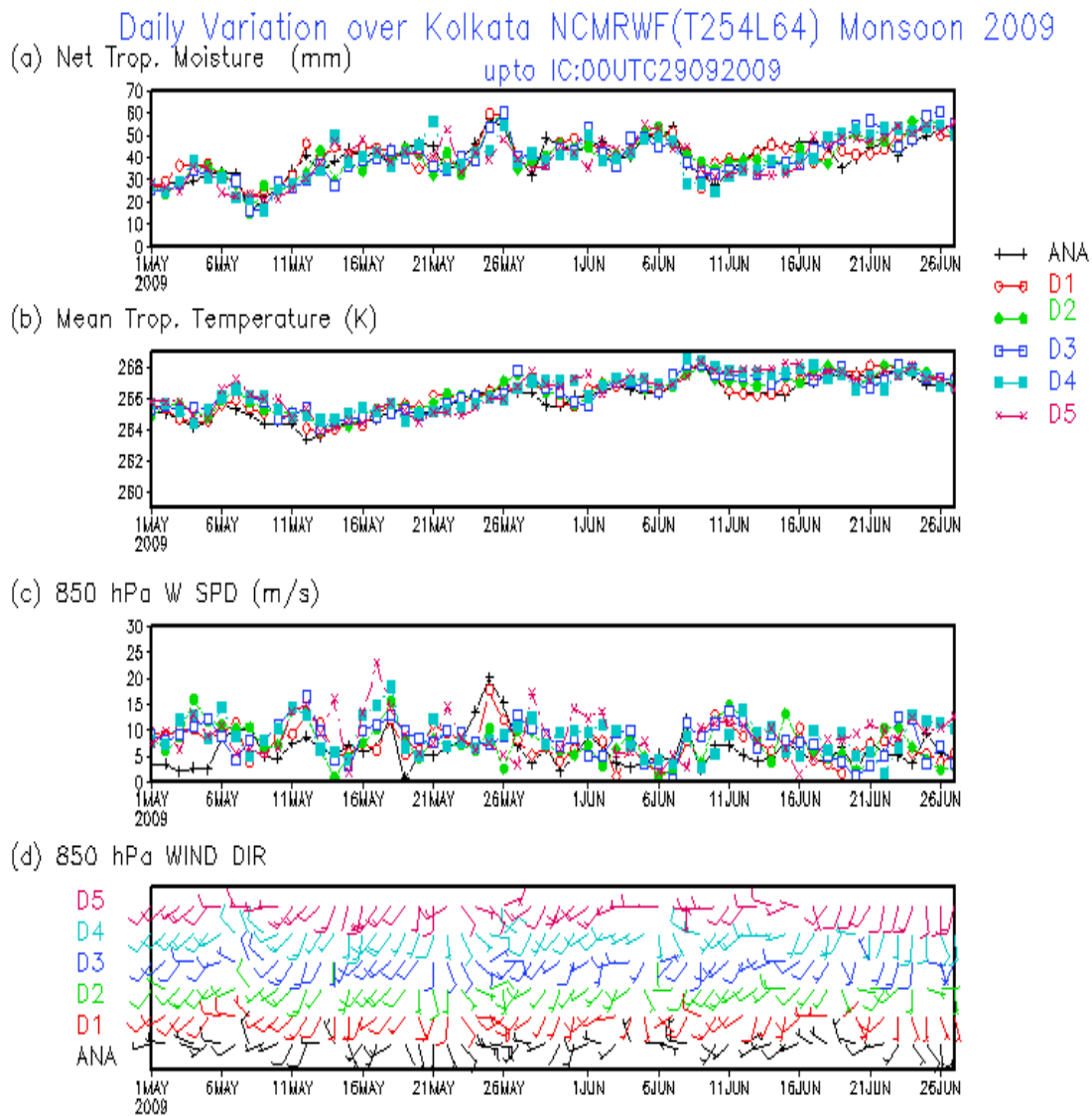


Fig.3 Daily variation of (a) NTM, (b) Net MTT (c) Wind Speed at 850 hPa and (d) Wind direction at Kolkata (IC: 1st May- 27th June 2009)

According to NCMRWF objective criteria, the advancement of monsoon over west coast of India was also sluggish. The advancement of monsoon in south peninsular stations during 2009 was not clearly captured by T254L64 system using the above mentioned criteria. However, apart from west coast of India (below 17°N), most of the places the date of advancement of monsoon by objective method and date declared by IMD differ by 0-7 days.

Table 1. Date of advancement of monsoon

Locations	Date determined by NCMRWF objective criteria	Date declared by IMD
Kolkata	27 th May	25 th May
Cochin	24 th June	23 rd May
Mumbai	27 th June	24 th June
Raipur	27 th June	27 th June
Patna	28 th June	29 th June
Varanasi	30 th June	29 th June
Allahabad	2 nd July	29 th June
Agra	6 th July	30 th June
Delhi	6 th July	30 th June
Jodhpur	7 th July	3 rd July
Jaisalmer	10 th July	3 rd July

This year withdrawal of monsoon was also late due to presence of systems in westerlies over northwest India and IMD declared withdrawal of monsoon from north and north-west India from 25th September onwards. The objective criteria for withdrawal of monsoon are as follows:

- (i) value of NTM below 30-35mm for three consecutive days after the progression of Tibetan anti-cyclone at 200 hPa and formation of anti-cyclonic circulation over NW India

Reduction of NTM below 30mm over Jaisalmer and Jodhpur (west Rajasthan) was noticed from 10th September onwards and it remained below 30mm till to the end of the season. Accordingly NCMWRF analysis-forecast system suggested the withdrawal of monsoon from northwest India by 10th September. However the stations in Northern region like Jammu, Dehradun, Delhi showed subsequent increase of NTM in day3-day5 predictions again above 35mm, from 14th September onwards. All these stations showed steady decrease in NTM below 30mm in predictions from 23rd September onwards till the

end of season, suggesting the date of withdrawal of monsoon over that region as 23rd September.

5. Summary

First time the objective criteria for onset/progress of monsoon developed based on analysis and forecast data from a coarser resolution global model (T80L/18) was tested during monsoon 2008 with data from a higher resolution global model (T254L64). It was concluded that the parameters related to the objective criteria of onset and progress of monsoon over India were also well captured by analysis and the medium range predictions from higher resolution model. But during 2009, it is seen that some of these features were not captured well by T254L64 system for southern peninsular stations. This may be related to the early weak onset of Arabian Sea branch of monsoon and subsequent weakening of cross-equatorial flow. Mechanism for incorporating rainfall predictions from high resolution models, in the objective method could be explored in future. However, the advancement of monsoon, based on the objective criteria, over other part of the country is captured well by T254L64 analysis-forecast system. Withdrawal of monsoon based on objective criteria also showed early withdrawal compared to the date declared by IMD.

References:

Das Gupta M., A. K. Mitra 2009: Onset and Advancement of Monsoon, “MONSOON-2008: Performance of the T254L64 Global Assimilation Forecast System“, Report no. NMRF/MR/01/2009, 117 pages, Published by NCMRWF (MoES), A-50 Institute Area, Sector- 62, NOIDA, UP, INDIA 201 307

Ramesh, K.J, Swati Basu, and Z.N. Begum, 1996: Objective determination of onset, Advancement and Withdrawal of the summer monsoon using large scale forecast fields of a global spectral model over India, Meteor. and atmospheric Physics,61, 137-151.

Swati Basu, K.J. Ramesh and Z.N. Begum,1999: Medium Range Prediction of summer monsoon activities over India vis-avis their correspondence with observational features, Adv. in Atmos. Sci.,16,1,133-146.

Monsoon Indices: Onset, Strength and Withdrawal

D. Rajan and G. R. Iyengar

1. Introduction

Precipitation in India has clear seasonal variation and the onset of the Indian summer monsoon is of great interest as not only a research target but also a socio-economic factor for water resources in India. The annual reversal of wind and rainfall regimes in monsoon is spectacular. Because of the need of referring to monsoon variability with reference to specific features and the time of their occurrence, many monsoon indices have been developed and used in research. The onset date of the monsoon has been defined by several methods in past studies. The onset and withdrawal of the broad scale Asian monsoon occur in many stages and represent significant transitions in the large-scale atmospheric and ocean circulations (Fasullo and Webster 2003), which can be examined by analyzing various monsoon indices. Useful indices provide a simple characterization of the state of the monsoon during different epochs and also the inter-annual variability. While there is no widely accepted definition of these monsoon transitions at the surface, the onset is recognized as a rapid, substantial increase in rainfall within a large scale.

The arrival of the summer monsoon over the Kerala coast is found to be reasonably regular either towards the end of May or beginning of June (Ramesh et al. 1996; Prasad and Hayashi 2005; Taniguchi and Koike 2006, Goswami and Gouda 2010). The monitoring and forecasting of the summer monsoon onset over the Indian subcontinent is very important for the guidelines for the operational forecaster reference. This migration and location of the heat source associated with summer monsoon has important implications for the withdrawal of monsoon over South Asia. However, to date there has been no systematic investigation of the retreat of the monsoon system despite its key contribution to total rainfall variability. But it is known that, in terms of rainfall, the onset is better defined than the withdrawal. In this section of the report, data from T254L64 global analysis forecasts system have been used to compute various monsoon indices to monitor onset, strength and the withdrawal of the monsoon during 2009 season.

2. Monsoon circulation indices for onset, strength and withdrawal

Though a definition of monsoon onset based on Indian rainfall is somewhat arbitrary, it has the significance of being the date which signals (Goswami and Gouda 2010) the beginning of the main agricultural season for a significant fraction of the world's population. Kerala state, situated in the southwest part of the Indian sub-continent is the gateway for the Indian summer monsoon. Based on Kerala rainfall, the mean onset date occurs around 1 June and varies with a standard deviation of 8-9 days from year to year. Given the relatively small scale of Kerala that is less than 200 km in breadth, sensitivity of the declaration of onset based solely on the district's rainfall to spatial area in the monsoon transitions is also likely to be large. The onset date is normally declared based on rainfall, wind, temperature, moisture, cloud pattern, and the state of the sea, etc. For a forecaster it is a difficult job to declare the date of onset because all the above parameters are highly variable in space and time. It is difficult to quantify these parameters precisely and so the experience of the forecaster plays a key role in declaring the date of monsoon onset subjectively for individual years (Wang et al., 2009).

The India Meteorological Department (IMD) has been using the qualitative method over a long period using rainfall to declare the onset date for the monsoon forecast. As per IMD's daily weather bulletins for the year 2009, the southwest monsoon set in over Andaman Sea around its normal date of 20 May. Ultimately it set over Kerala on 23 May, about a week earlier than the normal onset date.

Ramesh (1996) et al., suggested the following characteristics for the evolution of the onset over the Arabian Sea covering the area of $0^{\circ} - 19.5^{\circ} \text{N}$ and $55.5^{\circ}\text{E} - 75^{\circ}\text{E}$: (a) the net tropospheric (1000 – 300 hPa) moisture build-up, (b) the mean tropospheric (1000 – 100 hPa) temperature increase, (c) sharp rise of the kinetic energy at 850 hPa. The author read that the above objective study most of the time computed the onset date delayed by few (3–8) days than the actual date declared is 23 May. In the previous section of this report, onset and progress have been described with the above said criteria. This year also it is noted that the onset date is seen to be around 20 June.

In this chapter four monsoon dynamical indices are considered with data from the present NCMRWF high resolution T254L64 analysis and forecast system. These widely used monsoon dynamical indices of the South Asian summer monsoon are shown in the table (I) with their corresponding brief definition. These monsoon indices are based on circulation

features associated with convection centers related with rainfall during the summer monsoon for the Indian region.

In 1999 Goswami et al., defined the index based on the meridional wind (V) shear between 850 hPa and 200 hPa over the south Asian region $10^{\circ}\text{N} - 30^{\circ}\text{N}$, $70^{\circ}\text{E} - 110^{\circ}\text{E}$ which is related to the Hadley cell features. This index can be used to study the onset and advancement phases of the monsoon.

Wang et al., (2001) introduced a dynamical index based on horizontal wind (U) shear at 850 hPa called the circulation index. They recommend that the circulation index computed with the mean difference of the zonal winds (U) between the two boxes; one for southern region and the other for the northern region, i.e. $5^{\circ}\text{N} - 15^{\circ}\text{N}$, $40^{\circ}\text{E} - 80^{\circ}\text{E}$ and $20^{\circ}\text{N} - 30^{\circ}\text{N}$, $70^{\circ}\text{E} - 90^{\circ}\text{E}$ can be used as the criteria for identifying the onset date. The southern region box is taken over South Arabian Sea and the northern region box is taken over northern region. This circulation index describes the variability of the low-level vorticity over the Indian monsoon trough, thus realistically reflecting the large scale circulation. After that Fasullo and Webster (2003) defined the onset date in terms of vertically integrated moisture transport derived from reanalysis data sets. As per their discussions the inter-annual variation in the onset date modestly agreed with reality.

Taniguchi and Koike (2006) emphasized the relationship between the Indian monsoon onset and abrupt strengthening of low-level wind over the Arabian sea ($7.5^{\circ}\text{N} - 20^{\circ}\text{N}$, $62.5^{\circ}\text{E} - 75^{\circ}\text{E}$). This is a measure of the strength of the low-level jet over South Arabian Sea and indicates the strength of the monsoon over India. They showed that Indian summer monsoon onset is brought mainly by enhancement of low-level wind over the Arabian Sea.

Wang et al., (2009) found that the onset date can be objectively determined by the beginning of the sustained 850 hPa zonal wind (U) averaged over the southern Arabian Sea ($5^{\circ}\text{N} - 15^{\circ}\text{N}$, $40^{\circ}\text{E} - 80^{\circ}\text{E}$). This criterion is known as objective circulation index. The rapid establishment of steady westerly is an excellent parameters to correlate with the abrupt commencement of the rainy season over the southern tip of the Indian peninsula. In this index, the onset date is defined as a sustained zonal westerly exceeding 6.2 m/s and persists for more than six days. This definition is objective and depends on large scale circulation feature. This circulation index clearly omits the bogus onset or multiple onset dates. The bogus or double monsoon onset develops when the strong convection in the Bay of Bengal is accompanied by the monsoon like circulation and appears in the Indian Ocean.

Syroka and Toumi (2002, 2004) also defined a similar type of circulation index by taking the box slightly towards east of Wang's (2001) case. A daily circulation index was defined as the difference in average 850 hPa zonal winds between a southern region 5°N – 15°N, 50°E – 80°E and a northern region 20°N – 30°N, 60°E – 90°E. This daily circulation index is a physically sensible and practical tool to study the withdrawal of the monsoon also. According to them the date of withdrawal of the monsoon is defined as the first of seven consecutive days for which the index becomes negative. This daily circulation index can be used to define both the dates of onset and withdrawal of the Indian summer monsoon from these regions. The index changes sign, reflecting both the changing intensity of the low-level westerly monsoon flow and the vorticity associated with the monsoon trough and synoptic activity. The above index suggest that the average date of withdrawal is 16 October with a standard deviation of 7 days. In this section we have computed the above described for circulation indices based upon the various definitions that are tabulated in table (I).

3. Results and discussions

We use the daily NCMRWF high resolution version of T254L64 analysis and forecast (up to 120 hrs) data sets for the period May to September 2009. Details of the NCMRWF assimilation and forecast systems are described in chapter 1 of this report. The IMD Climate Diagnostics Bulletin of India (2009) daily/seasonal reports have been referred for the observation of rainfall, flow patterns, the dates for the declaration of onsets monsoon strength and withdrawal etc during the entire period of this study.

Figure (1 a) shows the objective circulation indices calculated by Wang et al ., (2009) for the analysis and forecast for the length of 24 hr, 72 hr and 120 hr. From this figure it is seen that the apparent onset date (bogus onset) is noticed as 23 May, by the sustained westerly (U) exceeding 6.2 m/sec and persisting for more than five days i.e. up to 28 May. This high value of U did not persist beyond 28 May. From this figure it is seen that another onset date is noticed around 20 June, by the sustained westerly (U) exceeding 6.2 m/sec and persisting for more than six days. This high value of U did not persist beyond 05 June also. Hence it is appropriate that the real dynamical onset occurred on 20 June only. The bogus onset date 23 May can be omitted safely by quoting these monsoon onset criteria. In the forecasted indices also broadly these features are captured well. However 72 hr and 120 hr forecasts have difficulty in capturing the transition of the onset.

Figure (1 b) shows the circulation indices calculated by Syroka and Toumi (2002, 2004) for the onset phase. From the figure (1 b) we infer that the apparent onset date around 22 May 2009, because on that day onwards the daily index is changing its sign from negative to positive and maintained there after. In this case also the bogus onset date 23 May is clearly brought out. From this figure we infer that the onset date is seen around 18 June only. The analysis and the 24 hr forecast, 72hr forecast, 120hr forecast also shows the change of sign, but with lag of few days.

Figure (1 c) shows the circulation indices/vertical shear suggested by Goswami et al., (1999) for the onset phase. This is popularly known as Goswami Hadley cell circulation index. From this figure we infer that the onset date is seen around 20 June only but not on the day 23 May, because on that day onwards the daily index is changing its sign from negative to positive and maintained the positive sign there after. The analysis and the 24 hr forecast, 72 hr forecast, 120 hr forecast also having the same trend and are able to capture the change of sign from negative to positive with a lag of 2-3 days.

Figure (2 a) shows the Wang (2001) circulation index for the 122 days of the monsoon 2009. From the IMD source it is seen that in association with the advance of monsoon over the northeastern states including West Bengal & Sikkim occurred earlier than normal. A prolonged hiatus in the advance of monsoon occurred during 8 – 22 June, which is clearly seen in the figure having circulation index at the order of 5 m/sec only. During 23 – 24 June one depression formed over the east central Arabian Sea, moved northwards along west coast and weakened after crossing Gujarat coast this synoptic features can be noticed in the figure (2 a) the circulation index have a sharp raise on 23 June onwards. The wind strength more than 8 m/sec in the circulation index scale is seen around after the period 24 June in the analysis of T254L64; which has been reflected in the monsoon rainfall reported by IMD. Hence the real onset is around 20 June 2009. As seen in the observation monsoon further advanced as a weak current over some more parts of peninsular India on 21 – 24 June, covering parts of north Arabian Sea, south Gujarat State, Konkan and some more parts of Maharashtra. The rainfall activity over the country as a whole was very much below normal during the month June. These corresponding circulation index are also showing very low values (<10 m/sec) throughout this period June. Monsoon covered the entire country on 3 July, about 12 days earlier than its normal date ie 15 July, when the interaction between monsoon flow and mid-latitude westerlies resulted in copious rainfall seen in the figure (2 b) over Rajasthan.

As shown in the figure (2 a) there are more than five peaks having the strength of more than 10 m/sec wind speed, those can be correlated with the peaks rainfall observed Figure (2 b) during this season with some time lag. The break monsoon conditions also prevailed over the country during the second half of July. It has affected the rainfall (- 0.39 %) over the central and South peninsular India during July. The cross equatorial flow was weaker than normal during major parts of the season except for a brief period from last week of June to third week of July; which can be correlated with the rainfall observation shown in figure (2 b). The less amount of rainfall distribution was mainly due to the break monsoon condition that developed during 12 – 20 September, which can be easily correlated with the circulation index shown in figure (2 a).

The figure (3) shows the wind circulation index as per Syroka & Toumi (2002) for the period of August – September 2009. From the IMD's climate diagnostics bulletin of India (2009) it is seen that in 2009 there was delay in the withdrawal of southwest monsoon due to rainfall activity over north India in associated with mid latitude westerly activities. From the figure it is seen that the circulation index values reduced sharply but it does not changes its sign to negative up to the date 15 September. So the withdrawal date can not be consider as the date 15 September. From 15 – 23 September the index curve is near to the vicinity of the axis ie it gets the minimum value around the 23 – 25 of September. Hence 23 – 25 September can be taken as withdrawal date of the southwest monsoon 2009. This date can be commented as the real withdrawal date. Thus the withdrawal of monsoon from west Rajasthan started only on 25 September which is delay of more than 3 weeks time from the normal date (1 September), of withdrawal from extreme western parts of Rajasthan. In the second occasion circulation index changes its sign from positive to negative on 25 September onwards; subsequently it persists for more than 5 days. This increase in the circulation index brought rainfall to the country as shown in the figure (2 b). Thus the day 25 September can be regarded as the withdrawal date of southwest monsoon for the year 2009. When we consider the IMD official information on withdrawal dates it is closer to our dates. It is reported that the withdrawal started on 25 September over the Rajasthan. In reality also the southwest monsoon withdrew from the entire country on 22 October 2009.

4. Summary

Several popular monsoon indices have been used to study the onset, strength and withdrawal of monsoon during 2009 season. In general, the indices are able to represent the onset, variability in strength of monsoon and the withdrawal in a reasonable way. The indices when used with medium range forecast data from the global model indicates that the same could be used to forecast the changes in phases of the monsoon system within a season. These indices have to be refined with more years of data from such a higher resolution system. In future use of thermodynamic parameters from the model will add value to the monitoring of monsoon by such indices.

Acknowledgement: Thanks are due to the observed rain information of IMD made available via IITM web site.

References

Climate Diagnostic Bulletin of India (2009) Issue No. 159 – 163. Issued by National Climate Center office of the Additional Director General of Meteorology (Research) India Meteorological Department, Pune.

Fasullo. J., and P. J. Webster, 2003: A hydrological definition of Indian monsoon onset and withdrawal. *J. climate*, **16**(14), 3200-3211.

Goswami. B.N., V. Krishnamurthy and H. Annamalai 1999: A broad scale circulation index for interannual variability of the Indian summer monsoon. *Quart. J. Roy. Meteor. Soc.*, **125**, 611-633.

Goswami. P., and K.C. Gouda 2010: Evaluation of a dynamical basis for advanced forecasting of date of onset of monsoon rainfall over India. *Monthly Weather Review.*, (online version, February 2010)

Prasad. V S and Hayashi.T. 2005: Onset and withdrawal of Indian summer monsoon. *Geophy. Res. Lett.*, **32** L20715.

Ramesh. K J., Swati Basu and Z N Begam 1996: Objective determination of onset, advancement and withdrawal of the summer monsoon using large-scale forecast fields of a global spectral model over India. *J of Meteo. and Atmospheric physics*, **61**, 137-151.

Syroka, J., and R. Toumi 2002: Recent lengthening of the south Asian summer monsoon season. *Geophy. Res. Lett.*, **29**, (DOI: 10.1029/2002/ GL015053).

Syroka, J., and R. Toumi 2004: On the withdrawal of the Indian summer monsoon. *Quart. J. Roy. Meteor. Soc.*, **130**, 989-1008.

Taniguchi. K., and T. Koike 2006: Comparison of definitions of Indian summer monsoon onset: better representation of rapid transitions of atmospheric conditions. *Geo. Res. Lett.*, **33**, L02709, 5 pages.

Wang, B., Q. Ding, and V. Joseph 2009: Objective definition of the Indian summer monsoon onset using large-scale winds. *J. Climate* **22**, 3303–3316.

Wang. B., R.Wu and K.M. Lau 2001: Interannual variability of the Asian summer monsoon: Contrasts between the Indian and Western North Pacific-East Asian monsoons. *J. Climate*, **14**, 4073-4090.

Name of the Index	Type of Index	Domain of application	Definition in terms of regions	Reference
Goswami	Meridional wind	South Asia	V850 – V200 over (10°N – 30°N, 70°E – 110°E)	Goswami et al., (1999)
Wang and Wu	Circulation index	Tropical Asia	U850 (5°N – 15°N, 40°E – 80°E) – U850 (20° N – 30°N, 70°E – 90°E)	Wang et al ., 2001
Wang and Ding	Circulation zonal wind	Tropical South Asia	U850 averaged over (5°N – 15°N, 40°E– 80°E)	Wang et al ., 2009
Syroka and Toumi	Circulation zonal wind	Tropical Asia	U850 (5°N – 15°N, 50°E –80°E) – U850 (20°N – 30°N, 60°E –90°E)	Syroka and Toumi (2002, 2004)

Table I

T254L64 Wang & Ding 850 hPa Circulation Index

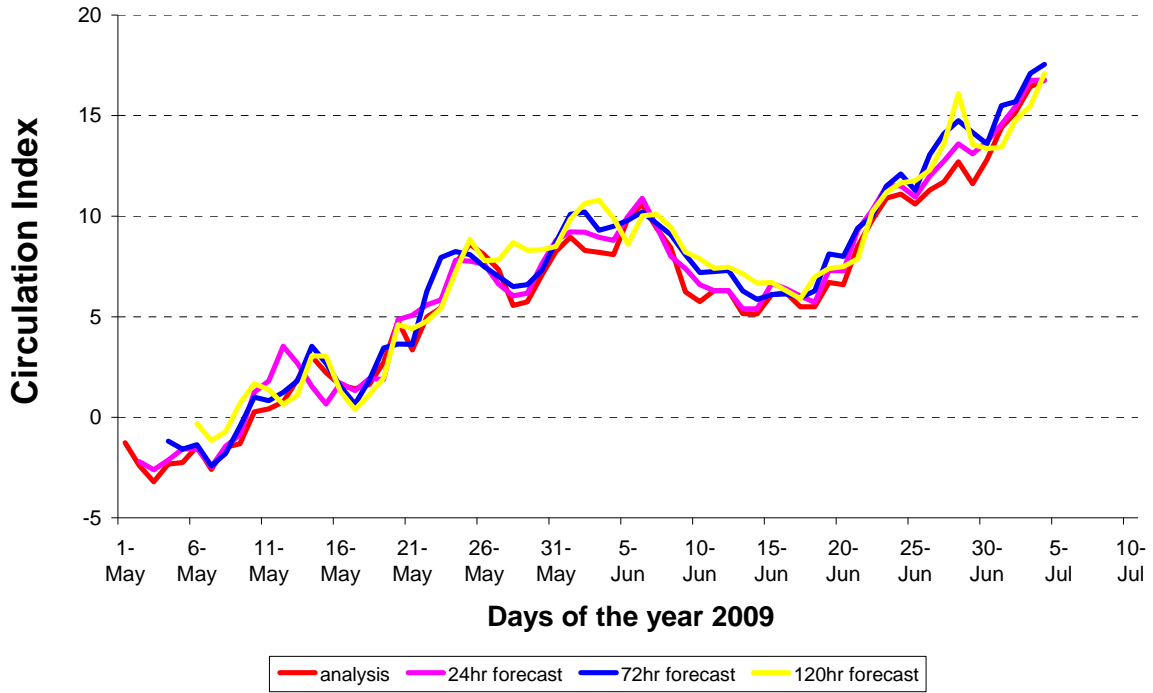


Figure 1(a)

T254L64 Syrok & Toumi Circulation Index

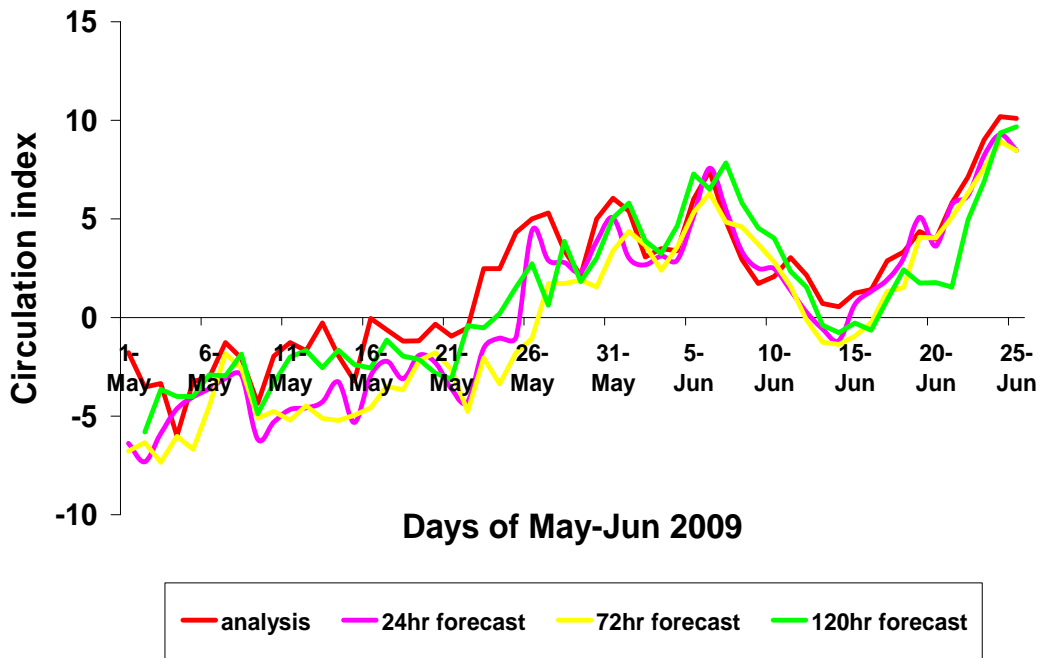


Figure 1(b)

T254L64 Goswami Hadley cell index

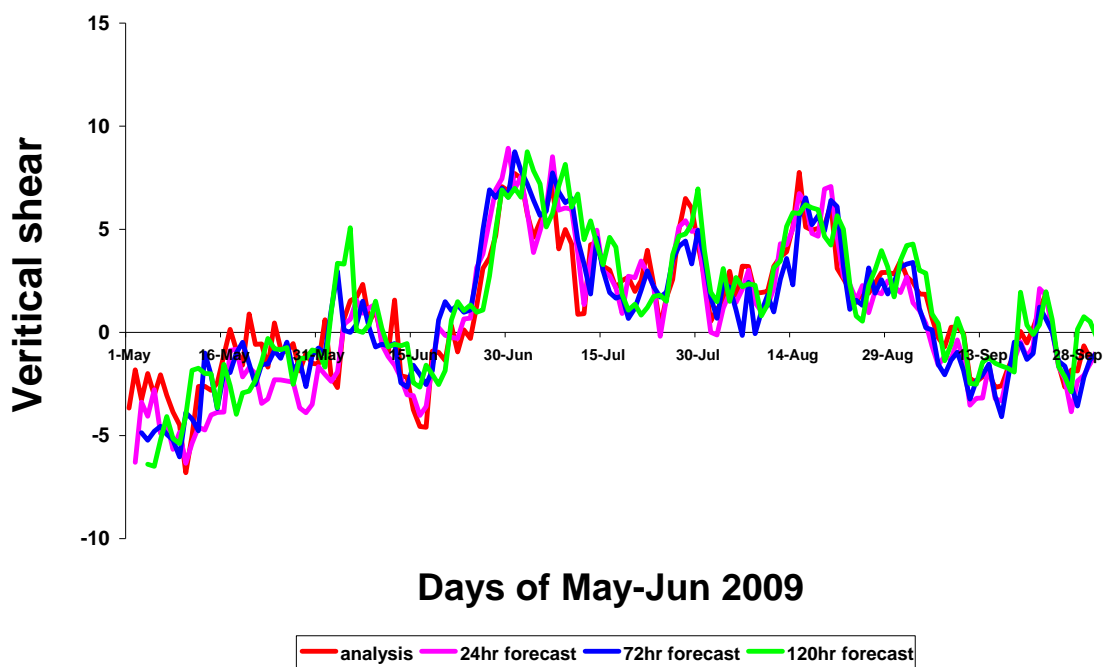


Figure 1(c)

T254L64 Wang & Ding Circulation Index

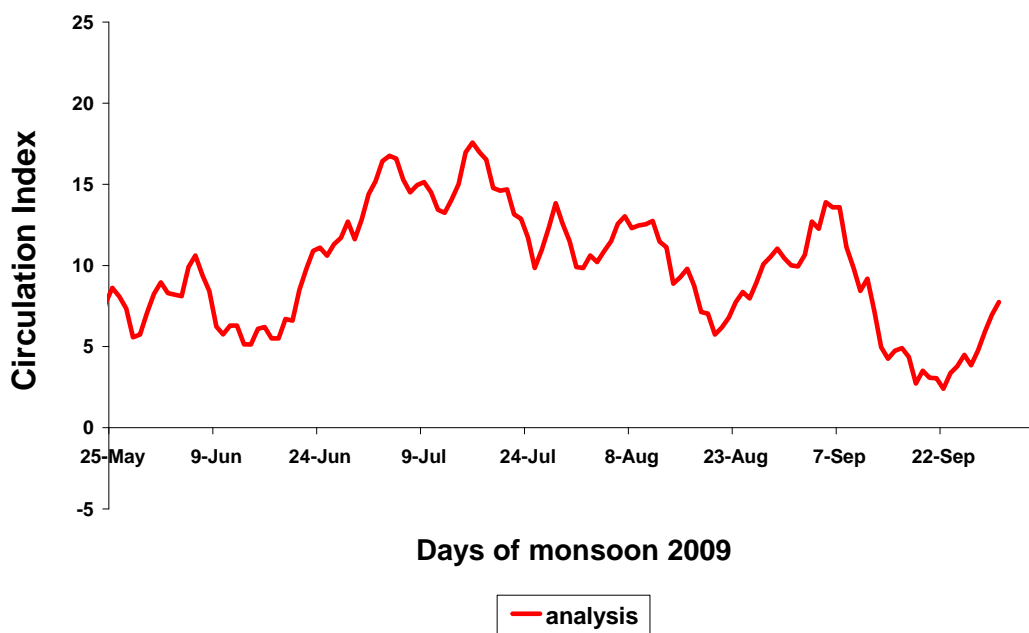


Figure 2 (a)

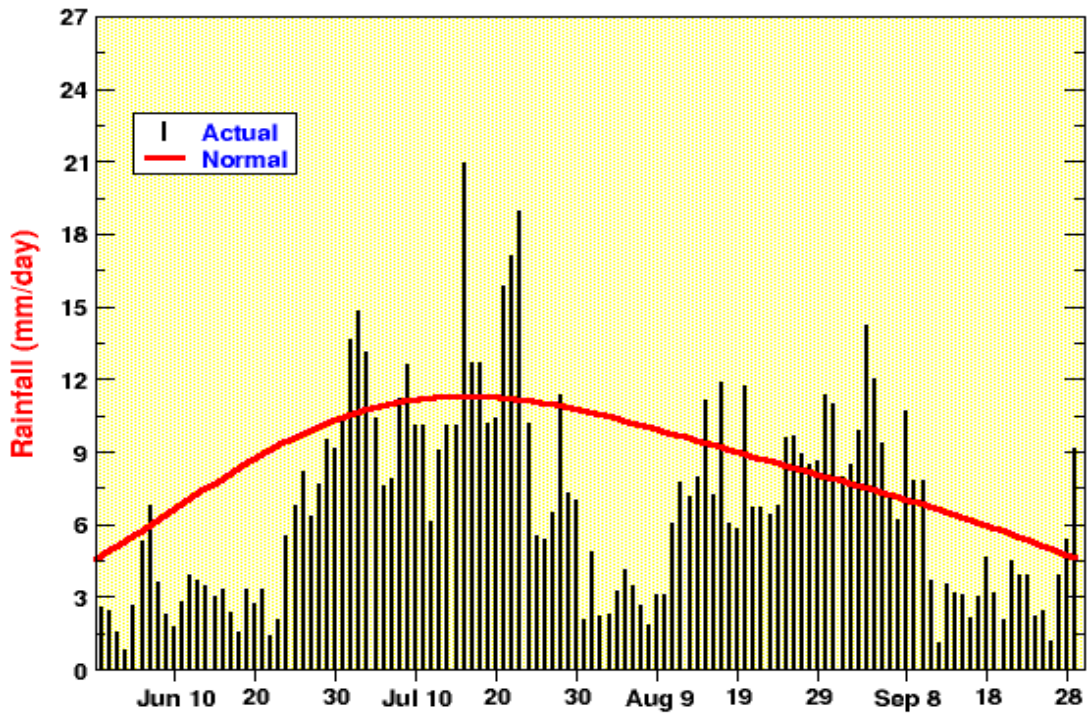


Figure 2(b)

T254L64 Syrok & Toumi Circulation Index

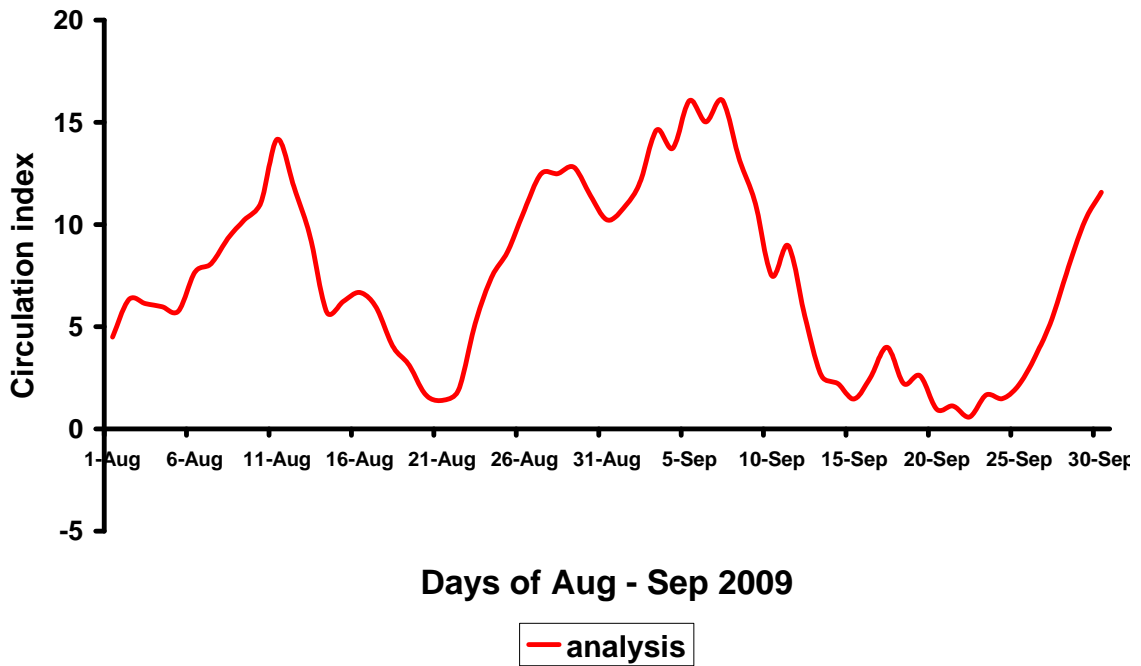


Figure 3

Heat Low, Monsoon Trough, Monsoon Lows and Depressions

R.G. Ashrit and John P. George

1. Introduction

The Heat low over northwest of India and monsoon trough over the Gangetic plains are the two most prominent quasi-permanent near surface features of monsoon circulation and are closely related to the large scale monsoon activity over the Indian sub-continent. Due to the intense heating in summer months a low pressure belt develops over the Afro-Asian continent running from North Africa to North-West (NW) India through Arabia and Pakistan. The deepest low pressure area over Pakistan and adjoining NW India is known as the heat low. The intensity of heat low is a good indicator of the continental heating and land-sea contrast which drives the monsoon. Deeper (shallower) heat low will usually be associated with stronger (weaker) North-South pressure gradient and enhanced (subdued) monsoon activity. The large scale monsoon activity is closely associated with the position of the monsoon trough. During the established phase of the monsoon, the monsoon trough normally runs at surface from Srirangapatna in NW India to the Head Bay of Bengal. A northward shift (towards the foothills of Himalayas in the extreme cases) of trough is usually associated with weaker monsoon activity over major parts of the country except over the Sub-Himalayan regions and South-East peninsula. A southward location of monsoon trough is favorable for good monsoon activity over large parts of the country. Monitoring and prediction of the position and the intensity of the monsoon trough is thus very important for assessment of monsoon activity. The characteristics of these two semi-permanent features, viz. Heat low and Monsoon trough in the global model analysis and day-1 forecasts, day-3 forecasts and day-5 forecasts during monsoon-2009 are examined in this chapter.

2. Heat Low

The intensity of the heat low is represented in this study by the magnitude of the innermost closed isobaric contour on a mean sea level pressure chart. By this terminology, a higher value of innermost closed isobar will mean shallower or less intense heat low. The average heat low centre pressure of the NCMRWF T254 model analyses and forecasts for different months during the monsoon season (Figure. 1) were examined to understand the behavior of the heat low during monsoon-2009. During June and July, the mean heat low position is around 70°E, 28°N in both in the analysis and forecast up to Day-5. In second

half of August and in the month of September, the mean MSLP values over this location were well above 1000 hPa. The Day-1, Day-3 and Day-5 forecast position of the heat low for all months, except September, are close to its analysis position. In June, the lowest MSLP contour in the analysis is 993 hPa whereas in the forecasts it is reduced to 991 hPa. In July, MSLP at heat low region is around 988 hPa in the analysis. The Day-1, Day-3 and Day-5 forecasts show values of 990, 990 and 991 hPa respectively during July. In the month of August, the heat low becomes weak in both analysis and forecast; particularly in the second half of August. In September no heat low is seen in both analysis and forecast. It is seen that the heat low is generally more intense in model forecast as compared to the analysis. Also the Day-1 and Day-3 forecast intensity is more than that of Day-5 forecast. In general, the model forecast tends to intensify the heat lows, compared to analysis.

3. Monsoon Trough

Monsoon trough is the most prominent semi-permanent feature of the Indian summer monsoon. Intensity and location of the monsoon trough is indicative of general monsoon condition over India and neighborhood. During JJAS of 2009 the north-south surface pressure gradient across the country was mostly weak throughout the season. The monsoon trough was also very shallow and during many occasions was situated north of its normal position. During 30-31 July and 13-19 September, the trough was close to the foothills of Himalayas. To identify the strength and position of the monsoon trough at surface level in the T254 analysis and forecast, the MSLP field is used in this study (Figure. 2).

In the month of June, compared to the mean analysis, Day-1, Day-3 and Day-5 forecasts show lower MSLP values over the monsoon trough region. The mean June position of the monsoon trough is the same in the analysis and the forecast, up to day-5 forecast and is over the Indo-Gangetic plains close to foot hills. The predicted MSLP over the eastern tip of the monsoon trough is lower than the analysis in June. In the July mean analysis, in the eastern part of the monsoon trough extends up to the head Bay, which was not the case in June where it extended only up to 88.0⁰ E. As in the case of June, the intensity of the monsoon trough is more in the forecast compared to analysis. It is also noted that monsoon trough intensity is more in Day-1 and Day-3 forecast compared to Day-5 forecast. The eastward and southward extension of the trough is also more in the initial days of the forecast, up to Day-3 forecast. In the month of August, the monsoon trough was weak. The T254 forecasts also clearly show the dramatic change from July to August.

However the MSLP values were much higher over the trough region in August compared to previous years. In September the monsoon trough is very weak both in analysis and in the corresponding forecasts.

4. Monsoon Depressions

As discussed before, the north-south surface pressure gradient across the country was mostly weak throughout the season leading to a shallow monsoon trough mostly situated north of its normal position. Further, the cross equatorial flow was weaker than normal during major part of the season except for a brief period from last week of June to third week of July. Due to these anomalous features, the activity of monsoon low pressure systems (lows and depressions) during this year was very much subdued compared to previous years. Only 4 depressions (2 each formed over the Arabian Sea and the Bay of Bengal) and 5 low pressure areas were formed during the season. The lifespan of most of these systems over land was short and therefore did not help for the persistent rainfall activity. The Figure.3 shows the tracks of depressions and deep depressions formed over Indian seas during the season.

The Global model forecast verification is carried out with the aim of studying the impact of higher resolution of the model and assimilation of satellite radiances. The study is carried out for the two depressions formed over Bay of Bengal and two depression formed over Arabian Sea.

- (1) Depression during 23-24 June 2009 over Arabian Sea near Gujarat coast.
- (2) Depression on 25th June 2009 over Arabian Sea near Gujarat coast.
- (3) Deep Depression during 20-21 July 2009 over coastal Orissa.
- (4) Deep Depression during 04-07 September 2009 over coastal Orissa.

(1) Depression during 23-24 June 2009 over Arabian Sea near Gujarat coast.

During the month of June, two depressions were formed. One depression formed over the east central Arabian Sea, moved northwards along the west coast and weakened after crossing the south Gujarat coast during 23-24 June. The location of this system in the T254 analysis and the forecasts valid for 23rd June 2009 is shown in Figure 4. The analysis and the Day-1 forecasts show the weak cyclonic circulation over west coast of India south of Gujarat.

While the Day-3 forecast shows that the system is located southwards and the Day-5 forecast suggests that the system is close to the coast but a much weaker circulation. Thus the short lived system is not predicted well by the model.

(2) Depression on 25th June 2009 over Arabian Sea near Gujarat coast.

The remnant of the Arabian Sea system during 23-24 June 2009 re-emerged over the northeast Arabian Sea and concentrating again into a depression moved northwards over the land during 25–26 June and weakened over Kutch and neighborhood. The analysis and the model forecast valid for 25th June 2009 are shown in Figure 5. The cyclonic circulation is rather weak in the analysis and in the forecasts it is completely missing.

(3) Deep Depression during 20-21 July 2009 over coastal Orissa.

During July, the synoptic activity was near normal. Two low pressure areas and a deep depression formed during the month. One of the low pressure areas (13-16 July) and the deep depression (20-21 July) formed over northwest Bay of Bengal, moved west northwestwards along the monsoon trough and caused normal to excess rainfall along west coast and over central parts of the country. The 850hPa winds in the analysis and the forecasts valid for 21st July are shown in Figure 6. The location of the depression after the landfall over Orissa is well captured in the analysis and the Day-1 and Day-3 forecasts. The location is correctly predicted in the Day-5 forecast, but the predicted intensity was rather weak.

(4) Deep Depression during 04-07 September 2009 over coastal Orissa.

In the month of September, one deep depression and one low pressure area were formed. The deep depression which formed over the northwest Bay of Bengal off Orissa coast (5 -7 September) initially moved northwestwards and then west northwestwards resulting an active monsoon conditions all along the west coast and central India. The interaction of the remnant of this system with trough in upper air westerlies also caused good rainfall activity over north India. The T254 model analysis and the forecasts valid for 6th September 2009 are shown in Figure 7. The model analysis shows an intense system over eastern India. The signature of the system is captured only upto the Day-1 forecast.

It is interesting to note that for the first two depressions discussed in Figure 4 and 5, the monsoon current is very weak in the analysis and the forecasts. However, for the next two depressions discussed in Figure 6 and 7, the monsoon current is enhanced. This clearly suggests that the model successfully captures and predicts the very well known classical feature of the low level monsoon circulation. The model predicted tracks of the four monsoon depression are shown in the Figure 8. A comparison with Figure 3 clearly suggests that none of the predicted track match accurately with the observation. It is generally noted that the movement of the cyclonic disturbances in the T254 model is generally rapid compared to the observations.

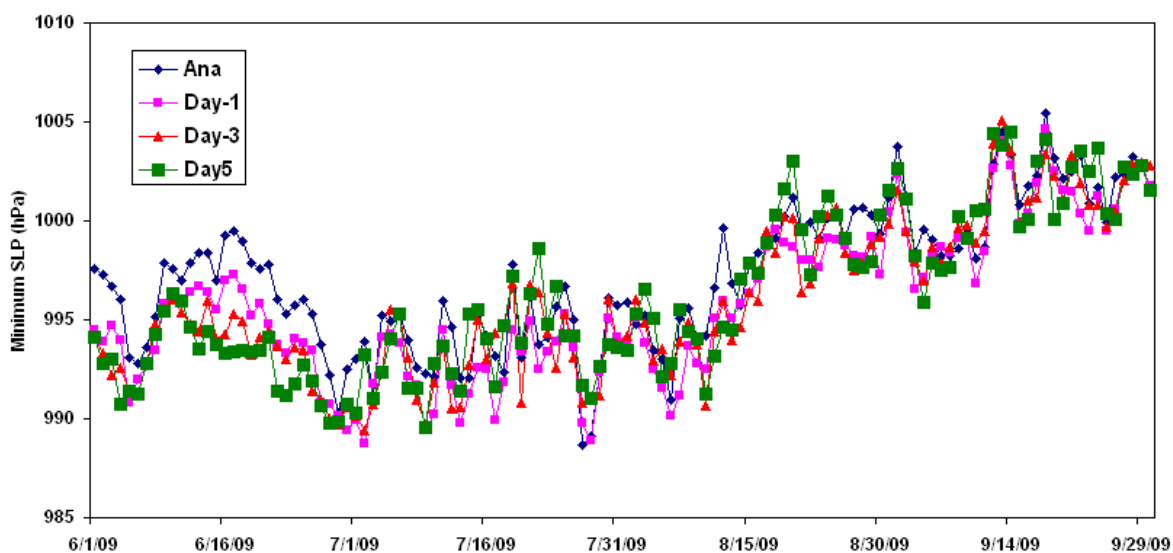


Figure 1. Central Pressure (SLP) of Heat Low in the T254 analysis and Day-1, Day-3 and day-5 forecasts

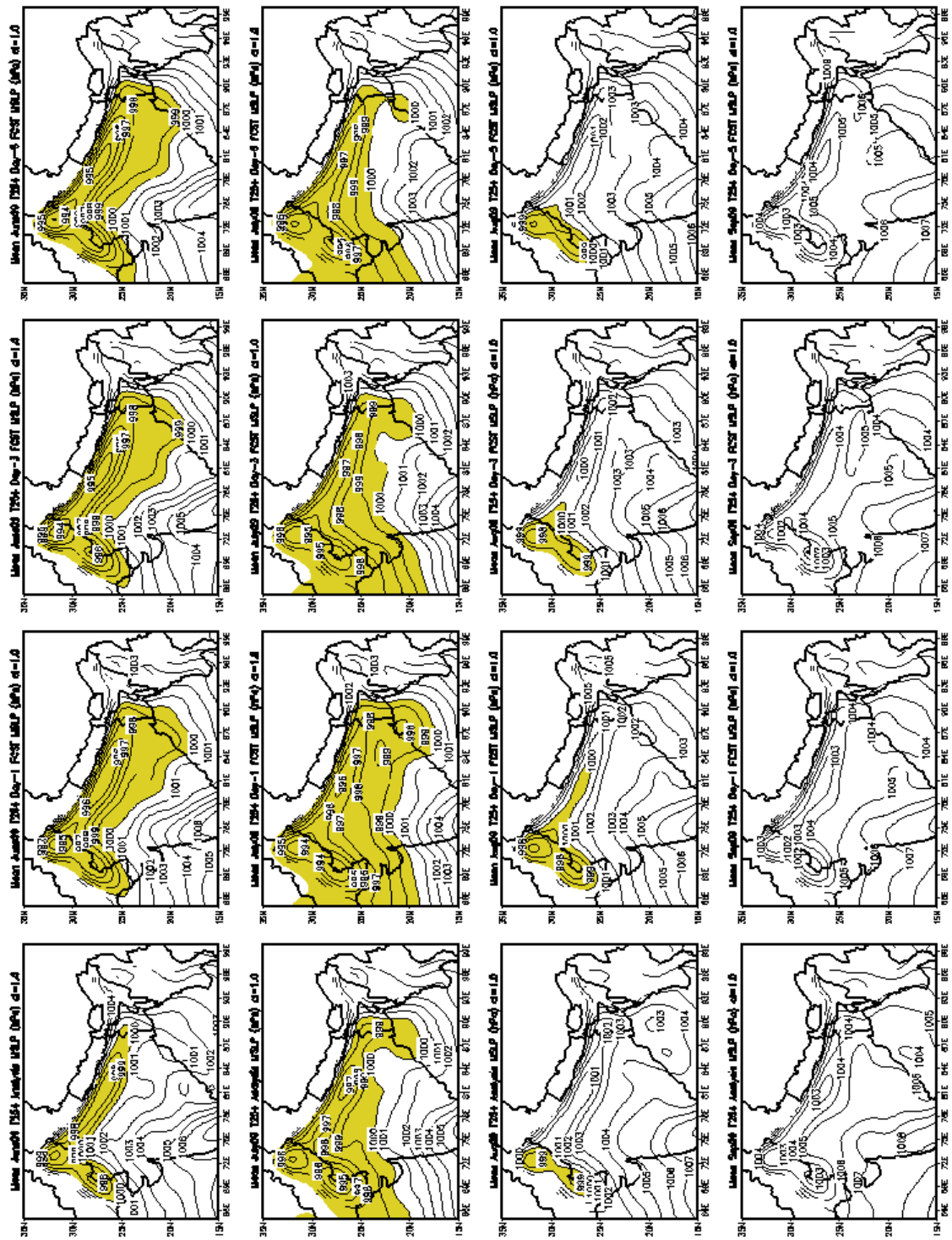


Figure.2 NCMRWF T254 model monthly mean of MSLP analysis and Day-1 (24 hrs), Day-3 (72 hrs) and Day-5 (120 hrs) forecast over the Indian region for June, July, August and September, 2009.

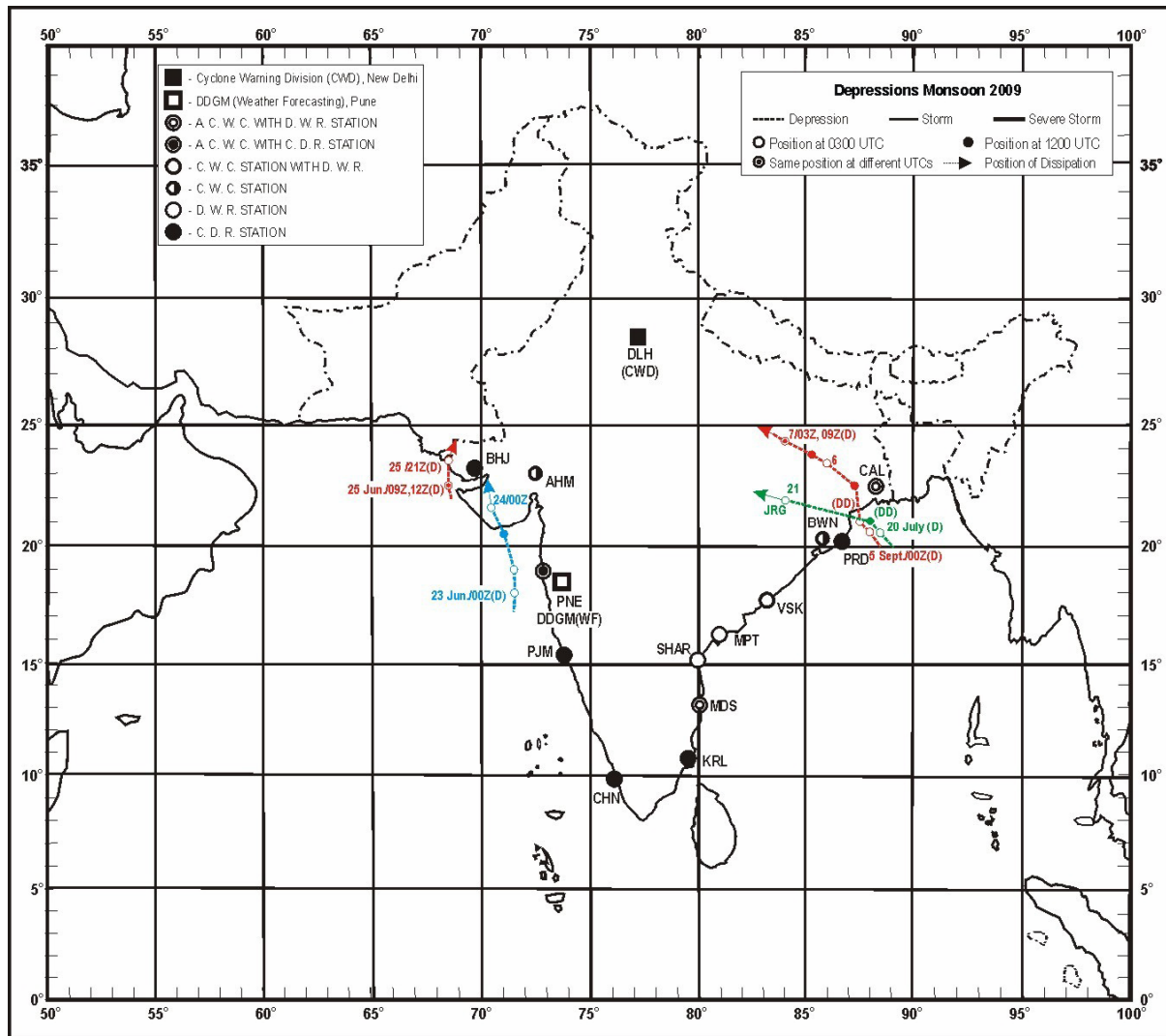


Figure 3. Observed tracks of the Arabian Sea and Bay of Bengal Monsoon depressions during JJAS 2009

T254: Winds at 850 hPa

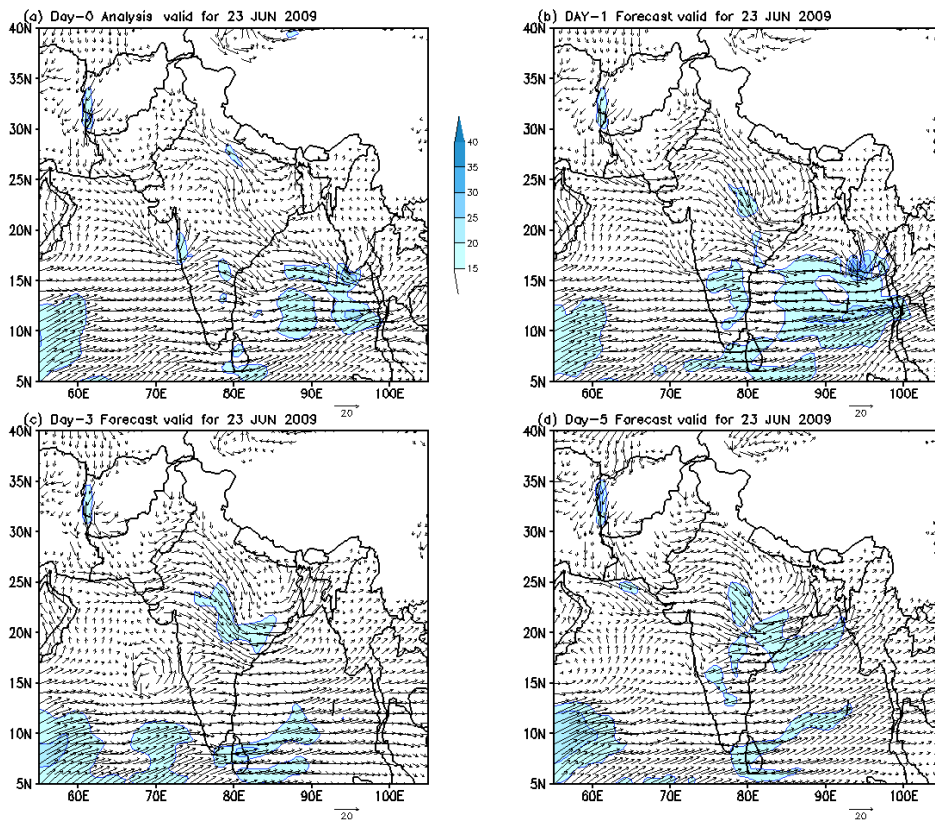


Figure 4. Winds at 850 hPa in the T254L64 analysis and forecasts valid for 23rd June 2009

T254: Winds at 850 hPa

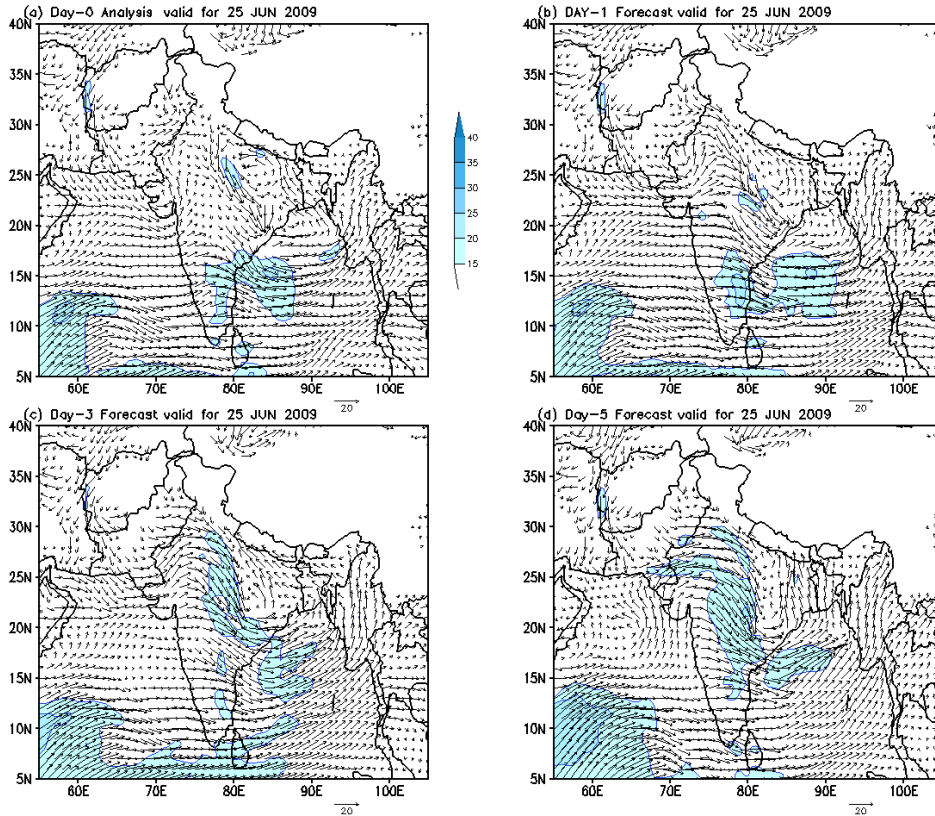


Figure 5. Winds at 850 hPa in the T254L64 analysis and forecasts valid for 25th June 2009

T254: Winds at 850 hPa

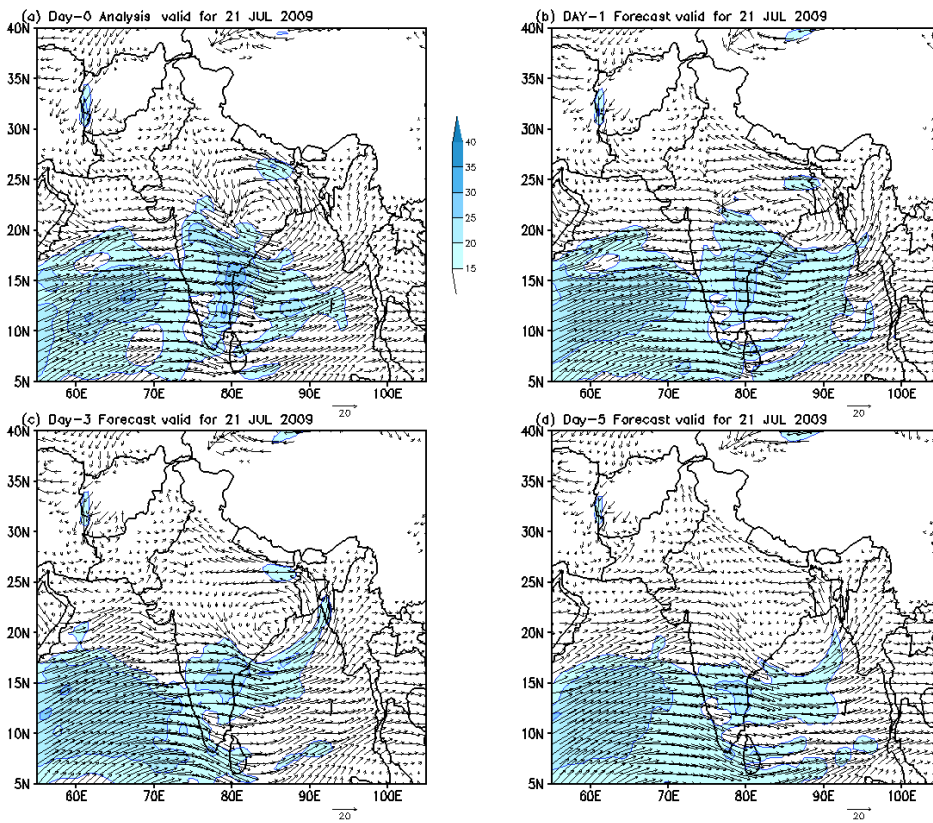


Figure 6. Winds at 850 hPa in the T254L64 analysis and forecasts valid for 21st Jul 2009

T254: Winds at 850 hPa

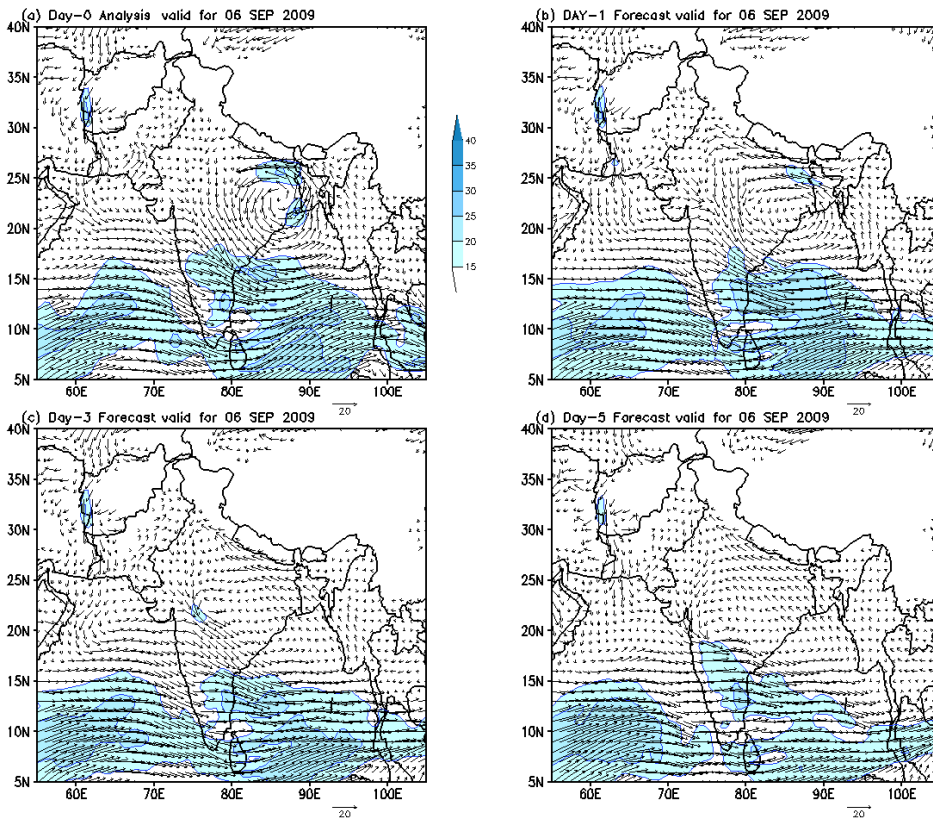


Figure 7. Winds at 850 hPa in the T254L64 analysis and forecasts valid for 6th Sept 2009

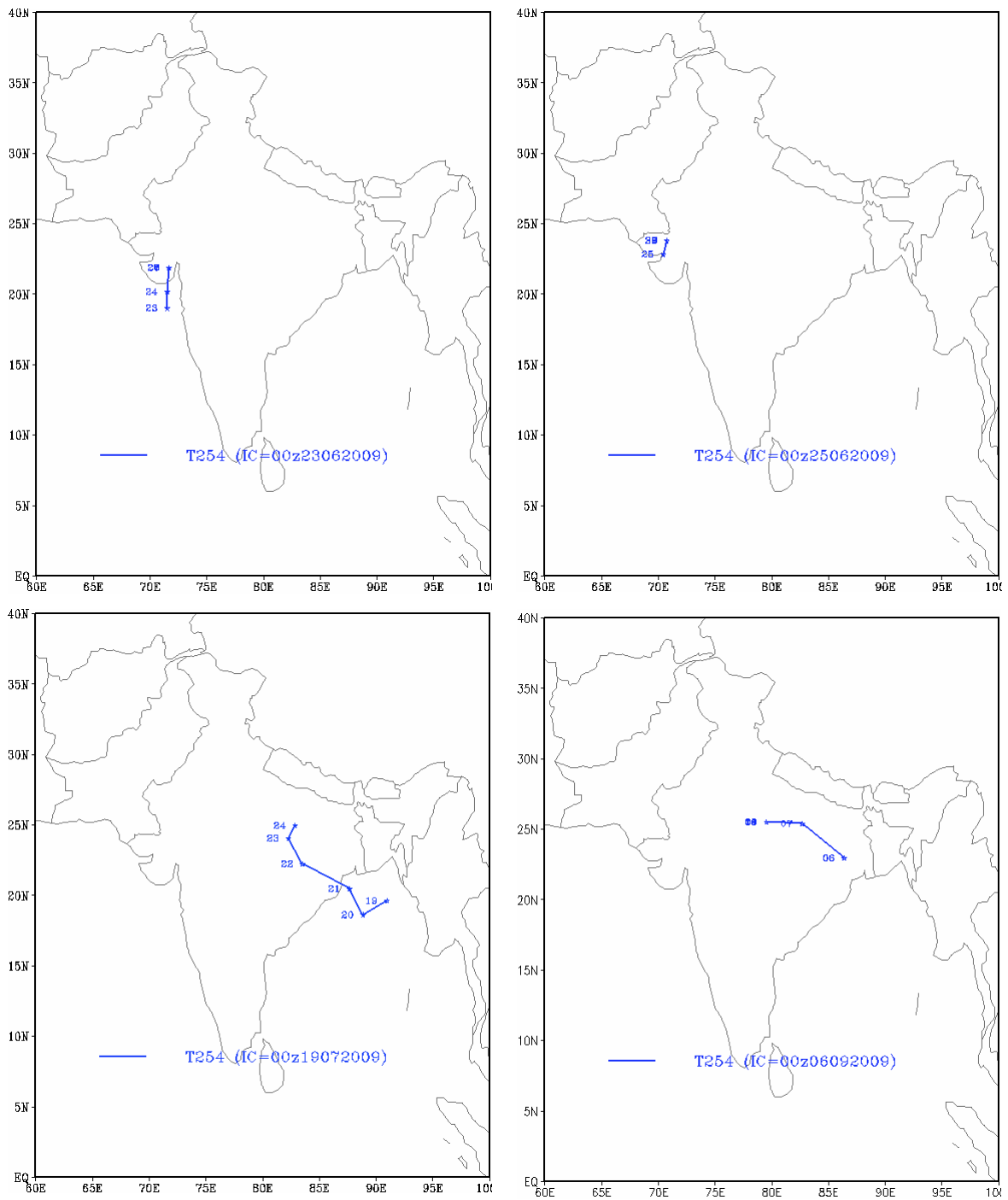


Figure 8. Model predicted tracks of the Monsoon depressions during JJAS 2009

Mascarene High, Cross-Equatorial Flow, Low-Level Westerly Jet and North-South Pressure Gradient During Monsoon 2009

A. K. Mitra, M. Das Gupta and G.R.Iyengar

1. Introduction

Low-level westerly jet is one of the most important feature of the south Asian summer monsoon system. Various features of this low level jet and associated inter-hemispheric moisture transport were documented four decades ago (Bunker, 1965; Tucker 1965; Findlatter, 1966; Joseph and Raman, 1966; Saha and Bavedkar, 1973). Through the cross-equatorial flow, southern hemisphere's Mascarene High influences the low level jet in the Arabian Sea. As this is associated with strong wind maxima offshore from Somalia, this jet is also known as Somali Jet. Indian monsoon rainfall and its active/break phases are linked to the weather systems in the southern hemisphere midlatitudes (Rodwell, 1997; Fukutomi and Yasunari, 2005). The low-level flow from the southern hemisphere interacts with the cross equatorial flow and the low level westerly jet in the Arabian Sea to shape the rainfall pattern (Anderson, 1976). Heating pattern over the southern Indian Ocean is linked to the strength/position of the East African jet, which modulates the flow over Indian monsoon region (Rodwell and Hoskins, 1995). In the southern Indian ocean significant high frequency (periods 2-6 days) transient eddy activity are seen associated with northern summer monsoon (James and Anderson, 1984). This tropical-extratropical connection in the Indian Ocean region has to be simulated correctly by the model to represent the monsoon precipitation in the medium range time scale. The final strength of the monsoon flow is manifested in the north-south pressure gradient along the west coast of India. Arabian Sea and the Bay of Bengal are among the few regions of earth, where the low-level jets (LLJ) are seen with some regularity in the annual cycle. These jets are related to the synoptic-scale forcing and have narrow zones of high-speed flow that extend for hundreds of kilometers. These LLJs have appreciable horizontal and vertical shear. These are also important for the fluxes of temperature and moisture (both horizontal and vertical) and are generally associated with the development and evolution of deep convection over the Indian sub-continent and the neighboring regions of south Asia. Under a wide variety of synoptic conditions, the proper representation of the development and the evolution of these LLJs in a global numerical model (with particular resolution) the physical mechanisms like the shallow baroclinicity (in PBL) interacting with many factors like the strong geostrophic forcing, the horizontal SST gradients, terrain effects are to be taken care of adequately (Stensrud, 1996; Krishnamurti et al., 1976). Surface winds, SST over Arabian Sea and

other associated parameters are related to the rainfall over Indian sub-continent during monsoon (Shukla and Misra, 1977; Raghavan et al., 1978). Similar relation of SST and low-level winds for the tropics in general was also shown in relation to the tropical deep convection (Lindzen and Nigam, 1987).

Oscillations in the strength of the components of monsoon flow have been linked to variability of monsoon rainfall. This low level jet is found to have large intraseasonal variability, affecting the moisture transport and finally the active/break conditions in convection over India and Bay of Bengal region (Joseph and Sijikumar, 2004). The splitting of the Somali Jet depends on the variable synoptic conditions, mean flow strength (dynamical feature of jet width and wavelength) and the evolving transients in the region (Thompson et al., 2008). Features of the large-scale monsoon circulation are related to the interaction of diabatic heating, orography (mountains) and their non-linear interactions with flow itself (Hoskins and Rodwell, 1995). Representations of these interactions in a model are essential to numerically simulate the low-level monsoon flow realistically (Krishnamurti et al., 1976; krishnamurti and Wong, 1979; Krishnamurti et al., 1983). The global model has to be realistic to capture the jet split. The model vertical and horizontal resolution should also be fine enough to represent adequately the forces responsible for maintenance and day-to-day variations in the strength of the low level westerly jet over the Arabian Sea. A higher resolution model is highly desirable for capturing the meso-scale convective structures in the monsoon system adequately and the associated details of monsoon rainfall distribution (Sperber et al., 1994; Martin, 1999; Teixeira, 1999). Since the low-level jet is very important in monsoon dynamics, monsoon modellers have to take adequate care to see that the low level flow and the associated deep convection and their variability are properly captured in model. This low level jet is intimately related to the cross-equatorial flow (inter hemispheric flow) deciding the moisture transport and hence the fate of the rainfall associated with Indian monsoon (Ramesh Kumar et al., 1999).

The performance of the high resolution global model's (T254L64) assimilation-forecast system running in real-time during the monsoon 2009 in respect of the Mascarene High (MH), Cross-equatorial flow (CEF), the low level westerly jet (LLWJ) and the north-south pressure gradient along west coast is described briefly in this chapter. Description of the global modeling system with its assimilation aspects are described in chapter one of this report.

2. Performance of Model

2.1 Mascarene High (MH)

During monsoon 2009, the analyzed mean intensity of the Mascarene High was 1032.8 hPa and its mean position was approximately at 67° E and 35° S, as seen from the data of T254L64 global modelling system. The observed analysed positions from the modeling system (during 2009) are to further south in latitudinal position of the long-term (80 years mean data) observed mean location of 69° E, 27° S with intensity of 1024 hPa (Gorshkov, 1977). Three panels in Fig. 1 show the day-to-day variations of the intensity of the Mascarene High produced by the T254L64 analyses (lines with square marks) during monsoon (June-September 2009). The corresponding intensities from the T254L64 model forecasts for Day-1, Day-3 and Day-5 are shown in lines with diamond marks. The intensities produced in Day-1 forecasts agree very well with the analysis. For the Day-3 forecasts, a very good agreement is seen in general, except few episodes. In Day-5 forecasts the disagreement is more compared to Day-1 and Day-3 forecasts. The root mean square errors (RMSE) of the predicted intensity of the Mascarene High for Day-1, Day-3 and Day-5 forecasts are 1.2 hPa, 3.3 hPa and 3.9 hPa respectively. These errors are lower compared to the errors seen during monsoon 2008 season.

The longitudinal positions of the Mascarene High (MH) produced from T254L64 system's analysis (lines with square marks) and forecast (lines with diamond marks) are shown in different panels of Fig.2 for the monsoon 2009 period. From the analyzed positions it is seen that the major Indian Ocean Anticyclone (MH) moves from west to east in association with the passage of southern hemisphere's westerly waves with variations in the amount of eastward movement in time. The Day-1 forecasts are able to reproduce these variations very well. The agreement between the analysis and the Day-3 forecasts are also generally very good, with just few noticeable mismatches. The Day-5 forecasts indicate that the variability in longitudinal positions are captured well, but have more errors compared to the Day-1 and Day-3 forecasts. The RMSE of the predicted longitudinal positions of the Mascarene High for Day-1, Day-3 and Day-5 forecasts are 9.4° , 16.5° and 18.5° respectively. These errors are lesser in magnitude compared to those during monsoon 2008 period.

Latitudinal positions of the Mascarene High during monsoon 2009 are shown in different panels of figures 3. Lines with square marks show the analysed (observed) positions, and the line with diamond marks show the predicted positions. From the analyzed positions it is clear that the MH also oscillates in north-south direction around its mean position during monsoon season. In

the T254L64 model, the Day-1 and Day-3 forecasts are agreeing well with the analyzed latitudinal positions, except few episodes. In Day-5 forecasts the positional errors are more compared to Day-1 and Day-3 errors. The RMSE of the predicted latitudinal positions of the Mascarene High for Day-1, Day-3 and Day-5 forecasts are 2.3° , 3.5° and 3.8° respectively. These errors are lesser to those compared for the monsoon 2008 period.

2.2 Cross-Equatorial Flow (CEF)

The time mean analyzed, Day-1, Day-3 and Day-5 forecasts of the meridional wind at equator over the sector 30° E- 100° E with mean taken over the entire monsoon period (June to September 2009) are shown in figure 4 in the form of longitude-height cross-sections. In T254L64 model, the analyzed field shows prominent maxima of 14 mps around 40° E at 875 hPa representing the core of the Arabian Sea branch of the cross-equatorial flow and a secondary maxima of 3 mps between 80° E - 90° E, representing the Bay of Bengal branch. The dual core of cross-equatorial flow in the Arabian Sea is not seen in this year's analysis, which was observed during monsoon season of 1995 and 1998. This dual core was also absent in recent monsoons of 2005, 2006, 2007 and 2008 (NCMRWF Report 2006a; NCMRWF Report 2006b; NCMRWF Report 2008; NCMRWF Report 2009). During monsoon 2009, all the forecasts (day-1 through day-5 predictions) of the cross-equatorial flow (Arabian Sea branch) indicate a slight intensification of the strength of cross equatorial flow to 15 mps (very similar to monsoon 2007 and 2008). The core of the Arabian Sea branch of CEF is well maintained during forecast at 15 mps in a very consistent way. The Bay of Bengal branch of the cross-equatorial flow is also maintained well in the T254L64 model. The 3 mps contour over bay of Bengal(BoB) region is seen to descend to lower levels further, indicating a slight weakening of the BoB branch of low-level jet in terms of its vertical extent. Overall, the skill of the T254L64 model is very good during monsoon 2009, in terms of capturing and maintaining the low-level cross equatorial flow both in the Arabian Sea and the Bay of Bengal.

The mean (June to September 2009) vertical profiles of meridional wind averaged over the domain 2.5° S - 2.5° N; 39° E - 51° E from the analysed, Day-1, Day-3, and Day-5 prediction fields from T254L64 are shown in figure 5. It is seen that the maxima of the cross-equatorial flow occurs at around 875 hPa in the mean analysis. The intensity and location forecasts of CEF from the T254L64 model agrees very well with the observations (analysis), indicating that the CEF is well maintained in the T254L64 model. Only marginal intensification is noticed on day-3 and day-5 between 900 and 800 hPa.

2.3 Low-Level Westerly Jet (LLWJ)

The mean analyzed and predicted positions and strength of the low-level westerly jet (LLWJ) in the Arabian Sea at 850 hPa from T254L64 are shown in different panels of figure 6 for the whole monsoon season. This diagram brings out clearly the well maintenance of the strength and location of LLWJ during monsoon 2009 in the Arabian Sea throughout the forecast length (day-1 through day-5) in this high-resolution model. The contour of 15 mps adjacent to Somalia coast in the Arabian Sea is very consistent in analysis and the forecasts. The winds in the Bay of Bengal and peninsular India are also very well maintained in the forecasts compared to the analysis. As a result the monsoon trough over the central India is also well maintained in the forecasts in the T254L64 model.

The north-south cross-sections of seasonal mean analyzed and predicted (Day-1, Day-3 and Day-5) zonal component of wind along 54° E, a longitude which falls within the climatological location of LLWJ, from T254L64 model are given in figure 7. The observed core of the jet matches with the climatological location. The jet core is observed to be at 16 mps in T254L64 model. Here the second core (dual core) of 10 mps at around 14° N is also seen during 2009 monsoon. The model forecasts (Day -1 through Day -5) are matching very well with the observed jet strength and position. Even the dual core system is very well maintained in the model. Throughout the forecast length the LLWJ is seen to be very consistent in structure among each other and also with the observed analysis. The strength is seen to be slightly intensifying from day-3 (16 mps) to day-5 (17 mps) forecasts. In general, the representation and maintenance of LLWJ is very good in the high resolution T254L64 model.

The latitude-height cross-sections of seasonal mean analyzed and predicted zonal wind along 75° E (a longitude where the low-level westerlies interact with the west coast orography leading to heavy rainfall) from T254L64 system is given in figure 8. The maximum zonal wind in analysis is seen to be around 9 mps. The second core at 16° N represents the monsoon trough region (a very important feature of monsoon system) is seen to be quite strong at 9 mps. During the forecast in general the strength is well maintained, with slight intensification to 11 mps in day-3 and day-5. The position and intensity of the monsoon trough is also well maintained. The strength of the core at 9° N is well maintained. Unlike 2007 and 2008, this season the monsoon trough is not seen to move southward during forecasts. Therefore the rainfall forecast associated with monsoon trough should be better in 2009 compared to 2007 and 2008 season. Figure 9 shows the daily verification

of day-1, day-3 and day-5 forecasts of the zonal winds (u) at a station (Goa) against RS/RW observed values at 850 hPa during monsoon 2009. It is seen that daily variability of wind at a station is also captured well in the model forecasts. The RMS errors of the day-1, day-3 and day-5 forecasts are 4.27, 4.35 and 4.85 mps respectively. The error of the analysis itself (from the data assimilation system) is seen to be 2.21 mps during the season. This shows that the high resolution model forecasts do a fairly good job in capturing the zonal wind variability even at a station like Goa. The remarkable day-to-day agreement of the analysis with the station values during the season show the efficiency of the NCEP based GSI data assimilation system for monsoon.

2.4 North-South Pressure Gradient

The daily variations of analyzed (line with square marks) and predicted (line with diamond marks) values of north-south pressure gradient along the west coast of India from T254L64 model are shown in different panels of figure 10, for the monsoon 2009 season. In T254L64 model, the day-1 forecasts match very well with the corresponding analyzed values. Even in day-3 forecasts the feature of north-south pressure gradient along west coast of India is captured reasonably well. However, day-5 forecasts have higher errors (in amplitude and phases) compared to day-1 and day-3 forecasts. In T254L64 model the RMSE of the predicted north-south pressure gradient along the west coast of India for Day-1, Day-3 and Day-5 forecasts are 1.6, 2.0 and 2.1 hPa respectively. These errors are lesser in magnitude as compared to monsoon 2008 season from the same model. Overall, in high resolution T254L64 model the day-to-day variability in the north-south pressure gradient (a measure of strength of monsoon) in terms of amplitude and phases are captured well.

3. Summary

The T254L64 global model running in real time with its assimilation system is able to represent the low level features of monsoon circulation system adequately. During monsoon 2009, in general the medium range forecasts from the model are able to bring out the order of variability in the intensity and positions of Mascarene High. The cross-equatorial flow near its core is captured well in the model having less error. The low level westerly jet's strength and positions near Somalia coast are represented well. All these features are manifested in the T254L64 model representation of low-level wind flow, north-south pressure gradient and the monsoon trough over India sub-continent. Overall the global modelling system captures the low-level circulation features well. In most of the features examined here, it is noticed that the errors during 2009 season are generally lesser compared to those noticed during previous monsoon season.

Legends for Figures

Fig. 1. Intensity of the Mascarene high in the analysis against Day-1, Day-3 and Day-5 forecasts during monsoon 2009.

Fig. 2. Longitudinal position of Mascarene high in the analysis against Day-1, Day-3 and Day-5 forecasts during monsoon 2009.

Fig. 3. Latitudinal position of Mascarene high in the analysis against Day-1, Day-3 and Day-5 forecasts during monsoon 2009.

Fig. 4. Time mean analyzed, Day-1, Day-3 and Day-5 forecasts of meridional wind at equator over the sector 30°E - 100°E , during monsoon 2009.

Fig. 5. Time mean vertical profiles of meridional wind averaged over the domain 2.5°S - 2.5°N & 39°E - 51°E , during monsoon 2009.

Fig. 6. Mean analyzed, Day-1, Day-3 and Day-5 forecasts of 850 hPa flow pattern and wind speeds, during monsoon 2009.

Fig. 7. North-south cross-section of seasonal mean analyzed, Day-1, Day-3 and Day-5 forecasts for Zonal component of wind along 54°E , during monsoon 2009.

Fig. 8. North-south cross-section of seasonal mean analyzed, Day-1, Day-3 and Day-5 forecasts for Zonal component of wind along 75°E , during monsoon 2009.

Fig. 9. Daily verification of day-1, day-3 and day-5, forecast zonal winds (u) at a station (Mumbai) against RS/RW observed values during monsoon 2009, at 850 hPa

Fig. 10. Analyzed, Day-1, Day-3 and Day-5 forecasts of North-South Pressure Gradient along west coast during monsoon 2009

Reference

Anderson,D.L.T., 1976: The low level jet as a western boundary current , MWR, 104 , 907 - 921

Bunker,A.F., 1965: 'Interaction of the Summer Monsoon air with the Arabian Sea (preliminary analysis)', Proceedings of Symp. Meteor. Results from IIOE, July 1965, Bombay, India, 3-16

Findlatter,J., 1966 "Cross-equatorial jet streams at low level over Kenya ", Met. Mag., 95, 353-364

Fukutomi, Y., and Tetsuzo Yasunari, 2005, Southerly Surges on Submonthly Time Scales over the Eastern Indian Ocean during the Southern Hemisphere Winter, MWR, 133(6), 1637-1654

Gorshkov, S.G., (Ed.), 1977: World Ocean Atlas - Atlantic and Indian Oceans, Chief Directorate of Navigation and Oceanography, Former USSR

Hoskins, B. J., and M.J.Rodwell 1995: A model of the Asian summer Monsoon. part I : The global scale , JAS , 52 , 1329 - 1340

Joseph P.V., and S. Sijikumar, 2004, Intraseasonal Variability of the Low-Level Jet Stream of the Asian Summer Monsoon , J Clim., 17(7), 1449–1458

Joseph,P.V. and P.L.Raman 1966: Existence of LLWJ stream over Peninsular India during July, Ind. J. Meteor. Geophys., 17 , 407-410

Krishnamurti, T.N.K. , V. Wong , H. L. Pan , R. Pasch , J. Molinari and P. Ardanuy 1983 : A three dimensional planetary boundary layer model for the Somali Jet , JAS , 40 , 894 - 908

- Krishnamurti, T.N.K., and V. Wong 1979: A simulation of cross-equatorial flow over the Arabian Sea, *JAS*, 36, 1895-1907
- Krishnamurti, T.N.K., J. Molinari and H.L. Pan 1976: Numerical Simulation of the Somali Jet, *JAS*, 33, 2350-2362
- Lindzen, R.S. and R.S. Nigam 1987: On the role of SST gradients in forcing low-level winds and convergence in tropics, *JAS*, 44, 2418-2436
- Martin, G.M., 1999: Simulation of the Asian summer monsoon, and its sensitivity to horizontal resolution, in UK Met. Office UM, *QJRMS*, part A, 125(557), 1499-1525
- NCMRWF, DST(GOI), January 2006a: 'Monsoon 2005: Performance of the NCMRWF Global Assimilation Forecast System', Report no. NMRF/MR/01/2006, 139 pages, Published by NCMRWF(DST), A-50, Institute Area, Sector – 62, UP, India 201307, chapter 5, pages 71–88
- NCMRWF, MoES(GOI), December 2006b: 'Monsoon 2006: Performance of the NCMRWF Global Assimilation-Forecast System', Report no. NMRF/MR/02/2006, 114 pages, Published by NCMRWF(MoES), A-50, Institute Area, Sector–62, UP, India 201307, Chapter 4, pages 51–66
- NCMRWF, MoES(GOI), January 2008: 'Monsoon 2007: Performance of T254L64 Global Assimilation-Forecast System', Report no. NMRF/MR/01/2008, 143 pages, Published by NCMRWF(MoES), A-50, Institute Area, Sector–62, UP, India 201307, Chapter 5, pages 67–93
- NCMRWF, MoES(GOI), February 2009: 'Monsoon 2008: Performance of T254L64 Global Assimilation-Forecast System', Report no. NMRF/MR/01/2009, 117 pages, Published by NCMRWF(MoES), A-50, Institute Area, Sector–62, UP, India 201307, Chapter 6, pages 81–97
- Raghavan, K., P.V. Puranik and V.R. Majumdar, P. Ismail and D.K. Paul 1978: Interaction between the west Arabian Sea and the Indian Monsoon, *MWR*, 106, 719 - 724
- Ramesh Kumar M. R., S. S. C. Shenoi and P. Schluessel, 1999: On the role of the cross equatorial flow on summer monsoon rainfall over India using NCEP/NCAR reanalysis data, *MAP*, 70(3-4), 201-213
- Rodwell, M.J., 1997: Breaks in the Asian Monsoon: The influence of southern hemisphere weather system, *JAS*, 54(22), 2597-2611
- Saha, K.R. and S.N. Bavedkar 1973: Water vapour budget and precipitation over the Arabian Sea during the northern summer, *QJRMS*, 99, 273-278
- Shukla, J., and B.M. Mishra 1977: Relationships between SST and wind speed over the central Arabian Sea and monsoon rainfall over India, *MWR*, 105, 998-1002
- Sperber, K.R., S. Hameed, G.L. Potter and J.S. Boyle 1994: "Simulation of the northern summer monsoon in the ECMWF Model: Sensitivity to horizontal resolution", *MWR*, 122(11), 2461-2441
- Stensrud, D.J., 1996: Importance of Low-Level Jets to Climate: A Review, *J. of Climate*, 8(9), 1698-1711
- Teixeira, J., 1999: The impact of increased boundary layer vertical resolution on the ECMWF forecast system. *ECMWF Tec. Mem. No268*. Feb. 1999, ECMWF, Reading, UK, pp. 55
- Thompson A, L. Stefanova and T.N. Krishnamurti, 2008, Baroclinic splitting of jets, *MAP*, 100, 257-274
- Tucker, G.B., 1965: "The equatorial tropospheric wind regime", *QJRMS*, 91, 140-150

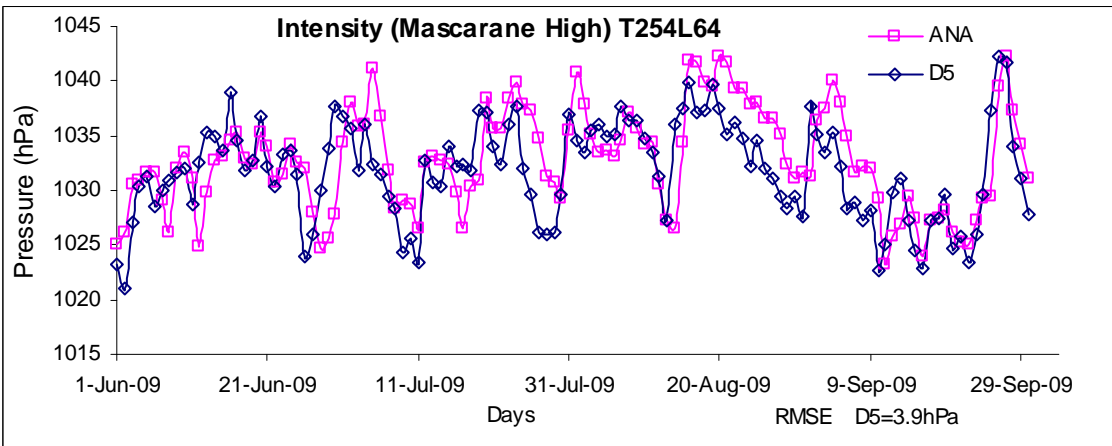
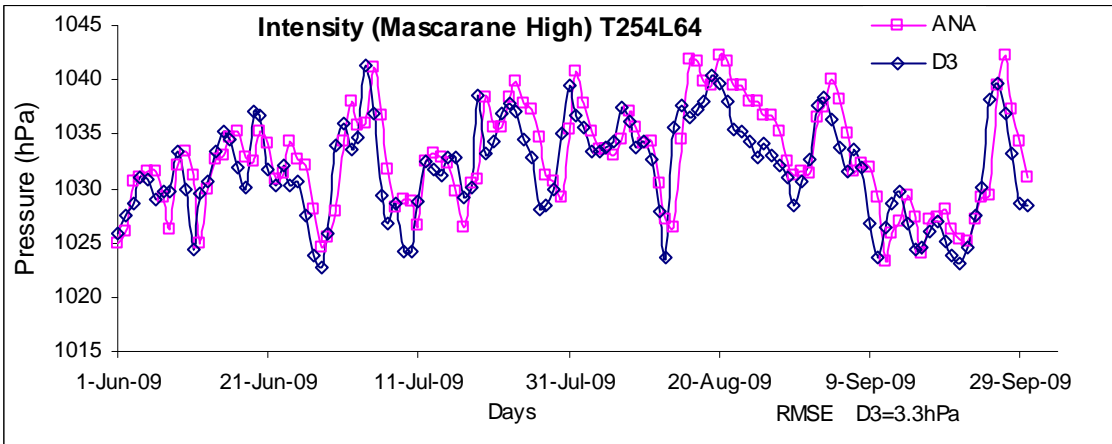
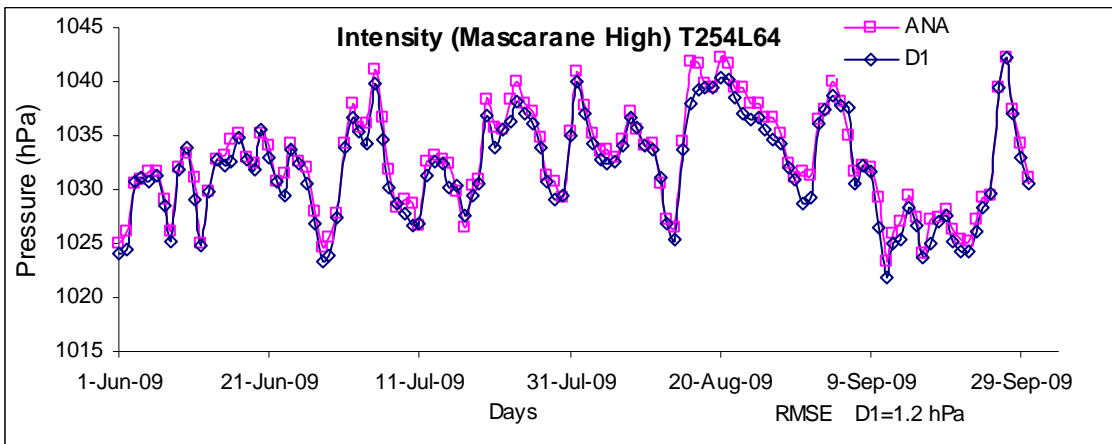


Fig. 1

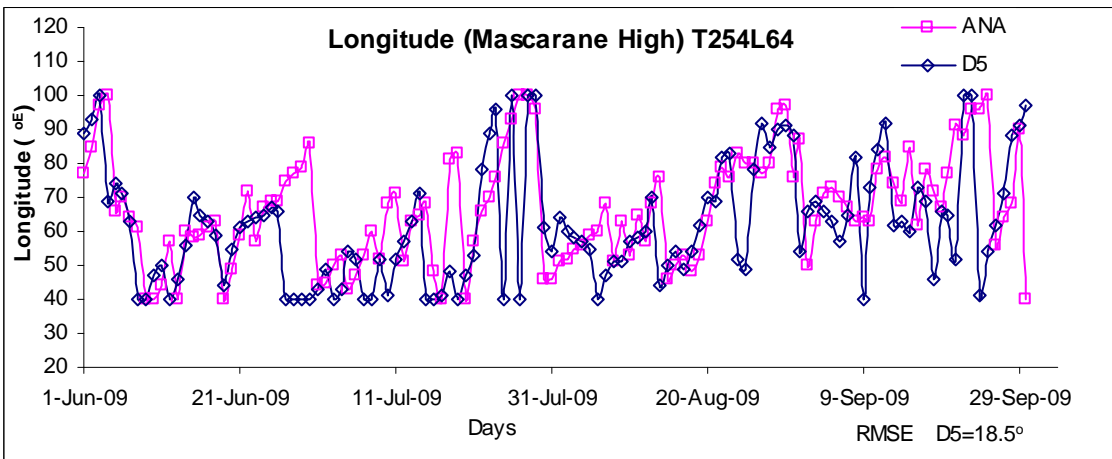
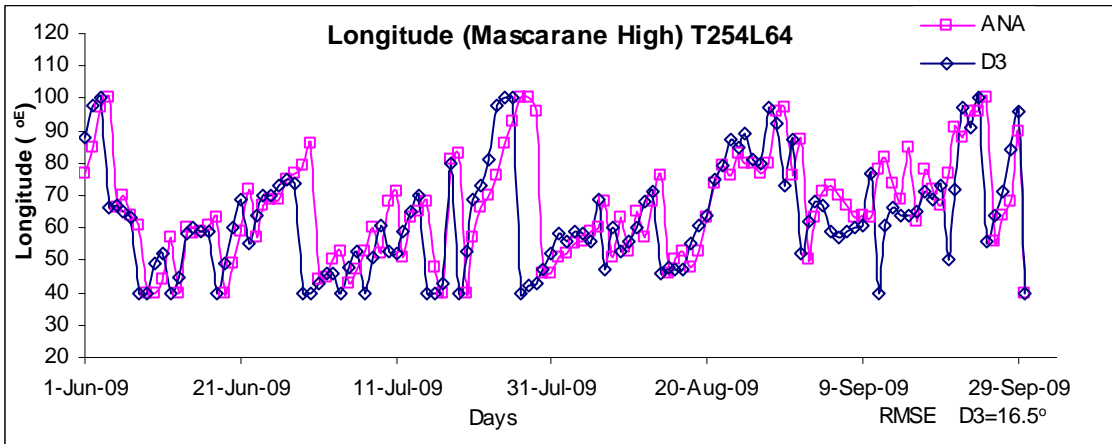
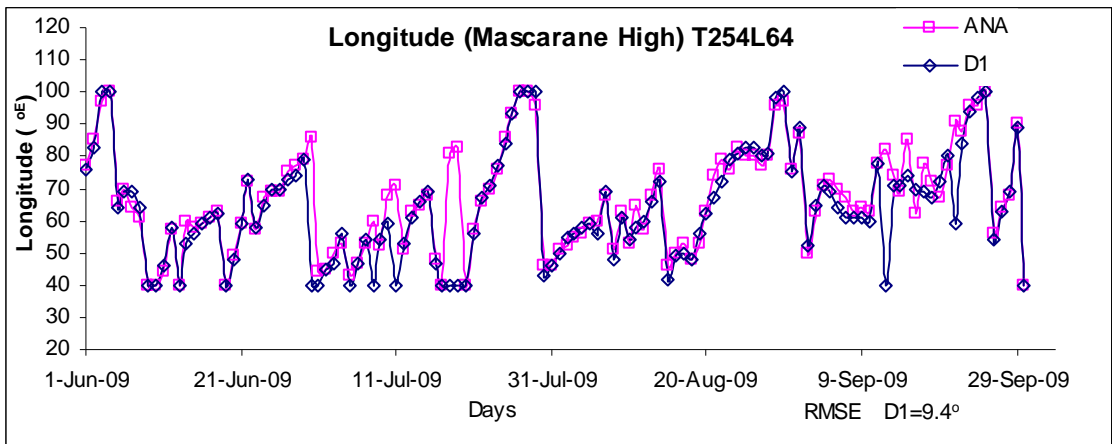


Fig. 2

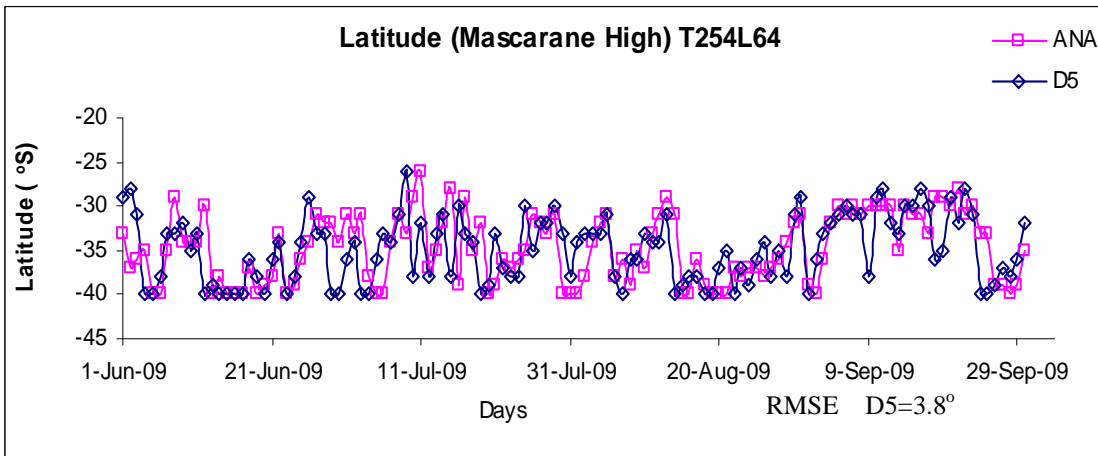
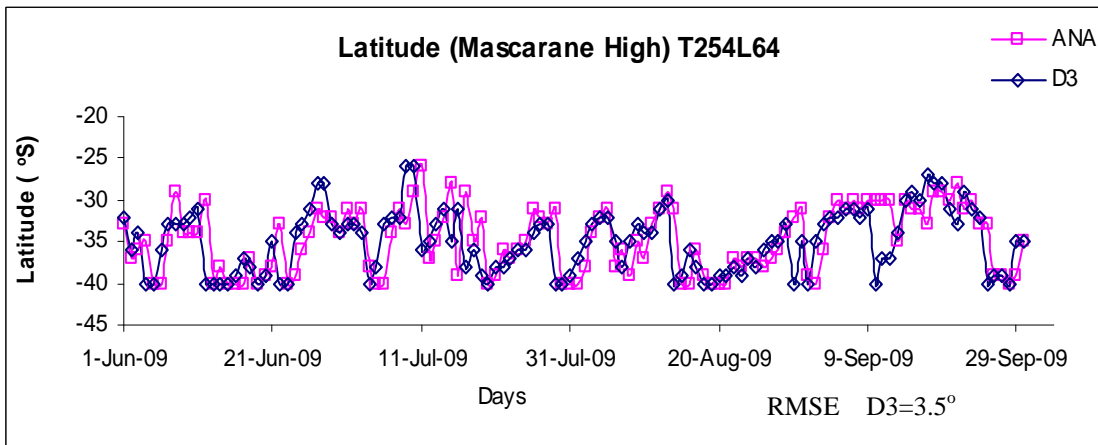
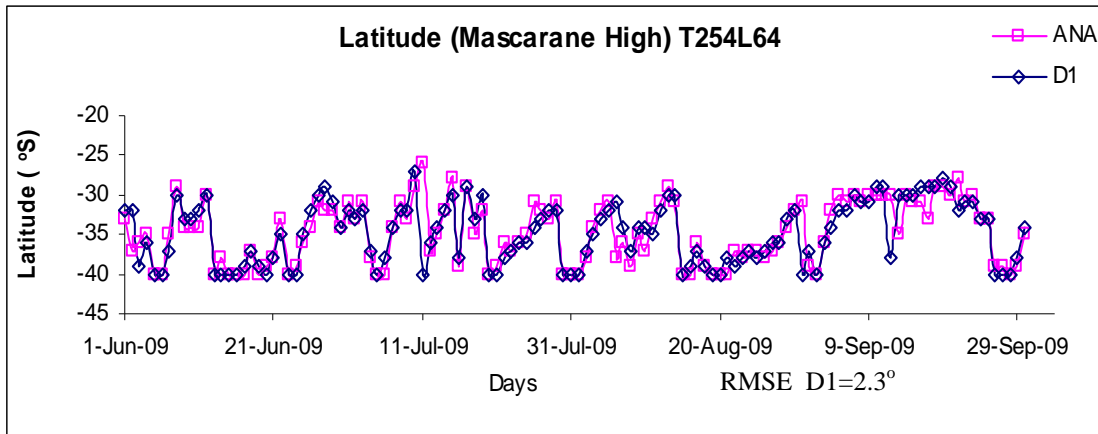


Fig. 3

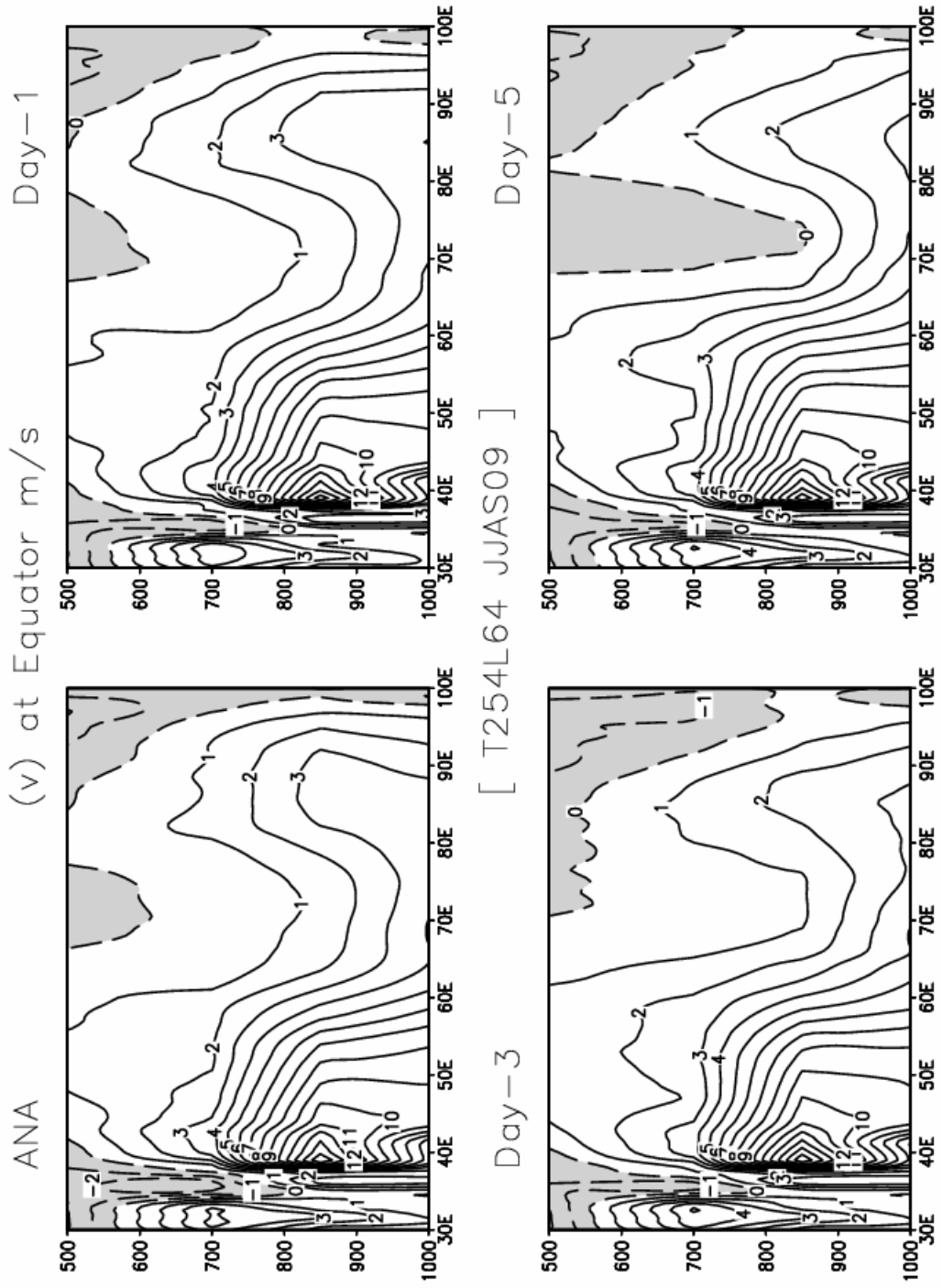


Fig. 4

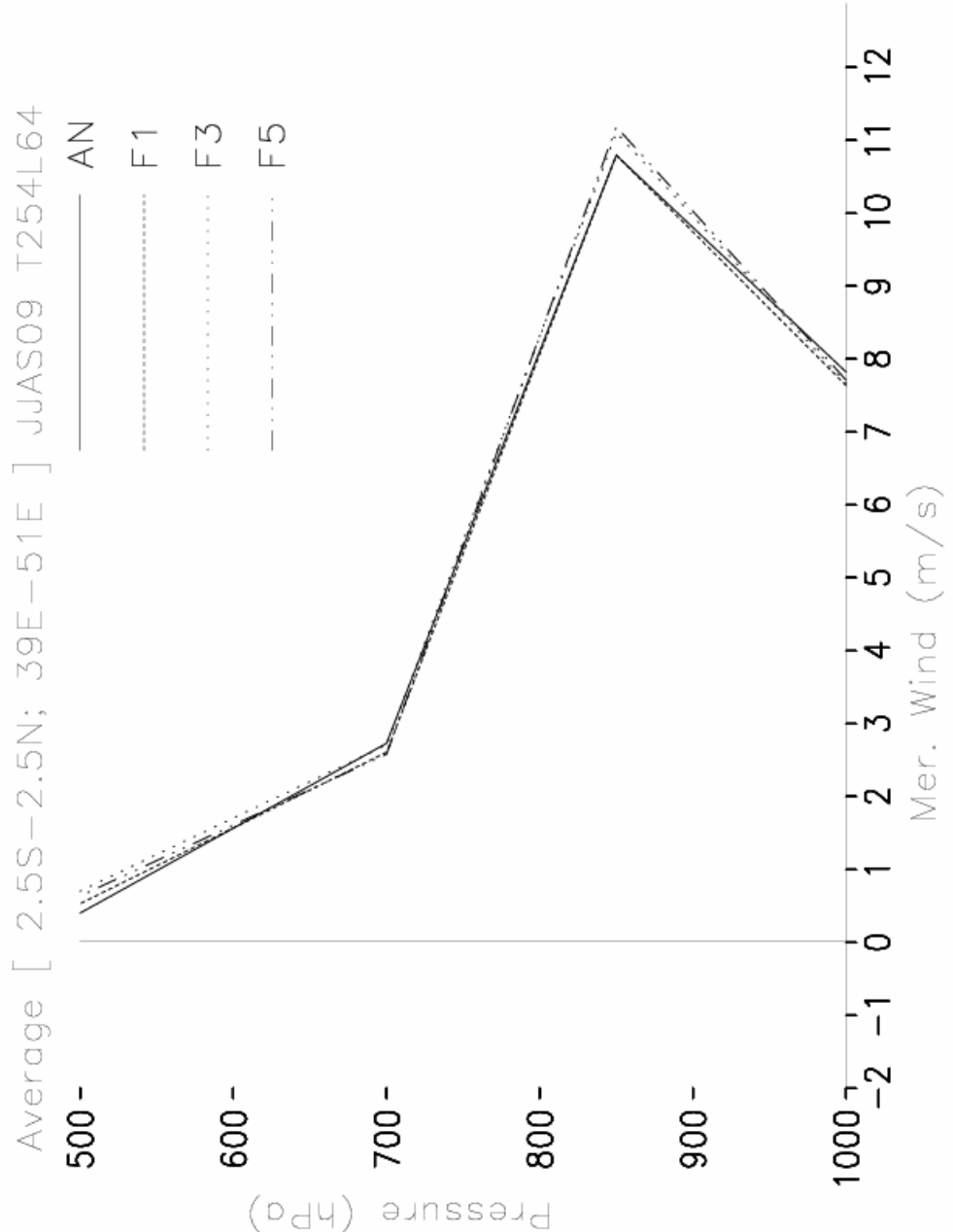


Fig. 5

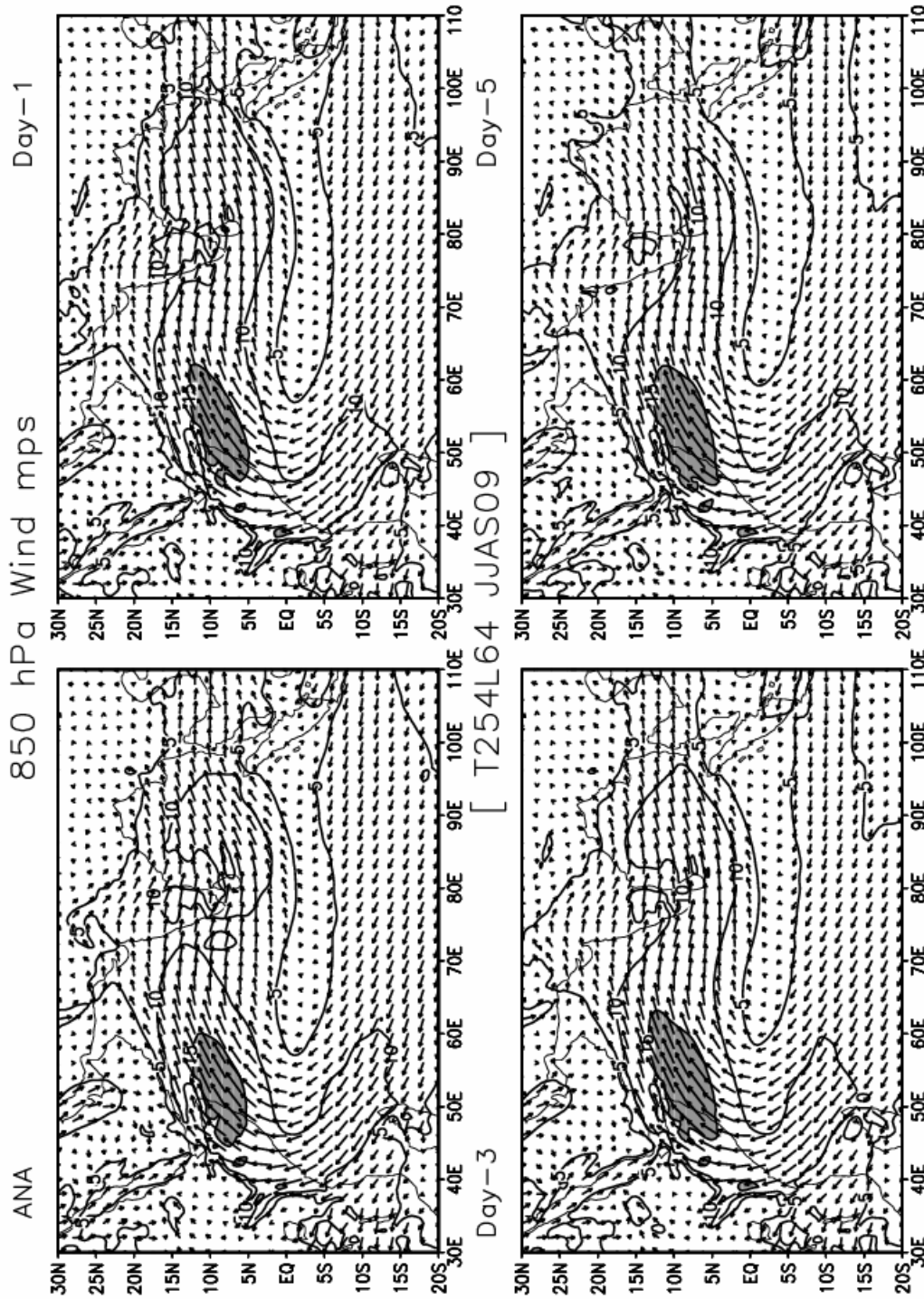


Fig. 6

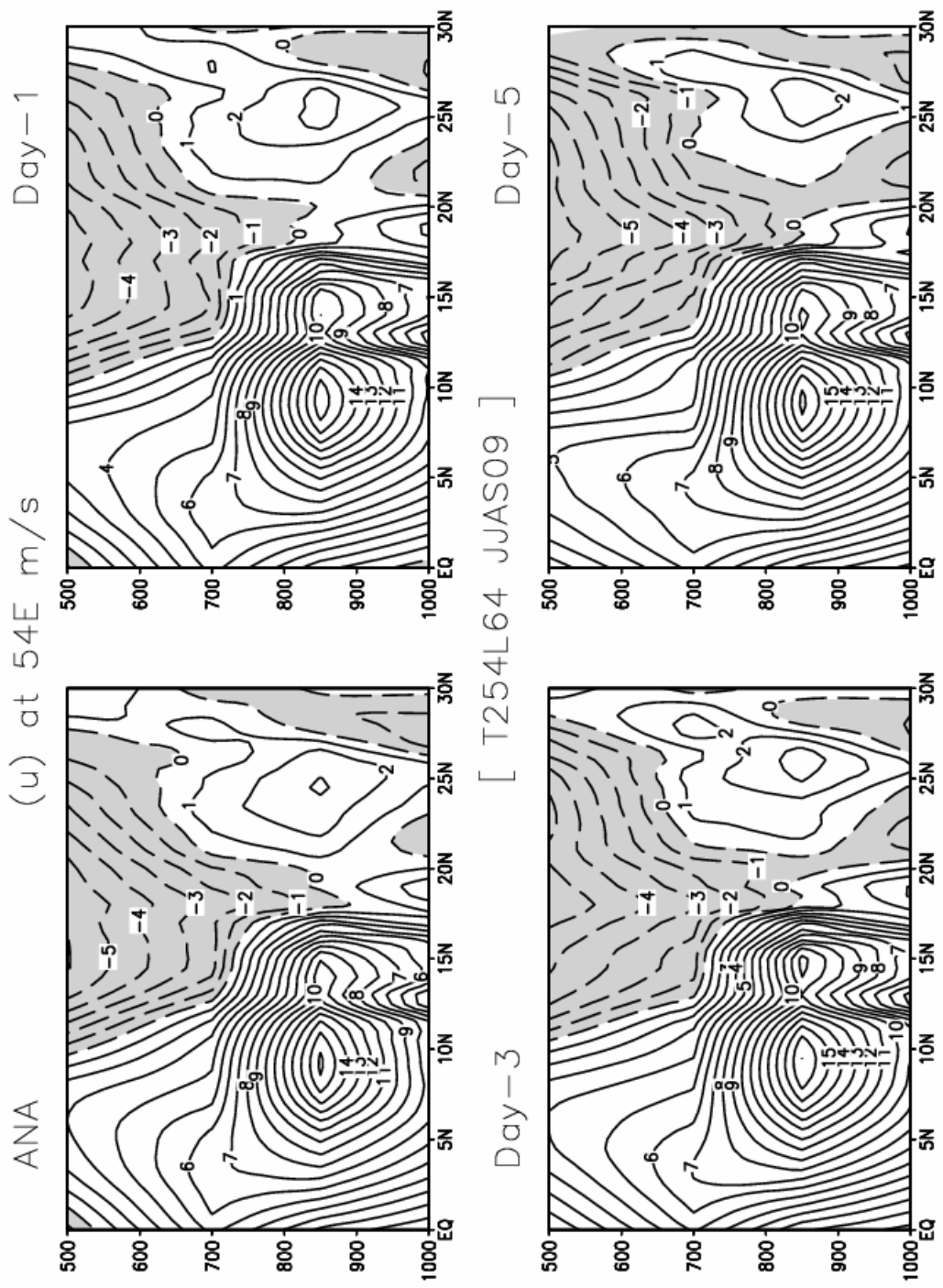
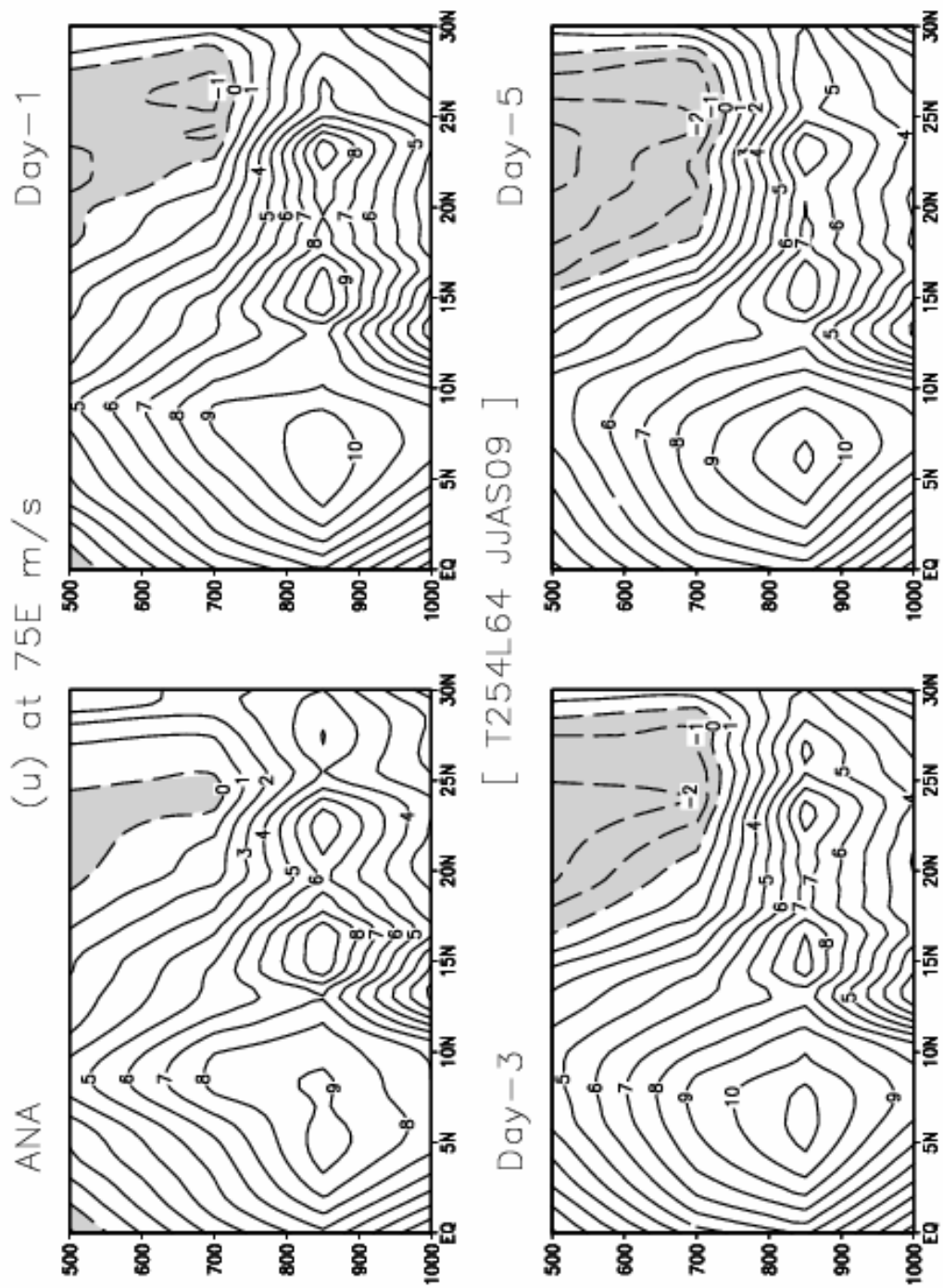


Fig. 7



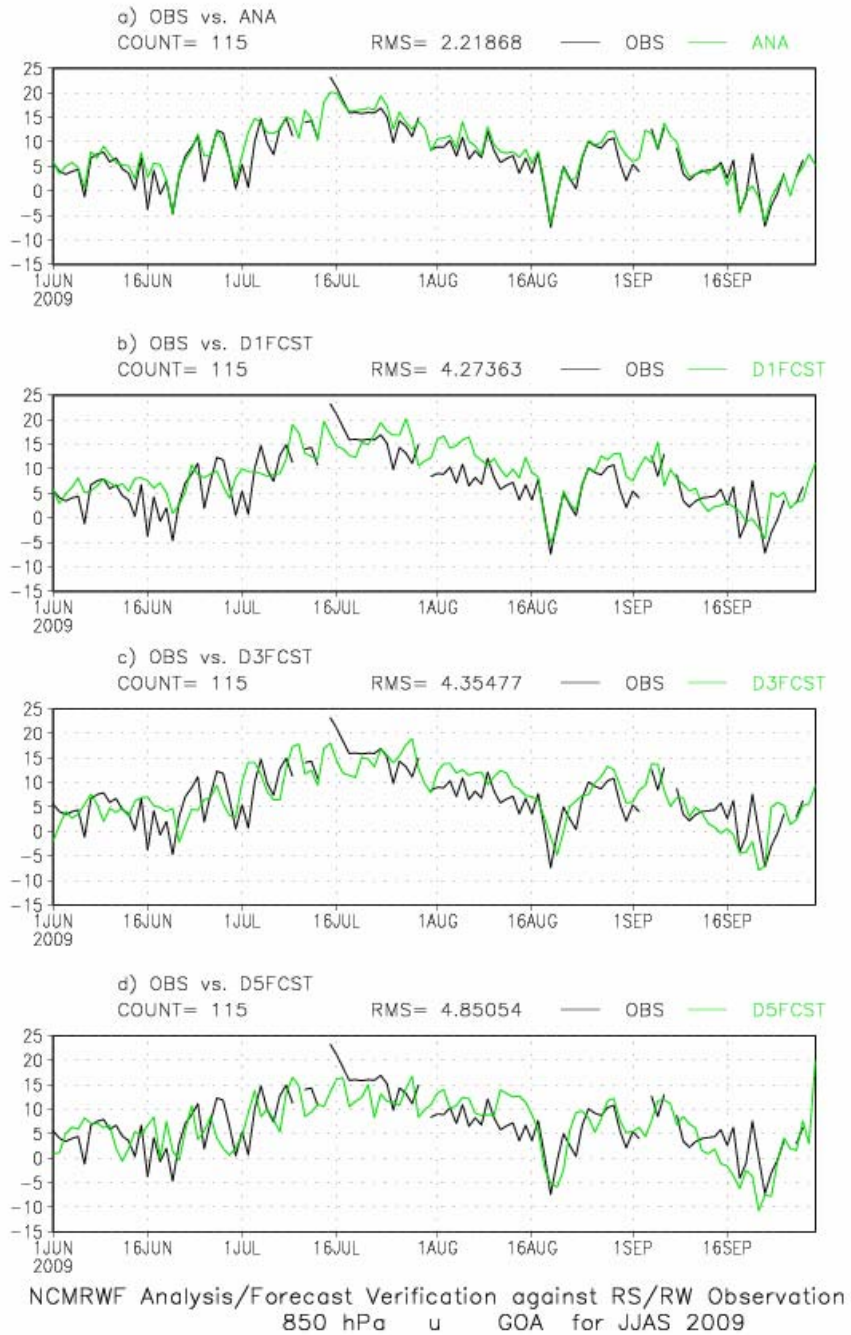


Fig. 9

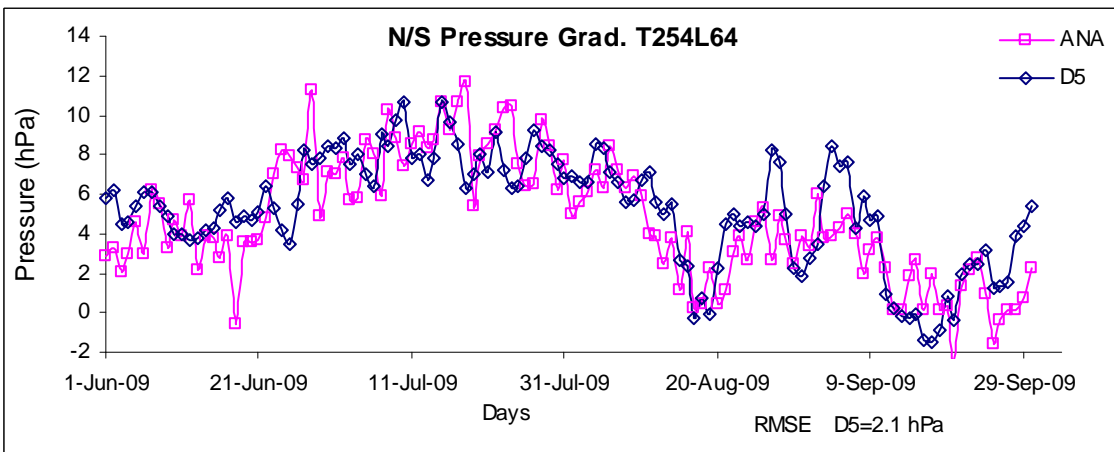
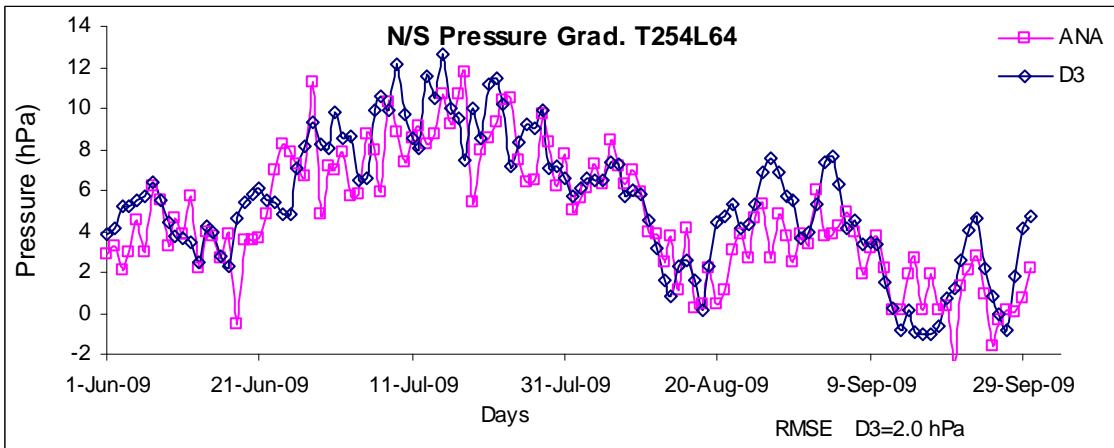
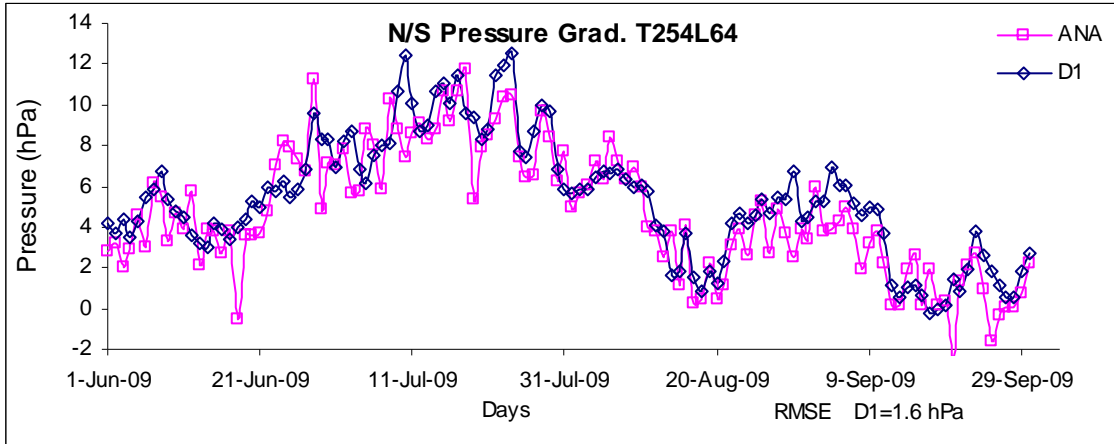


Fig. 10

Tropical Easterly Jet, Tibetan High and Mid-Latitude Interaction

Saji Mohandas and L. Harenduprakash

1. Introduction

Tropical Easterly Jet (TEJ) and Tibetan High are two prominent semi-permanent flow structures that exist during the Indian summer monsoon season (Koteswaram, 1958, Rao, 1976). The easterly jet is found to the south of subtropical ridge over Asia, which runs from the east coast of Vietnam to the west coast of Africa. Normally, the jet is at an accelerating stage from South China Sea to South India and decelerates thereafter, with latitudinal positions and speed fluctuating from day to day.

Tibetan High is a warm anticyclone, which gets established much later, after the onset of monsoon. Tibetan high prominently appears with its center being most marked at 300hPa level, approximately at 30 °N, 90 °E. It usually extends from 70 °E to 110 °E. There is also a ridge normally found at 700hPa level, with its axis along 40 °N, between 75 °E and 95 °E, just north of the Tibetan massif (Rao, 1976). In July another ridge also is normally observed to lie at about 700hPa and aloft, over Pakistan and northwest India to the west of 75 °E, with its axis along 30 °N. The high over Tibet from 500hPa upward, centred near Tibet at 500hPa and over Tibet at 300hPa and 200hPa levels is normally termed as Tibetan High. In June the axis of anticyclonic belt is at about 25 °N at 300hPa and 200hPa levels. In August, the anticyclone is more or less similar to July, but is shifted to more north and is slightly more intense. In September, the anticyclonic belt is nearabout 26 °N upto 200hPa level. Ramaswamy (1965) associates well-distributed rainfall over India with well-pronounced and east-to-west oriented anticyclone over Tibet at 500hPa and 300hPa levels.

During the onset period, the position of sub-tropical high is to the south and even middle latitude westerlies may be prevailing in northern India in the upper troposphere. When the southwest monsoon is fully established over India, middle latitude westerlies prevail mostly to the north of 30 °N. However, these westerlies appear to affect the monsoon weather over north India to a considerable extent (Rao et al., 1970; Chakravorty and Basu, 1957; Mooley, 1957). Weather produced by monsoon depressions could be accentuated by extra-tropical eastward moving disturbances at a higher latitude (Malurkar, 1958). The

weather on the southern side of the high latitude disturbance may be further increased by orography near Himalayas.

In this section, the significant features of the monsoon circulation over the Indian region at 200hPa level and its interactions with mid-latitude disturbances as seen from the model analysis and forecast during southwest monsoon season of 2009 are documented. The circulation at this level is characterized largely by anticyclone (Tibetan High) extending over the domain from 20°E to 140°E, with its axis along 28°N and the tropical easterly jet (TEJ) formed to the south of this anticyclone, covering most parts of the North Indian Ocean and the southern part of India. The Tibetan anticyclone may break into two distinct cells, one close to 65°E and the other close to 85°E and oscillates about its axis. This breaking up and oscillation of the anticyclone at 200hPa may be due to the intrusion of transient mid-latitude westerly troughs over to the Indian region. Some of these large amplitude troughs between 65°E and 100°E affect the weather over the Indian region. In this report, the time series of the fluctuations in the location of Tibetan Anticyclone along 65°E and 85°E, the location of strong easterlies (at 200hpa and along 75°E) and passage of westerly troughs between 65°E and 95°E are documented for the monsoon season of 2009.

The charts give a concise record of the variations of the features mentioned above and form the result of this work. The discussion therefore is brief.

2. Axis of the 200hPa Anticyclone

During the onset phase of Monsoon, seasonal anticyclone cell generally moves northwards accompanied by the northward shift of upper level westerly flow over to its northward fringes. Latitudinal positions of this 200hPa anticyclone along 65°E and 85°E have been extracted from the daily analyses, and day-1, day-3 and day-5 predictions by NCMRWF operational T254L64 analysis and forecast systems. These are shown in the panels a & b in the respective figures for day-1 (Fig. 1), day-3 (Fig. 2) and day-5 (Fig. 3) predictions. It is seen that the general features of all the three forecast leading times are similar.

The meridional movement of ridge axis in T254L64 analysis at 65°E during the period JJAS 2009 is marked with gradual northward progression in June. During July and August it remained at around 32°N and in September it gradually moved southwards to around 28°N. Around the middle of June it propagated down to even 12°N. The day-1 and day-3 forecasts

produced the variability in the ridge positions at 200hPa at 65°E fairly well. However in the day-5 forecasts the model forecasts deviated from the analysis and the southward shift of ridge in the month of June was not predicted. At 85°E, the meridional shift of the ridge axis in the analysis and forecasts was very less with the average latitudinal position being around 28°N. Compared to day-3 or day-5 forecasts, day-1 forecast curve showed the best match at 85°E. In general it can be seen that T254L64 forecasts up to day-3 are in good agreement with the corresponding analyses.

3. Tropical Easterly Jet

Strength of tropical easterlies at 200hPa along 75°E was monitored throughout the season as the strongest wind with speed exceeding 20 m/s (meter per second). Panels c & d of the respective figures show the latitudinal positions and strength of easterlies in the analyses and day-1, day-3 and day-5 forecasts. In the figures, latitudinal positions (where the strength of easterly is maximum along 75°E) have been marked by crosses and vertical lines show the strength of easterly in m/s for the day at that position. For simplifying the plot, 20 m/s has been subtracted from the strength of easterly and in the figures, 1 m/s represents one-degree latitude of the vertical axis.

T254L64 analysis clearly displayed an intraseasonal variability in the northward movement of the position of the strongest easterly wind. As a part of the monsoon onset spell in the first week of June, the tropical easterly jet stream position as observed at 200hPa analyses progressed northward till 10°N with core wind speed less than 25 m/s and thereafter weakened during the hiatus. Again after the break period, TEJ became more prominent during the end of June and attained a maximum wind speed exceeding 30m/s and maximum northward displacement upto 20°N. During July, TEJ remained quiet strong throughout and fluctuated around 10°N. Again during the first half of August the position of core easterly wind at 200hPa level shifted north and by the middle of August it started shifting southward gradually.

The forecasts (panel d) in the figures 1-3 (corresponding to day-1, day3 and day5) are shown side by side with the analysis (panel c). The strength and meridional displacement of the core easterly wind at 200hPa level is best captured in day-1 forecasts compared to day-3

and day-5 forecasts. Generally the TEJ strength was underpredicted in all forecasts during the last part of September. Day-3 and day-5 forecasts could not sustain the intensity of TEJ core whereas day-3 predictions are less intense and less organized as compared with day-5.

4. Troughs in Upper Level Westerlies

Panels e & f show the north south extension of the westerly troughs that passed through Indian region between 65°E and 85°E in the analyses and day-1, day-3 and day-5 forecasts (Figs. 1-3) at 200hPa level. It may be noted that these figures do not show any other characteristics of the trough such as its orientation and strength. Also in these figures almost all long and smaller wave activities even up to 50°N are presented whereas the major activities affecting the Indian region may be related to those extending southward of 40°N. Still these may give some indication of the variations in the zonal index.

Westerly trough activity is found to be quiet strong at 200 hPa level in T254L64 analysis during the middle of June and the first week of July with the trough extending southward even upto around 23°N. During July and August, the westerly activity is somewhat subdued and in September, there are again a couple of spells of westerly trough activity observed in the analyses. The day-1 forecast captured the active and weak spells of westerly activity fairly well and overpredicted the southward propagation of trough during the middle of June. Day-3 forecast also displays some resemblance with the analysis though the activity was somewhat underpredicted in September. In the day-5 forecasts, the skill drops drastically.

Figure Legends

Fig. 1: Latitudinal positions of ridge axis at 200hPa level along 65°E (a) and 85°E (b) for both T254L64 analysis (dotted curve) and corresponding T254L64 forecasts (solid curve) for day-1. Latitudinal positions of maximum easterly wind along 75°E at 200hPa level (marked by crosses) and the wind speed in knots above 20 knots denoted by the length of the vertical lines in terms of degrees of latitude, for analysis (c) and day-1 forecasts (d). Meridional extend in terms of degrees of latitude of the prominent trough(s) in westerlies at 200 hPa level over north India and the neighbouring parts to the north of India denoted as vertical lines for analysis (e) and day-1 forecasts (f). The x-axis is the number of days starting from 1 June, 2009 through 30 September and y-axis is latitude in degrees.

Fig. 2: Same as Fig. 1, except for day-3 forecasts.

Fig. 3: Same as Fig. 1, except for day-5 forecasts.

References

- Chakravorty , KC and SC Basu, 1957, The influence of western disturbances on the weather over north-east India in monsoon months, *Indian J. Met. Geophys.*, 8, 261 – 272
- Koteswaram, P, 1958, The Easterly Jet Stream in the Tropics, *Tellus*, 10, 43 – 57
- Malurkar, S.L., 1958, “ Monsoons of the world – India Monsoon”, *Monsoons of the World*, 92 – 100
- Mooley, DA, 1957, The role of western disturbances in the production of weather over India during different seasons, *Indian J. Met. Geophys.*, 8, 253 – 260
- Ramaswamy, C, 1965, “On synoptic methods of forecasting the vagaries of southwest monsoon over India and neighbouring countries”, *Proc. Symp., IIOE*, 317 – 326
- Rao, YP, 1976, “Southwest Monsoon”, *Meteorological Monograph, Synoptic Meteorology No. 1/1976*, India Meteorological Department, June 1976, 367pp
- Rao, YP, V Srinivasan and S Raman, 1970, “Effect of middle latitude westerly systems on Indian monsoon”, *Symp. Trop. Met., Hawaii*, N IV 1 – 4

RIDGE, TEJ & TROUGH 200hPa JJAS2009

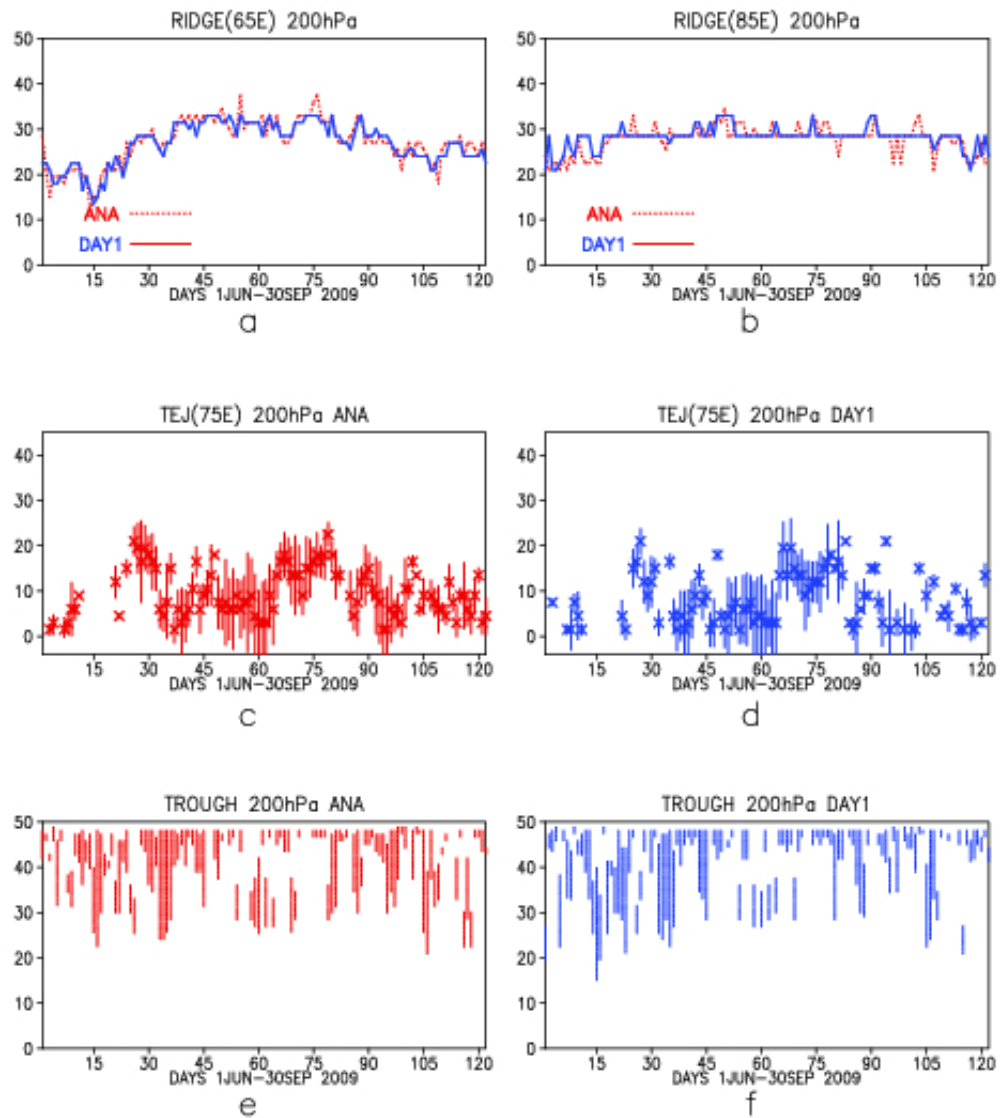


Fig. 1

RIDGE, TEJ & TROUGH 200hPa JJAS2009

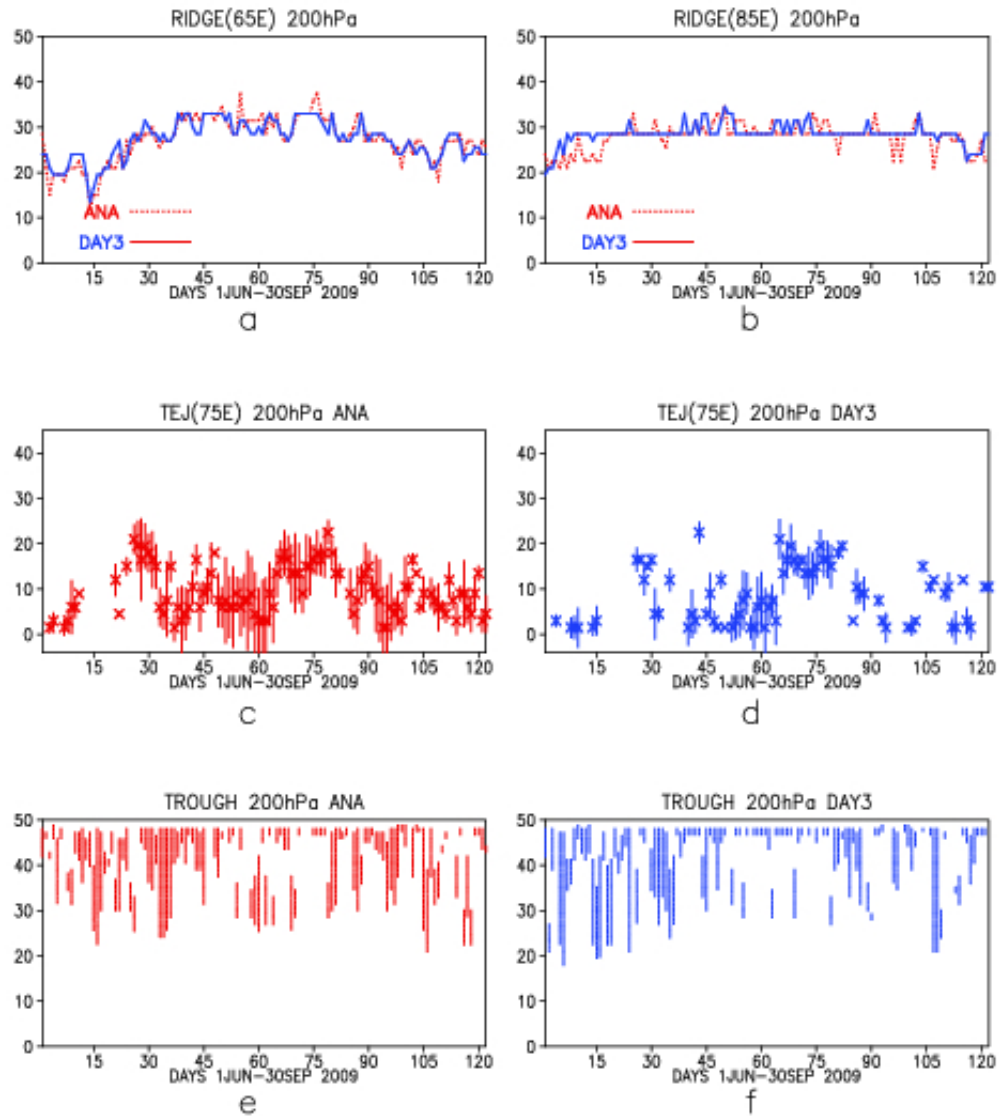


Fig. 2

RIDGE, TEJ & TROUGH 200hPa JJAS2009

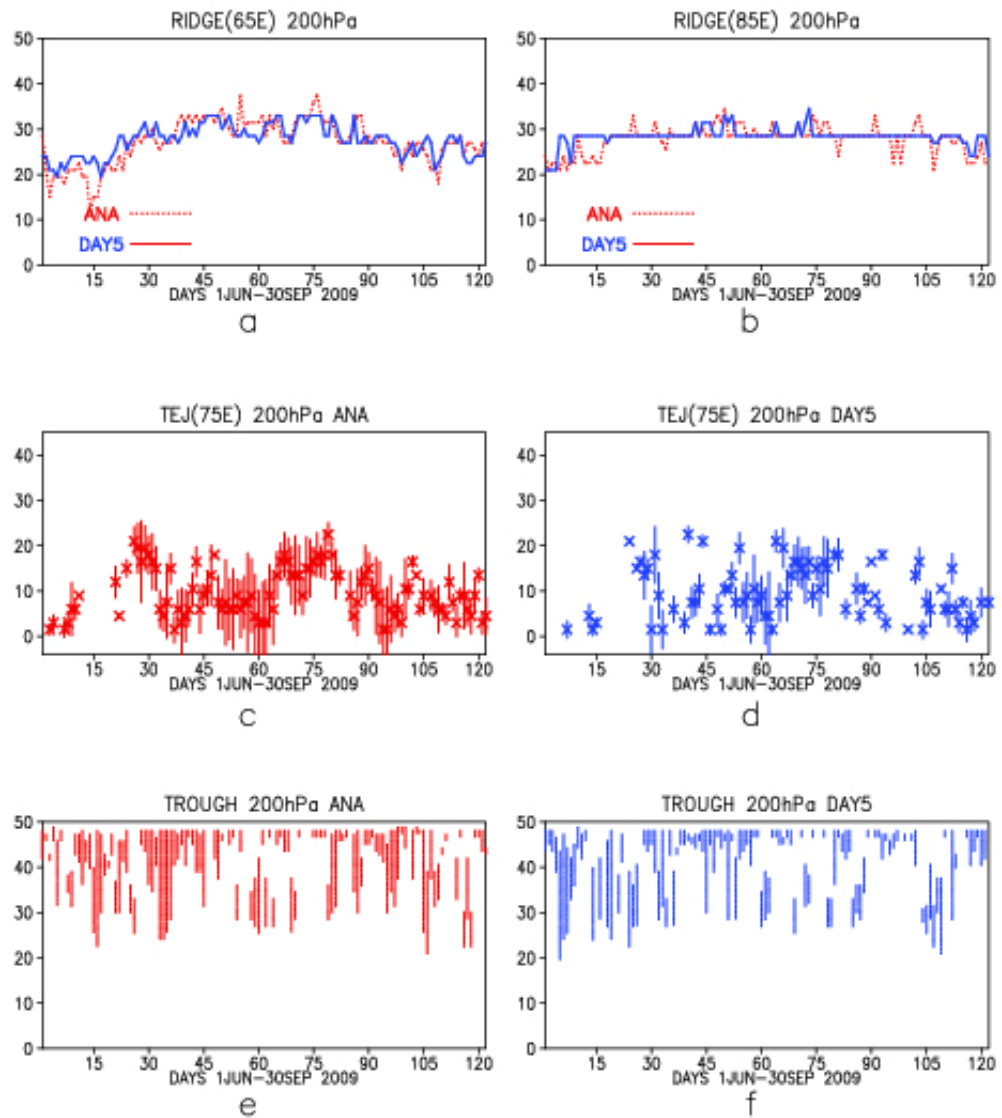


Fig. 3

Location Specific and Customized Weather Forecast for Cities and Districts: Evaluation of Forecast Skills

Ashok Kumar, E.N.Rajagopal, J.V.Singh and Ranjeet Singh

1. Introduction:

The location specific weather forecast products are generated regularly based upon the NWP models operational at NCMRWF. Initially these products were based upon global R-40, T-80 and T-170 coarser models and now these forecasts are based upon global T-254 general circulation model installed in January-2007.

Location specific weather forecasts in medium range are extremely useful, as 3-5 days lead time is very essential for taking precautionary measures to save crops from bad weather in agriculture and managing other agriculture related activities. Over the years a fully operational location specific forecast system for agriculture was successfully developed on the basis of the T80L18 medium range weather forecasts. (Kumar et.al.,1996) Later on location specific weather forecast system was also developed based upon T-254 model and by monsoon 2008 it was operational for all the 127 agro advisory service units in India. The location specific weather forecasting for agriculture sector was transferred to the India Meteorological Department in 2008.

Besides this two major location specific weather forecast products are generated every day, one is for major cities of India and other is for all the 602 districts of India and are put on NCMRWF website every day. These forecasts are easily accessible for media, general public, district authorities and farmers for planning their activities. A detailed verification study for these forecasts is conducted at the end of each monsoon season and is found up to the mark almost every year. The forecast performance in monsoon 2009 is presented in the following sections.

Location specific forecasts also play an important role in managing different activities and resources in other sectors like mountain expeditions, sea expeditions, organizing games, resources in power sector, aviation and satellite launching. These forecasts are used for civil and military operations both. These special customized forecasts are issued as and when demanded by the various user departments. These forecasts had always been found matching well with the prevailing weather at the place of work as per the information received at NCMRWF. The customized forecasts are demanded and well appreciated.

2. Direct model output(DMO) forecast

The current NCMRWF T254/L64 Global Spectral Model is obtained from NCEP and is made operational at NCMRWF in January 2007, (Rajagopal *et. al.* 2007). The details of the model assimilation/forecast system are described in chapter 1 of this report.

2.1 Nearest grid and interpolated forecast values

As the forecasts are obtained at gaussian grids and not at a particular location, hence the simplest way to get forecast at a specific location is to use the interpolated value from the four grid points surrounding it. But if the location is very near to a grid point, then the forecast at that grid point can also be taken as the forecast for the location. In order to decide as to which forecast among the two should be given more

weightage for a location, it is necessary to know the distance of the location from the four grid points surrounding it. If the distance of the location from the nearest grid is less than one-fourth of the diagonal distance between any two grid points, then more importance is given to the nearest grid forecast values otherwise the interpolated value is considered, Fig 1(Kumar et.al.,1999).

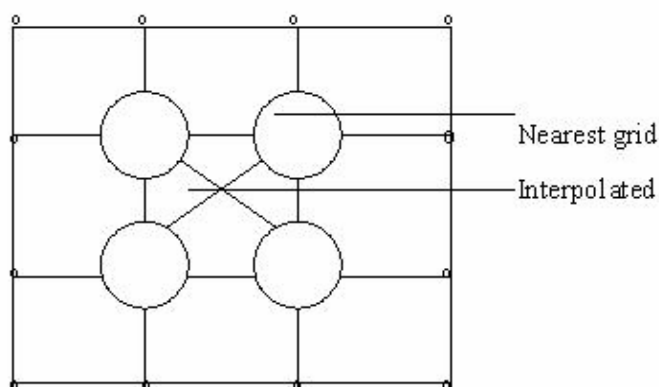


Fig. 1 Area considered around a grid point for deciding the relative importance of nearest grid and the interpolated DMO forecast values for a particular location.

2.2 DMO Forecast

DMO forecast values of both types i.e. nearest grid and interpolated, for each location of interest are obtained. Five day forecast for the following parameters is obtained by using forecast values at each time step of 15 minutes for T.80 model , 7.5 minutes for T.170 model or from every hour forecast values obtained from each time step of 7.5 minutes for T-254 model.

- Average Mean Sea Level Pressure (hPa)
- Cloud Amount (Morning and Evening) (okta)
- Rainfall (24 hours accumulated) (mm)
- Maximum Temperature($^{\circ}$ c)
- Minimum Temperature($^{\circ}$ c)
- Average Wind Speed (kmph)
- Predominant Wind Direction (deg)
- Maximum Relative Humidity (%)
- Minimum Relative Humidity (%)

Here, the validity of the forecast values for a particular day is for the subsequent 24 hours starting from 0003UTC(0830 hrs IST) of that day. As at NCMRWF earlier T-80 model and later on T-254 model are run only for 7 days based on 0000UTC analysis, hence only the 24,48,72 ,96,120 hours forecasts are obtained.

The forecast thus obtained are biased and bias free forecasts are obtained for 70 major cities of India and all the districts of India, as explained in the following sections. The bias free forecasts are obtained from the following weather parameters every day

- Rainfall (24 hours accumulated)(mm)
- Maximum Temperature ($^{\circ}$ c)
- Minimum Temperature ($^{\circ}$ c)

The meteograms are also obtained for the metropolitan cities, other important major cities every day and as and when required for the customized forecasts. In meteograms every six hourly accumulated rainfall values and six hourly wind speed and wind direction values are shown, besides this every time step or every hour values are also plotted for mean sea level pressure, maximum temperature and minimum temperature(Fig.2)

3. Bias free rainfall and Kalman filtered temperature forecast

The systematic error(bias) free forecast is obtained by using the direct model output obtained from the T-254 general circulation model during monsoon 2009.

3.1. Bias free rainfall forecast

An optimal rainfall threshold value is set to maximise the skill score. The optimal threshold value means that if the forecasted rainfall amount is less than the threshold then the forecasted value is taken as a zero otherwise it is taken as the forecasted rainfall amount(Maini.. *et. al.* 2002). The optimal threshold is calculated as follows:

Let the forecasted rainfall series during the seasons considered is denoted as R_{fi} , $i = 1, 2, \dots, n$. and Th be the threshold up to which the rainfall is taken as zero and beyond the Th value rainfall is taken as the actual value.

Then using the Th value forecasted YES/NO rainfall series is derived from the forecasted rainfall series as

if $R_{fi} \leq Th$ then no rain case i.e. 0(or N) case
and if $R_{fi} > Th$ then rainfall case i.e. 1(or Y) case

i.e value of 1(or Y) is taken for rainfall case and value of 0(or N) for no-rain case.

Similarly let the observed rainfall series during the seasons under consideration is denoted by R_{oi} , $i = 1, 2, \dots, n$; and threshold value as 0.1 mm and the observed YES/NO rainfall series is derived from the observed rainfall series using the similar logic.

As scores used for verification of the rainfall forecast are the ratio score and Hanssen and Copiers(H.K) skill score. Hence HK skill score is calculated by using the observed and forecasted YES/NO rainfall series based upon the data from the previous 2 to 3 seasons. Then HK skill score is maximized by varying the threshold(Th) value used for deriving forecasted YES/NO rainfall series. This threshold value which maximizes the HK skill score during previous seasons is applied for deriving YES/NO rainfall forecast from the DMO rainfall forecast during the current season. In the present study the thresholds correction factors are calculated based upon monsoon season (June, July, August and September) of 2003 for T-80 model. These thresholds correction factors are also calibrated and verified further using the monsoon 2005 and 2006 data for T-80 and T-170 models and these are further calibrated using monsoon 2007 and 2008 data for T-254 model. These threshold correction factors are explained further in section 5.

3.2. Basis of Kalman filtered temperature forecast (Anders o.Persson,1991)

It is a common fact that NWP models exhibit systematic errors in the forecasts of the near surface weather parameters. The 2m-temperatures for example are often systematically biased, though the magnitude of the bias varies with geographical location and time of the season. Such systematic errors may not only be due to short comings in the model but also depend on the sub-grid location of the station.

Individual mountains or different parts of a large city with their specific climate can hardly be fully resolved in any NWP model.

Mathematically a correction formula for a given station and for the specific lead time can be formulated as

$$Y = X1 + X2 * \text{Temp. forc.}$$

If X1 and X2 were constant over the seasons they could be computed with good accuracy by linear regression techniques. To avoid storage of old data a recursive regression technique could be used applying weights to make more recent data have a larger impact. X1 and X2 would then reflect more recent conditions. However, in a pure statistical sense this method is only a way to smooth the data, the weights pushing the emphasis towards a more recent time. In contrast to smoothing, filtering techniques actually tries to estimate today's value, in light of historical data. Thus a simple one parameter Kalman filter can be applied for removing the systematic errors in the temperature forecasts (Rashmi et.al. 2009).

3.3. Kalman filter equations

The Kalman filter consists of two sets of equations, the observation equations and the system(or prognostic) equations.

The observation equation:-

Let TFC(tau) be the forecasted value and the verifying observation TOBS(tau) at a certain location and time of the year tau.

The observed forecast error is then

$$\text{TFC}(\tau) - \text{TOBS}(\tau) = Y(\tau) \quad \text{----- (1)}$$

Where Y(tau) is the time varying bias and can be assumed to be a stochastic variable, which contains noise, i.e. factors that we can not describe: errors in synoptic part of the forecast, deficiencies in the physical parametrization and unexplained small scale disturbances.

$$Y(\tau) = X1(\tau) + v(\tau) \quad \text{----- (2)}$$

Where X1(tau) is the applied correction and v(tau) is the unexplained, non-systematic noise. A part of this noise might be explained by another statistical model e.g. containing more predictors. For example the bias might seem to be dependent on the forecasted parameter, TFC(tau) or function of it:

$$Y(\tau) = X1(\tau) + X2(\tau) * \text{TFC}(\tau) + v(\tau) \quad \text{----- (3)}$$

(2) and (3) are examples of observation equations, since they relate the observed errors to the statistical error model. If there is only a bias in the forecasts, then X2 = 0. If there are only non-systematic errors both X1 and X2 will be = 0.

The System (or prognostic) equation:

So far we have only considered the static part of the Kalman filter. The "clue" of the Kalman filter is a second stochastic and dynamic model that tries to describe the time evolution of the model coefficients X(tau) in the form

$$X(\tau+1) = A(\tau) * X(\tau) + u(\tau) \quad \text{----- (4)}$$

Where A (tau) is a time dependent transition matrix, known a priori, describing how X involves from one time period to the next during the season and u(tau) is a stochastic variable describing the "model noise", i.e. those part of the model development we do not know a priori.

Since we do not know the "ideal" coefficients X(tau) and u(tau), we have to make estimates: X(tau/tau) and e(tau/tau) is the corresponding co-variance of X.

In our applications A(tau) = 1 for all times tau, because we lack any theory (or even empirical formulas) describing how the coefficients develop over time. In other words, we will apply estimates valid "today" as a forecast some days ahead.

All changes in X will in our examples be due to random /unexplained variations due to the noise u(tau). Both v(tau) and u(tau) as well as e(tau/tau) are supposed to be

normally distributed and uncorrelated with means 0(white noise) and standard deviations D(tau), C(tau) and Q(tau) respectively.

3.4. Kalman filter forecast

The estimates for the standard deviations is obtained based upon the data for past 30-40 days and in turn the estimates for X1(tau) and X2(tau) are obtained and the same estimates are used for getting the prediction for forecast error in the temperature for the next day as per the following equation;

$$Y(\text{tau}) = X1(\text{tau}) + X2(\text{tau}) * \text{TFC}(\text{tau})$$

and the systematic error free temperature is forecasted.

4. Bias free rainfall and trend based temperature forecast

The direct model output forecast used for this was the forecast obtained T-170 earlier and T-254 model presently..

4.1. Bias free rainfall forecast

The technique used for getting bias free rainfall forecast is explained in section 4 The threshold values obtained here are for the forecasts obtained from T-80,T-170 or T-254 models and these are given in Table 1. This table also include the threshold values for T-80 model also as these values for T-80 and T-170 are same. These thresholds values are representative of a region and are obtained as the most probable value for the stations in a particular region(Rashmi *et.al.* 2007).

4.2. Trend based temperature forecast

Let Tf(I) and To(I) be the forecasted and observed temperatures(°C) respectively on day I (I = 1,.....,n),where n is the number of observations considered during the season. Let Tf(I) and To(I) for I = 1,.....,n, are having positive correlations. Forecasted temperature values are for 24,48,72 and 96 hour forecast from T-170 & T-254 models.

If Td_f(I) and Td_o(I) are the forecasted and observed temperature trends respectively on day I (I = 1,n).

Then

$$\text{Td}_f(I) = \text{Tf}(I) - \text{Tf}(I-1) \quad \text{-----}(1)$$

$$\text{Td}_o(I) = \text{To}(I) - \text{To}(I-1) \quad \text{-----}(2)$$

Let Tb_f and Tb_o is the minimum value of the forecasted and observed temperatures considered respectively and Tb is the minimum of Tb_f and Tb_o. Then considering Tb as base value we can represent the forecasted and observed temperatures in terms of the new series of positive values as;

$$\text{Tf}(I) = \text{Tb} + \text{c}(I) \quad \text{-----}(3)$$

$$\text{To}(I) = \text{Tb} + \text{d}(I) \quad \text{-----}(4)$$

where c(I) and d(I) are positive for all I, I = 1,.....,n and are having positive correlations.

Then as;

$$\begin{aligned} \sum_{I=2}^n (\text{Td}_f(I) - \text{Td}_o(I))^2 &= \sum_{I=2}^n ((\text{Tf}(I) - \text{Tf}(I-1)) - (\text{To}(I) - \text{To}(I-1)))^2 \quad (\text{from } 1 \& 2) \\ &= \sum_{I=2}^n ((\text{c}(I) - \text{c}(I-1)) - (\text{d}(I) - \text{d}(I-1)))^2 \quad (\text{from } 3\&4) \end{aligned}$$

As $c(I)$ and $d(I)$ are +ve and having positive correlations, $I=1, \dots, n$. Hence it is expected that per unit rate of change in $c(I)$ and in $d(I)$ is expected to be same. Hence $(c(I)-c(I-1))$ and $(d(I) - d(I-1))$ are expected to be of same order and thus $((c(I)-c(I-1)) - (d(I) - d(I-1)))^2$ is expected to be less than or equal to $(c(I) - d(I))^2$, for $I=1, \dots, n$.

$$\begin{aligned}
 \text{Hence, } \sum_{I=2}^n (T_{d_f}(I) - T_{d_o}(I))^2 &\leq \sum_{I=1}^n (c(I) - d(I))^2 \\
 &= \sum_{I=1}^n ((c(I) + T_b) - (d(I) + T_b))^2 \\
 &= \sum_{I=1}^n (T_f(I) - T_o(I))^2 \quad \text{-----}(5) \quad \text{(from 3 \& 4)}
 \end{aligned}$$

Hence from relation (5) it is clear that root mean square error for the observed and forecasted temperature trends is less than the root mean square error for the observed and forecasted temperatures.

This simple relation is due to the NWP model's bias i.e. the tendency of the model to over predict or under predict the temperatures always. Hence if we use the temperature trends, such biases will get removed and will not contribute to the root mean square error."

Hence the temperature trend forecast is obtained for maximum and minimum temperature for all the 602 districts of India based upon T-170 or T-254 model.. The user can add the present day temperature to the trends in order to get the temperature forecasts for the future days. But during monsoon 2009 these forecasts are based upon T-254 models only.

5. Customized forecast for user departments

The customized forecasts had been continuously issued as and when demanded by the various user departments as per their requirements. In this direction following are worth mentioning.

- Forecast bulletins containing the forecast for rainfall, temperature, wind speed and direction had been issued along with the meteograms to various teams mainly from Army adventure wing, ITBP, National Institute of Mountaineering who had carried out expeditions to various peaks ranging from lower ranges to Mount Everest. (Fig. 3). This forecast had been issued since over last decade.

- Forecast bulletins containing the forecast for cloud, rainfall, temperature, wind speed and wind direction had been issued along with the vertical wind profile and meteograms to SHAR centre for satellite launching missions of ISRO like PSLV and GSLV and also for the Chandrayan mission.. These forecasts had been issued for almost all such missions starting from the beginning.

- A forecast bulletin containing the general statements on weather systems and rainfall situation in general for Indian region and also for the different zones of the country along with the forecast table containing the objective forecast for cloud/rain, maximum and minimum temperature for 20 major cities had been continuously issued to media everyday including holidays, Saturdays and Sundays.

- Presentations during the map discussion or the statements by e.mail. in regard to forecasts from the NWP models operational NCMRWF, presently T-254 model,

during the monsoon season, STORM project during pre-monsoon season and FDP-Cyclone during post-monsoon had been continuously made or sent to IMD.

- Besides this meteograms for any place in India or any other country had been issued as and when such request received. Customized forecasts had also been sent to Power Grid Corporation of India(PGCIL) and also to Navy for their sea expeditions as and when required.

- Last but not least is the district wise forecast for rainfall , maximum/minimum temperature , which is available on NCMRWF website and can be utilised by the district authorities and farmers for managing different activities at their end.

6. Verification of the forecast

6.1 Skill scores used for verification.

The scores used for verification of rainfall forecast are the ratio score and Hanssen and Kuipers(H.K) skill scores. The ratio score (RS) measures the percentage of correct forecasts out of total forecasts issued. The Hanssen and Kuipers' discriminant (HK) is the ratio of economic saving over climatology. H.K Score can be explained by the following contingency table.

Forecasted	Observed	
	Rain	No Rain
Rain	YY	YN
No Rain	NY	NN

$$\text{Ratio Score} = (YY+NN) / N$$

$$\text{H.K.Score} = (YY*NN-YN*NY)/(YY+YN)*(NY+NN)$$

If the H.K Score is closer to 1 then the forecasts are the best and when the H.K Score is near 0 or less than 0 then the forecasts are bad. In the case of MAX/MIN temperatures, cloud amount, wind speed and wind direction the correlation and RMSE values are calculated for evaluating the skill of the forecast.

For further comprehensive study for the skill of rainfall amounts hit rate and threat scores and hit rates for different categories of rainfall amounts are calculated. Following four rainfall categories are considered;

- o_1, f_1 ; less than threshold(Th) is no rain
- o_2, f_2 ; greater than Th and less than 3.5 cm is light to moderate rain
- o_3, f_3 ; greater than 3.5 cm and less than 12.5 cm is heavy rain
- o_4, f_4 ; greater than 12.5 cm is very heavy rain.

Then a 4x4 contingency table is defined as follows,

	o ₁	o ₂	o ₃	o ₄
f ₁	a	b	c	d
f ₂	e	f	g	h
f ₃	i	j	k	l
f ₄	m	n	o	p

Then the hit rate for quantitative precipitation is defined as ,

$$H = (a + f + k + p) / N$$

where N is the total of all the frequencies shown in the table.

Hit rate for different categories of rainfall viz. light to moderate, heavy and very heavy is calculated as no. of matching cases divided by total no of observed rainfall cases in a particular rainfall category.

For a given rainfall category;

$$\textit{Threat Score} = \frac{\textit{hits}}{\textit{hits} + \textit{misses} + \textit{false alarms}}$$

6.2 Verification results(monson-2009)

For rainfall, minimum temperature and maximum temperature, the skill scores are calculated for selected major cities and districts of India for which more data are easily available , these are a good sample representative of major cities and districts of India. These skill scores for 72hr forecast are given in Table 2. for major cities and in Table 3. for districts of India.

For most of the selected major cities of India ,HK score varies from 0.02 to 0.76 and ratio score varies from 55 to 88 percent for rainfall, root mean square error(RMSE) varies from 1.10 to 2.99 and correlation varies from 0.04 to 0.84 for minimum temperature and RMSE varies from 1.99 to 3.98 and correlation varies from 0.23 to 0.90 for maximum temperature. Some of these are shown in Fig. 4.

For most of the selected districts of India ,HK score varies from 0.02 to 0.79 and ratio score varies from 56 to 89 percent for rainfall, root mean square error(RMSE) varies from 0.98 to 2.5 and correlation varies from 0.21 to 0.87 for minimum temperature and RMSE varies from 1.64 to 3.5 and correlation varies from 0.18 to 0.90 for maximum temperature. Some of these are shown in Fig. 5

For rainfall amounts the hit rate, hit rates and threat scores for different rainfall categories are also obtained for these selected major cities and districts of India. These scores for 72hr forecast are given in table 4. for major cities and Table 5 for districts of India.

For most of the selected major cities of India the overall hit rate for rainfall amounts varies from 0.51 to 0.77. The hit rate for individual categories has the value up to 0.88 for no rain, 0.89 for light to medium rain , 0.43 for heavy rain and only a very few stations are having very heavy rains and hit rate is zero for these. Threat score for individual rainfall categories has the value up to 0.73 for no rain , 0.70 for light to medium rain, 0.25 for heavy rain and only a very few stations are having very

heavy rains and threat score is zero for these. The threat score for some of the major cities are given Fig. 6.

For most of the selected districts of India the overall hit rate for rainfall amounts varies from 0.54 to 0.82. The hit rate for individual categories has the value up to 0.98 for no rain, 0.94 for light to medium rain , 0.75 for heavy rain and only a very few stations are having very heavy rains and hit rate is zero for these. Threat score for individual rainfall categories has the value up to 0.77 for no rain , 0.71 for light to medium rain, 0.33 for heavy rain and only a very few stations are having very heavy rains and threat score is zero for these. The threat scores for some of the districts are given in Fig. 7.

The skill for all the above mentioned forecast decreases with prognosis hour.

As per the information provided by the various user departments about the validity of the customized forecast issued from NCMRWF, the forecast has been reported as matching well with the prevailing weather and has been quite useful in taking strategic decisions by these departments.

8. Prospects and Future Plans:-

The forecast skill during monsoon 2009 are more stable and up to the mark.

There are some of the points which needs to be considered as the basis for future plans.

- District wise forecast is made operational for 602 districts, using the temperature trend and area wise estimates of the threshold value for rainfall starting from monsoon 2008 based upon T-254 model.

- Bias free forecast using kalman filter and threshold values for rainfall is obtained on operational basis for 70 major cities of India, using GTS data and T-80 initially and T-254 models output later respectively. Only last forty day data is being considered for every day run. This forecast gives the direct forecast value on a particular day, for next five days.

- The customized forecasts issued from NCMRWF had always been widely demanded and appreciated and reported to be quite useful in taking various strategic decisions by various user departments.

Following are some of the future plans;

- (i). MME forecast based upon different models for rainfall and cloud amount using Canonical variates and previous 2-3 seasons data.

- (ii) Kalman filter models based upon single best model for Max/Min Temp and Wind speed(or U & V),using online data for last 30 to 40 days for every day forecast.

- (iii) Kalman filter prediction models for rainfall based upon single best model using observed values of rainfall and forecasted values of directly related parametrical functions from NWP model using online data for last 30 to 40 days for every day forecast.

- (iv) SI forecast models based upon single best model for PoP and PoPT using previous five to six seasons data and Logistic Regression and Discriminant Analysis.

References

- Anders O. Persson., 1991, "Kalman Filtering --- A new approach to adaptive statistical interpretation of Numerical Meteorological Forecasts" PSMP report series no. **34**, pp. XX-27 TO XX-30
- Ashok Kumar & Parvinder Maini 1996: Statistical interpretation of general circulation model: A prospect for automation of medium range local weather forecast in India. *Mausam (formerly Indian Journal of Meteorology, Hydrology & Geophysics)*, **47(3)**:229-236
- Ashok Kumar, Parvinder Maini & Singh, S. V., 1999: An operational model for forecasting probability of precipitation and YES/NO forecast. *Wea. and Forecasting*, **14**: 38-48
- Maini, Parvinder, Ashok Kumar, Singh S V and L S Rathore, 2002: Statistical interpretation of NWP products in India. *Meteorol. Appl.*, **9** : 21-31
- Rashmi Bhardwaj, **Ashok Kumar**, Parvinder Maini, S.C. Kar and L.S. Rathore, 2007, 'Bias free rainfall forecast and temperature trend based temperature forecast based upon T-170 model during monsoon season' *Meteorological Applications* **14(4)** ,pp 351-360.
- Rashmi Bhardwaj , **Ashok Kumar** and Parvinder Maini, 2009, 'Evaluation of bias free rainfall forecasts and Kalman filtered temperature forecasts of T-80 model over Indian monsoon region, *Mausam*, **60(2)**,pp 147-166.

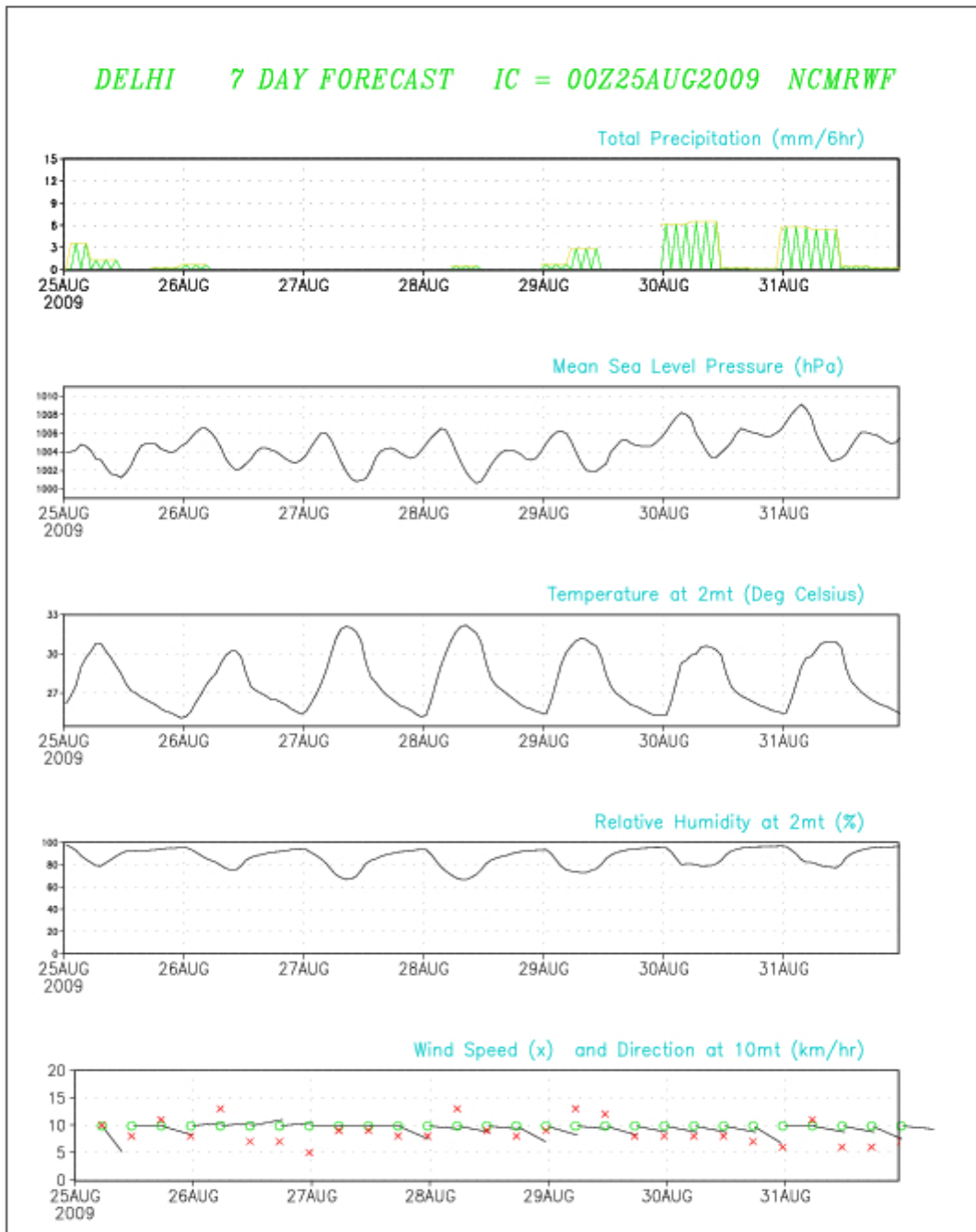


Fig 2. The meteogram for Delhi showing seven day forecast based upon initial condition of 0000UTC of 25 Aug. 2009.

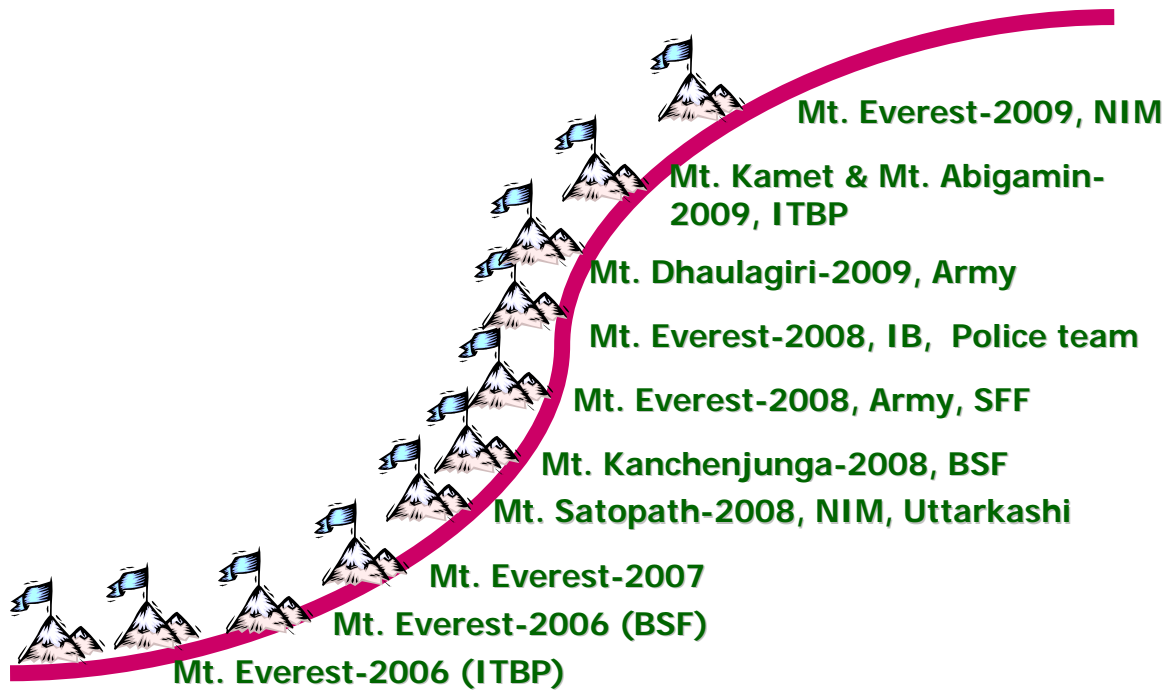


Fig. 3. NCMRWF's Customized Forecast for Mountaineering Expeditions

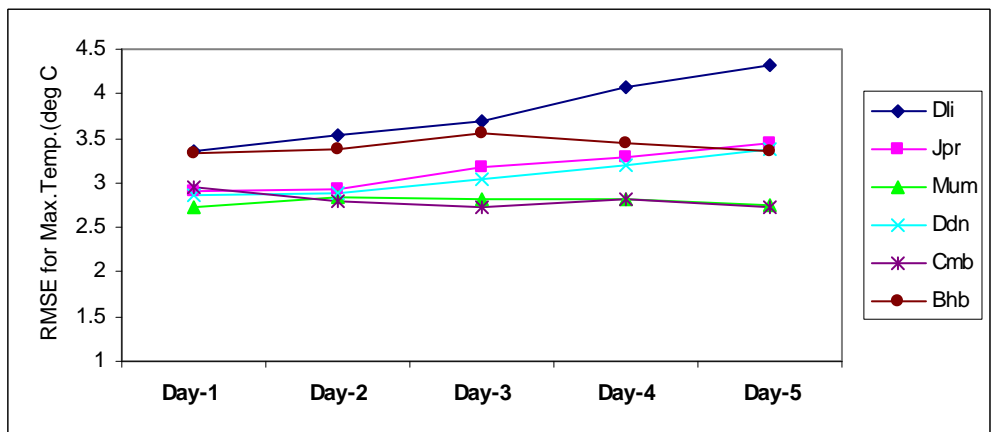
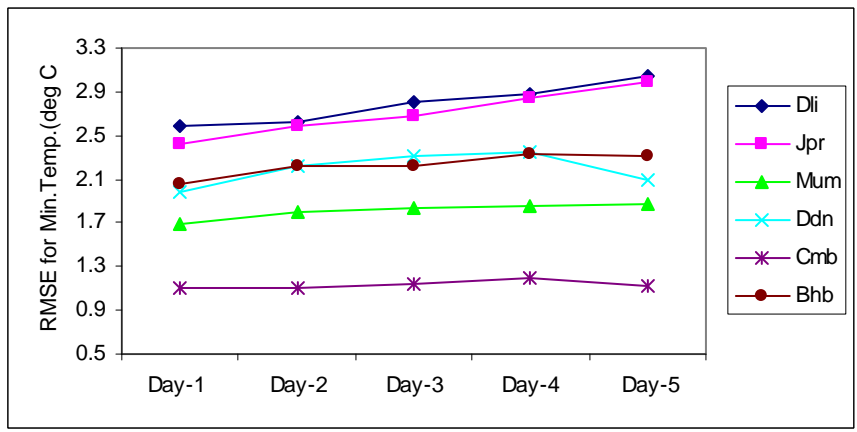
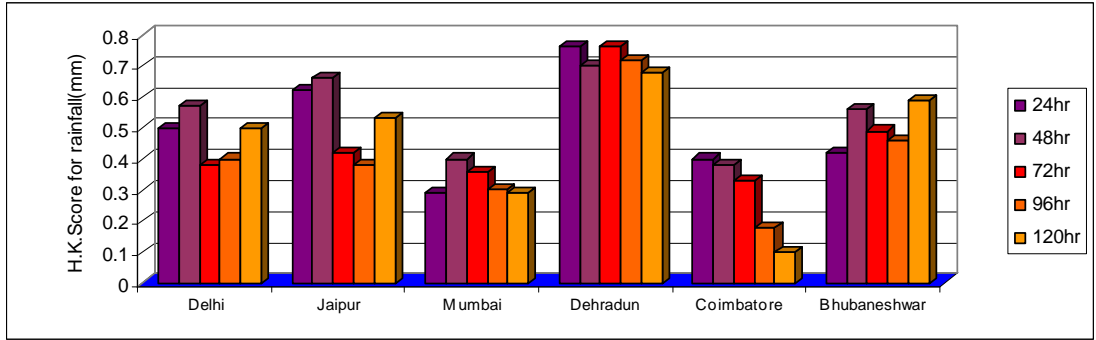


Fig. 4. Skill scores for Bias free rainfall and Kalman filtered Temperature forecast based upon T-254 model for selected major cities of India (monsoon-2009)

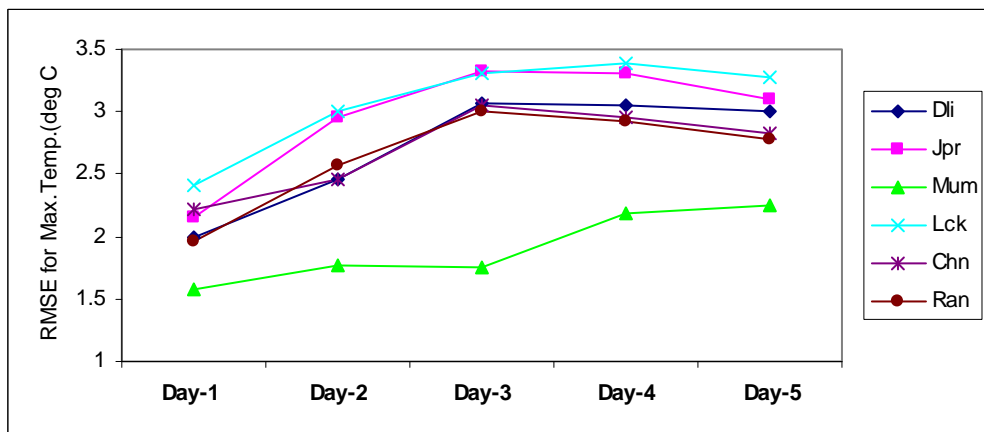
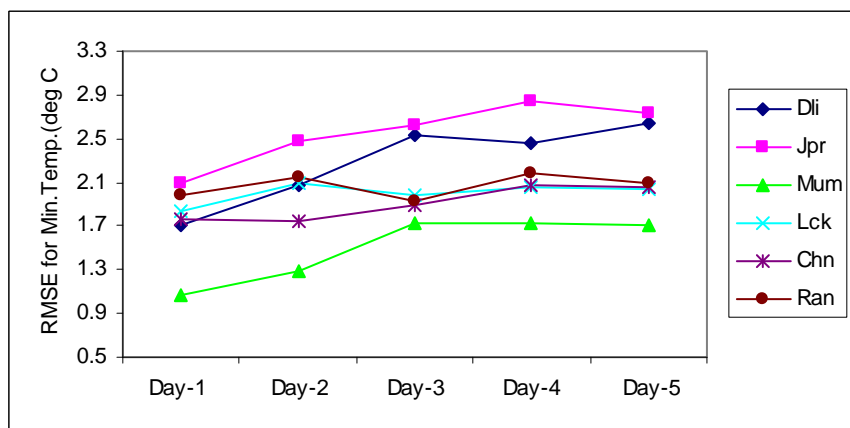
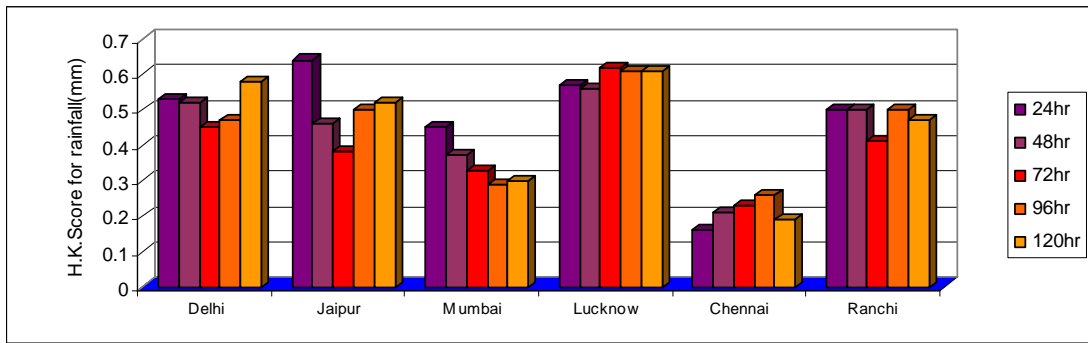


Fig. 5. Skill scores for Bias free rainfall and trend based Temperature forecast based upon T-254 model for selected districts of India (monsoon-2009)

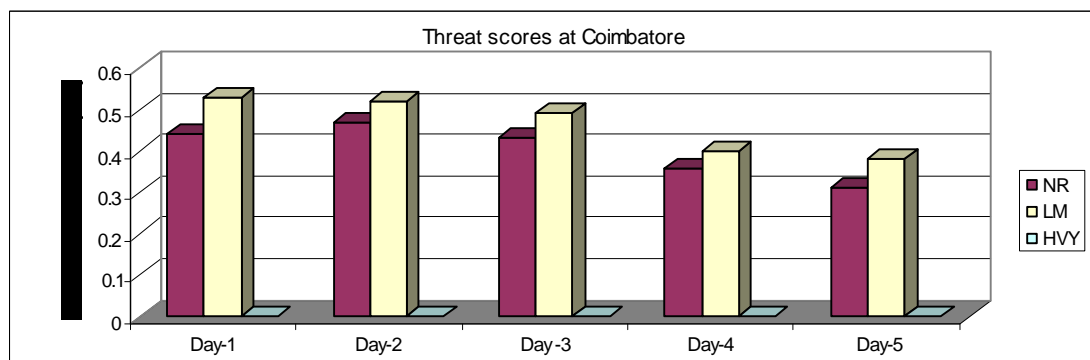
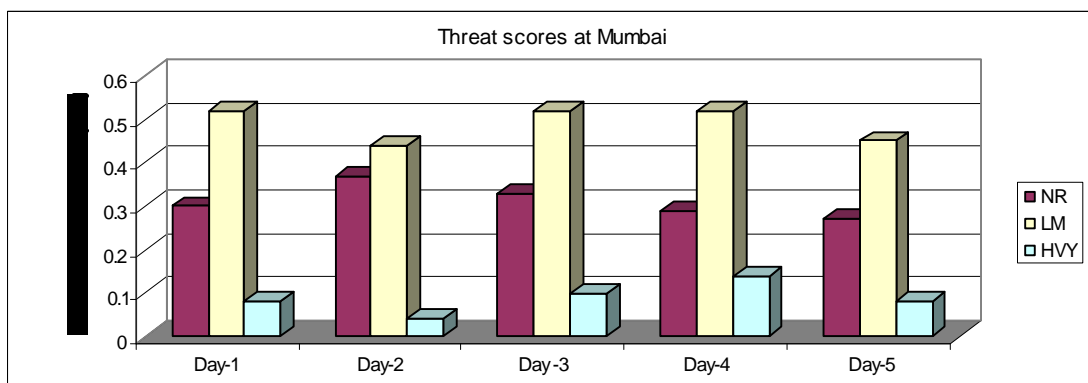
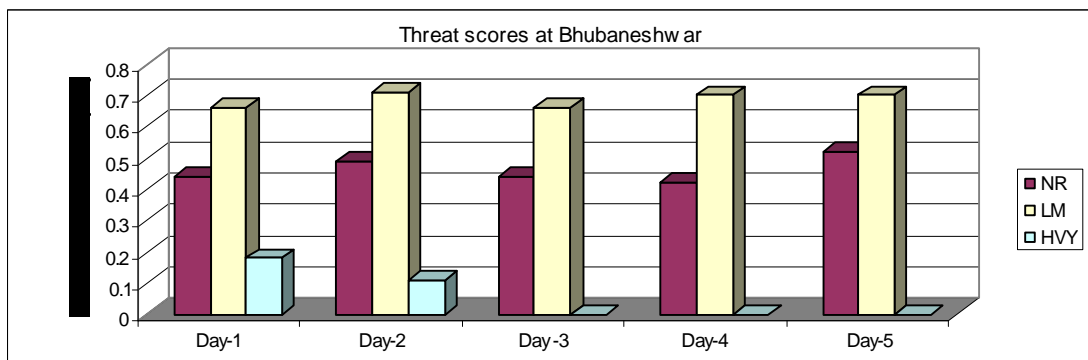
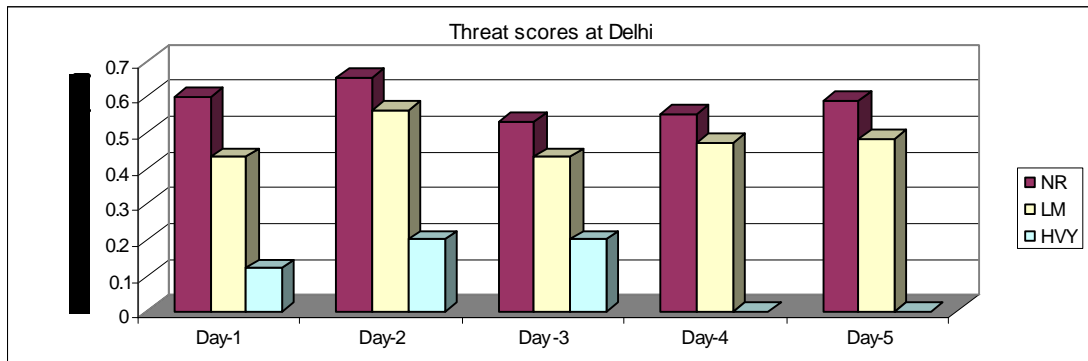


Fig. 6. Threat scores for Bias free rainfall amounts based upon T-254 model for selected major cities of India (monsoon-2009)
 (NR: no rain ; LM: light to medium rain ; HVY: heavy rain)

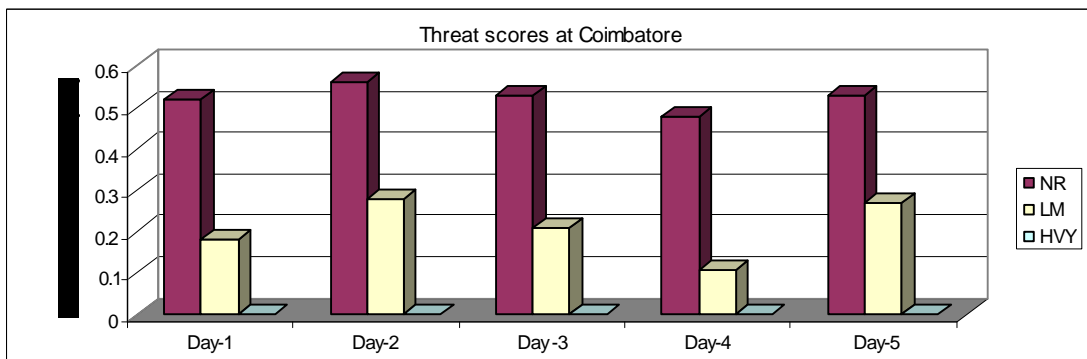
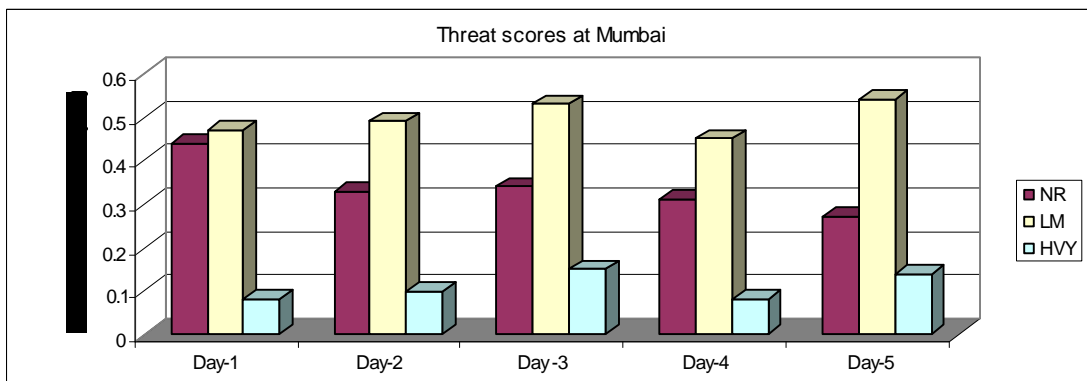
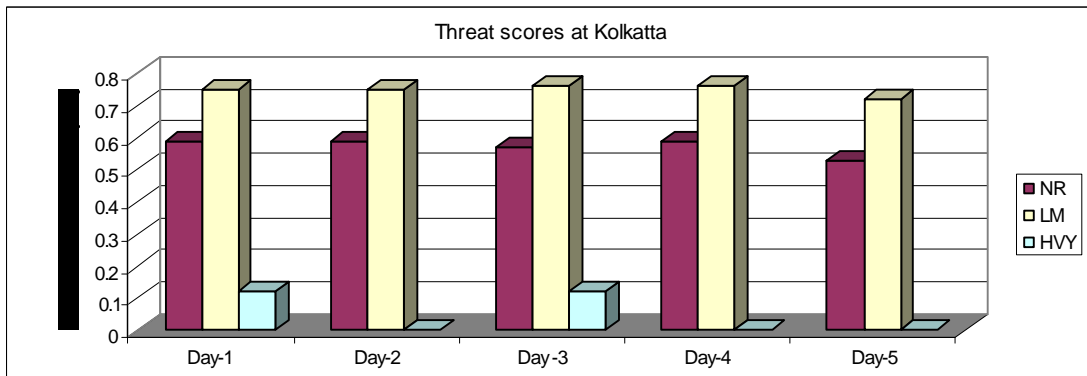
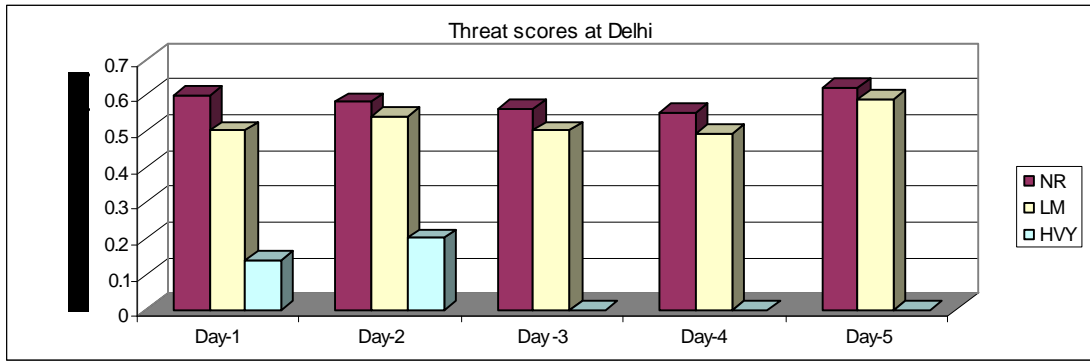


Fig. 7. Threat scores for Bias free rainfall amounts based upon T-254 model for selected districts of India (monsoon-2009)
(NR: no rain ; LM: light to medium rain ; HVY: heavy rain)

Table 1

State specific threshold values for T80/T170 and T-254 model rainfall forecasts

SN	States/UT	Threshold rainfall values(mm) (T-80/T-170 models)	Threshold rainfall values(mm) (T-254 model)
1	Andhra pradesh	5.0	5.0
2	Assam	2.0	2.0
3	Arunachal pradesh	2.0	2.0
4	Bihar	2.0	1.0
5	Chhatisgarh	2.0	2.0
	Gujarat	0.5	0.5
7	Haryana	0.1	1.0
8	Himachal pradesh	0.5	0.5
9	Jammu & Kashmir	0.5	0.0
10	Jharkhand	2.0	2.0
11	Karnataka	7.0	7.0
12	Kerala	7.0	7.0
13	Madhya pradesh	1.0	1.0
14	Maharashtra	2.0	2.0
15	Manipur	2.0	2.0
16	Meghalaya	2.0	2.0
17	Mizoram	2.0	2.0
18	Nagaland	2.0	2.0
19	Orissa	2.0	0.0
20	Punjab	0.1	1.0
21	Rajasthan	0.1	0.5
22	Sikkim	2.0	2.0
23	Tamil nadu	5.0	5.0
24	Tripura	2.0	2.0
25	Uttaranchal	0.5	0.5
26	Uttar pradesh	0.5	0.0
27	West Bengal	2.0	0.0
28	Delhi	0.1	1.0
29	Goa	2.0	2.0
30	Pondichery	2.0	2.0
31	Lakshdweep	7.0	7.0
32	Daman & Diu	2.0	2.0
33	Dadra & nagar	2.0	2.0
34	Chandigarh	0.1	1.0
35	Andaman & Nicobar	7.0	7.0

Table 2
Skill score for biasfree rainfall and Kalman filtered maximum and minimum
temperature ; 72 hr forecast; based upon T-254 model for major cities during
Monsoon (Jun.-Sep)-2009

Sn.	Station	Rain		Min		Max	
		Ratio	HK	RMSE	Corr	RMSE	Corr
1.	Agartala	78	0.03	1.35	0.13	2.23	0.53
2.	Ahmadabad	80	0.60	1.86	0.55	3.55	0.75
3.	Akola	72	0.43	1.95	0.78	3.14	0.80
4.	Allahabad	78	0.58	2.83	0.43	3.52	0.85
5.	Bangalore	66	0.21	1.40	0.10	2.34	0.28
6.	Bhopal	71	0.41	2.52	0.76	3.30	0.85
7.	Bhubaneshwar	80	0.49	2.22	0.35	3.56	0.64
8.	Coimbatore	67	0.33	1.14	0.04	2.73	0.40
9.	Dehradun	89	0.76	2.32	0.41	3.05	0.81
10.	Delhi	69	0.38	2.81	0.57	3.70	0.83
11.	Hisar	71	0.37	2.89	0.57	3.73	0.65
12.	Indore	79	0.56	2.03	0.77	2.69	0.87
13.	Jabalpur	72	0.44	2.26	0.83	2.72	0.88
14.	Jodhpur	63	-0.02	2.48	0.41	2.95	0.71
15.	Jaipur	72	0.42	2.67	0.66	3.18	0.76
16.	Lucknow	80	0.58	2.81	0.49	4.11	0.81
17.	Mumbai	81	0.36	1.83	0.26	2.82	0.53
18.	Nagpur	77	0.53	2.75	0.80	3.24	0.83
19.	Raipur	69	0.41	2.71	0.66	2.68	0.90
20.	Udaipur	75	0.52	2.58	0.42	2.65	0.85
21.	Vishakhapatnam	70	0.34	1.73	0.39	2.40	0.38

Table 3
Skill score for biasfree rainfall and trend based maximum and minimum
temperature; 72hr forecast; based upon T-254 model for selected districts during
Monsoon (Jun.-Sep)-2009

Sn.	Station	Rain		Min		Max	
		Ratio	HK	RMSE	Corr	RMSE	Corr
1.	Agartala	69	0.02	1.31	0.43	2.66	0.51
2.	Ahmadabad	83	0.66	1.91	0.40	2.39	0.78
3.	Akola	68	0.36	1.62	0.73	3.42	0.69
4.	Allahabad	78	0.57	2.42	0.25	2.73	0.79
5.	Baroda	79	0.58	1.48	0.52	2.55	0.65
6.	Bhopal	68	0.35	2.11	0.59	3.03	0.80
7.	Bikaner	69	0.17	2.54	0.54	2.87	0.48
8.	Chennai	62	0.23	1.90	0.47	3.05	0.44
9.	Coimbatore	58	0.19	1.17	0.21	2.45	0.18
10.	Dehradun	82	0.64	2.28	0.40	3.07	0.73
11.	Delhi	73	0.45	2.54	0.52	3.06	0.70
12.	Gwalior	85	0.69	2.43	0.66	3.42	0.76
13.	Hisar	72	0.41	2.43	0.61	3.88	0.56
14.	Hyderabad	67	0.34	1.94	0.29	3.31	0.41
15.	Indore	72	0.45	1.34	0.79	2.80	0.79
16.	Jabalpur	73	0.46	1.82	0.76	3.19	0.80
17.	Jodhpur	64	0.00	2.68	0.30	2.75	0.60
18.	Jaipur	70	0.38	2.62	0.50	3.33	0.62
19.	Kolkatta	88	0.67	1.50	0.47	2.65	0.44
20..	Lucknow	83	0.62	1.99	0.50	3.31	0.72
21.	Madurai	64	0.22	1.43	0.37	2.07	0.46
22.	Mumbai	78	0.33	1.72	0.54	1.76	0.63
23.	Nagpur	74	0.45	2.03	0.57	3.18	0.78
24.	Patna	83	0.61	1.72	0.31	2.99	0.58
25.	Pune	70	0.22	1.55	0.16	2.17	0.71
26.	Ranchi	75	0.41	1.92	0.36	3.00	0.69
27.	Raipur	68	0.49	2.32	0.56	3.14	0.81
28.	Shimla	83	0.65	2.20	0.49	3.08	0.59
29.	Udaipur	68	0.39	2.57	0.43	2.97	0.74
30.	Varanasi	81	0.60	1.74	0.48	3.05	0.75

Table 4
Skill score for biasfree rainfall amounts 72hr forecast based upon T-254
model for major cities during Monsoon (Jun.-Sep)-2009

Sn	Station	Hit Rate	Hit Rate for rainfall Amounts				Threat Score for rainfall amounts			
			NR	LM	HVY	VHY	NR	LM	HVY	VHY
1.	Agartala	0.71	0.05	0.97	0.14	----	0.05	0.71	0.11	-----
2.	Ahmadabad	0.74	0.81	0.73	0.00	----	0.69	0.50	0.00	-----
3.	Akola	0.63	0.69	0.65	0.00	---	0.54	0.44	0.00	-----
4.	Allahabad	0.70	0.62	0.93	0.00	----	0.60	0.54	0.00	----
5.	Bangalore	0.64	0.17	0.13	0.00	----	0.35	0.56	0.00	----
6.	Bhopal	0.64	0.61	0.79	0.00	0.00	0.50	0.51	0.00	0.00
7.	Bhubaneshwar	0.71	0.60	0.86	0.00	----	0.44	0.66	0.00	----
8.	Coimbatore	0.62	0.51	0.76	0.00	----	0.43	0.49	0.00	----
9.	Dehradun	0.77	0.84	0.86	0.10	----	0.73	0.69	0.08	----
10.	Delhi	0.64	0.68	0.62	0.25	----	0.53	0.43	0.20	----
11.	Hisar	0.66	0.77	0.50	0.00	----	0.62	0.32	0.00	----
12.	Indore	0.67	0.71	0.74	0.00	----	0.60	0.50	0.00	----
13.	Jabalpur	0.62	0.66	0.79	0.00	0.00	0.53	0.48	0.00	0.00
14.	Jodhpur	0.61	0.78	0.15	0.00	-----	0.60	0.09	0.00	----
15.	Jaipur	0.70	0.82	0.58	0.00	-----	0.61	0.47	0.00	----
16.	Lucknow	0.69	0.65	0.86	0.00	0.00	0.59	0.56	0.00	0.00
17.	Mumbai	0.57	0.42	0.69	0.29	0.00	0.33	0.52	0.10	0.00
18.	Nagpur	0.71	0.74	0.78	0.00	----	0.49	0.66	0.00	----
19.	Raipur	0.63	0.74	0.62	0.00	0.00	0.41	0.52	0.00	0.00
20.	Udaipur	0.69	0.69	0.79	0.00	-----	0.61	0.49	0.00	----
21.	Vishakhapatnam	0.68	0.53	0.83	0.00	----	0.43	0.59	0.00	-----

Note:- NR: No rain ; LM: Light to moderate rainfall ; HVY: Heavy rain ; VHY : Very heavy rain

Table 5
Skill score for biasfree rainfall amounts 72hr forecast based upon T-254
model for selected districts during Monsoon (Jun.-Sep)-2009

Sn	Station	Hit Rate	Hit Rate for rainfall				Threat Score for rainfall			
			NR	LM	HVY	VHY	NR	LM	HVY	VHY
1.	Agartala	0.62	0.20	0.79	0.14	----	0.12	0.60	0.12	----
2.	Ahmadabad	0.80	0.86	0.82	0.00	----	0.77	0.60	0.00	----
3.	Akola	0.62	0.71	0.60	0.00	----	0.51	0.42	0.00	----
4.	Allahabad	0.71	0.63	0.93	0.00	----	0.60	0.56	0.00	----
5.	Baroda	0.75	0.69	0.89	0.00	----	0.63	0.63	0.00	----
6.	Bhopal	0.62	0.63	0.72	0.00	0.00	0.47	0.48	0.00	0.00
7.	Bikaner	0.67	0.89	0.24	0.00	----	0.66	0.18	0.00	----
8.	Chennai	0.64	0.95	0.31	0.00	----	0.58	0.29	0.00	----
9.	Coimbatore	0.57	0.91	0.24	0.00	----	0.53	0.21	0.00	----
10.	Dehradun	0.72	0.81	0.81	0.00	----	0.60	0.63	0.00	----
11.	Delhi	0.67	0.68	0.75	0.00	----	0.56	0.50	0.00	----
12.	Gwalior	0.75	0.76	0.79	0.00	----	0.70	0.55	0.00	----
13.	Hisar	0.64	0.74	0.50	0.00	----	0.60	0.30	0.00	----
14.	Hyderabad	0.70	0.84	0.55	0.00	0.00	0.62	0.44	0.00	0.00
15.	Indore	0.65	0.70	0.69	0.00	----	0.53	0.48	0.00	----
16.	Jabalpur	0.59	0.68	0.70	0.00	0.00	0.55	0.40	0.00	0.00
17.	Jodhpur	0.62	0.80	0.15	0.00	----	0.62	0.09	0.00	----
18.	Jaipur	0.67	0.82	0.50	0.00	----	0.61	0.41	0.00	----
19.	Kolkatta	0.80	0.68	0.93	0.12	----	0.57	0.76	0.12	----
20..	Lucknow	0.73	0.67	0.90	0.00	0.00	0.62	0.62	0.00	0.00
21.	Madurai	0.64	0.95	0.23	----	----	0.60	0.22	----	----
22.	Mumbai	0.59	0.48	0.68	0.43	0.00	0.34	0.53	0.15	0.00
23.	Nagpur	0.63	0.68	0.67	0.00	----	0.43	0.55	0.00	0.00
24.	Patna	0.77	0.68	0.93	0.00	----	0.62	0.69	0.00	----
25.	Pune	0.54	0.26	0.85	0.00	----	0.23	0.49	0.00	----
26.	Ranchi	0.69	0.57	0.85	0.00	----	0.44	0.64	0.00	----
27.	Raipur	0.64	0.91	0.65	0.00	0.00	0.46	0.51	0.00	0.00
28.	Shimla	0.76	0.81	0.80	0.20	----	0.63	0.69	0.12	----
29.	Udaipur	0.62	0.60	0.75	0.00	----	0.51	0.43	0.00	----
30.	Varanasi	0.78	0.70	0.88	0.00	----	0.62	0.66	0.00	----

Note:- NR: No rain ; LM: Light to moderate rainfall ; HVY: Heavy rain ; VHY : Very heavy rain